



Scientific Report No. 51-2013

# Impacts of Climate Change and Adaptation in the Electricity Sector

## The Case of Austria in a Continental European Context (EL.ADAPT)

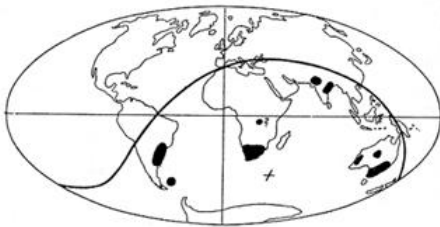
Gabriel Bachner, Birgit Bednar-Friedl, Steffen Birk,  
Gerald Feichtinger, Andreas Gobiet, Christoph Gutschli,  
Georg Heinrich, Veronika Kulmer, Armin Leuprecht,  
Franz Prettenthaler, Nikola Rogler, Thomas Schinko,  
Andreas Schüppel, Heinrich Stigler, Matthias Themeßl,  
Christoph Töglhofer, Thomas Wagner

April 2013



The **Wegener Center for Climate and Global Change** combines as an interdisciplinary, internationally oriented research institute the competences of the University of Graz in the research area „Climate, Environmental and Global Change“. It brings together, in a dedicated building close to the University central campus, research teams and scientists from fields such as geo- and climate physics, meteorology, economics, geography, and regional sciences. At the same time close links exist and are further developed with many cooperation partners, both nationally and internationally. The research interests extend from monitoring, analysis, modeling and prediction of climate and environmental change via climate impact research to the analysis of the human dimensions of these changes, i.e, the role of humans in causing and being effected by climate and environmental change as well as in adaptation and mitigation. (more informationen at [www.wegcenter.at](http://www.wegcenter.at))

The present report is the final report of the Austrian Climate Research Program (ACRP) project “EL.ADAPT” (project number B060380) which was conducted from February 2011 to March 2013. This project received financial support from the Climate and Energy Fund and is carried out within the framework of the ACRP program.



**Alfred Wegener** (1880-1930), after whom the Wegener Center is named, was founding holder of the University of Graz Geophysics Chair (1924-1930) and was in his work in the fields of geophysics, meteorology, and climatology a brilliant, interdisciplinary thinking and acting scientist and scholar, far ahead of his time with this style. The way of his ground-breaking research on continental drift is a shining role model — his sketch on the relationship of the continents based on traces of an ice age about 300 million years ago (left) as basis for the Wegener Center Logo is thus a continuous encouragement to explore equally innovative scientific ways: *paths emerge in that we walk them* (Motto of the Wegener Center).

## Wegener Center Verlag • Graz, Austria

© 2005 All Rights Reserved.

Selected use of individual figures, tables or parts of text is permitted for non-commercial purposes, provided this report is correctly and clearly cited as the source. Publisher contact for any interests beyond such use: [wegcenter@uni-graz.at](mailto:wegcenter@uni-graz.at).

ISBN 978-3-9503112-8-0

April 2013

Contact: *Birgit Bednar-Friedl.*  
[birgit.friedl@uni-graz.at](mailto:birgit.friedl@uni-graz.at)

**Wegener Center** for Climate and Global Change  
University of Graz  
Brandhofgasse 5  
A-8010 Graz, Austria  
[www.wegcenter.at](http://www.wegcenter.at)

# Impacts of Climate Change and Adaptation in the Electricity Sector - The Case of Austria in a Continental European Context (EL.ADAPT)

Final Report for Publication

Gabriel Bachner<sup>1</sup>, Birgit Bednar-Friedl<sup>1,\*</sup>, Steffen Birk<sup>2</sup>, Gerald Feichtinger<sup>3</sup>,  
Andreas Gobiet<sup>1</sup>, Christoph Gutschl<sup>3</sup>, Georg Heinrich<sup>1</sup>, Veronika Kulmer<sup>1</sup>,  
Armin Leuprecht<sup>1</sup>, Franz Prettenhaler<sup>4</sup>, Nikola Rogler<sup>4</sup>, Thomas Schinko<sup>1</sup>,  
Andreas Schüppel<sup>3</sup>, Heinrich Stigler<sup>3</sup>, Matthias Themeßl<sup>1</sup>, Christoph Töglhofer<sup>1</sup>,  
Thomas Wagner<sup>2</sup>

April 30, 2013

<sup>1</sup> Wegener Center for Climate and Global Change,  
University of Graz



<sup>2</sup> Institute of Earth Sciences,  
University of Graz



<sup>3</sup> Institute of Electricity Economics and Energy Innovation,  
Graz University of Technology



<sup>4</sup> POLICIES - Centre for Economic and  
Innovation Research, Joanneum Research



\* Project Leader. Contact: Wegener Center for Climate and Global Change, University of Graz,  
Brandhofgasse 5, A-8010 Graz, email: birgit.friedl@uni-graz.at

Program control: Climate and Energy Fund

Program management: Kommunalkredit Public Consulting GmbH (KPC)



TABLE OF CONTENTS

1	Introduction.....	3
2	Methodology.....	5
2.1	Regional climate modeling .....	6
2.1.1	Data and study region.....	6
2.1.2	Climate scenario selection .....	7
2.1.3	Error correction of selected RCMs .....	14
2.2	Hydrological modeling .....	19
2.3	Households' electricity demand modeling.....	24
2.4	Electricity sector model ATLANTIS .....	27
2.4.1	Model improvements within the project focus .....	30
2.4.2	Implementation of interfaces to other models .....	31
2.5	Multi-country multi-sector modeling .....	34
2.5.1	Model calibration .....	38
2.6	Iterative coupling of CGE model and ATLANTIS .....	38
2.6.1	Baseline .....	42
2.7	Uncertainty and reliability assessment.....	48
3	Results and conclusions.....	49
3.1	Regional climate change across Europe and uncertainties involved.....	49
3.2	Change in water availability in the GAR and uncertainties involved.....	50
3.2.1	Calibration and Validation .....	50
3.2.2	Runoff estimates based on four climate scenarios.....	52
3.2.3	Uncertainties involved.....	59
3.2.4	Concluding remarks .....	68
3.3	Climate change impacts on households' electricity demand across Europe .....	69
3.3.1	Cross-country comparison of heating and cooling electricity demand.....	70
3.3.2	Uncertainties related to future heating and cooling electricity needs.....	75
3.3.3	Impact on electricity demand .....	78
3.4	Climate change impacts on the electricity sector .....	79
3.4.1	Impacts on electricity generation.....	79
3.4.2	Impacts on the electricity demand.....	85
3.4.3	Impacts on the electricity market.....	86
3.4.4	Sensitivity analysis and uncertainties.....	91
3.5	Macroeconomic effects .....	97
3.5.1	Indirect effects of climate change impacts in the electricity sector .....	99
3.5.2	A comparison of direct and indirect effects of climate change impacts in the electricity sector	102
3.5.3	Environmental effects.....	106
3.5.4	Interactions with climate policy.....	108
3.5.5	Sensitivity analysis and uncertainty.....	109
3.6	Options for adaptation to climate change in the electricity sector.....	110
3.6.1	Overview on adaptation measures.....	110

EL.ADAPT

3.6.2	Hydro power .....	113
3.6.3	Wind power .....	114
3.6.4	Solar power (photovoltaics).....	115
3.6.5	Electricity demand.....	115
4	Outlook and recommendations for research .....	117
5	References .....	119
6	Annex .....	126

## 1 Introduction

The EU Green Paper (2007) on adaptation to climate change in Europe states mountain areas, particularly the Alps, as one of the most vulnerable areas in Europe. Austria already experiences rising annual average temperatures which are accompanied by significant and measurable impacts: Glaciers are retreating and snow covered periods are getting shorter, thus altering the timing and amplitude of melt water run-off. Also the intensity and frequency of precipitation in Austria is changing. With growing international recognition of the urgent need to adaptation to climate change, the mechanisms of adaptation, as well as the interplay with sectoral vulnerability, have to be better understood in order to devise cost-effective adaptation policies in the short, medium and long run.

This project intended to provide a sound scientific basis for assessing an adaptation strategy for Austria in the electricity sector, a sector highly vulnerable to climate change. Regarding power supply, especially hydropower plants but also new renewable energy sources will be affected by climate change. Changed evaporation and precipitation patterns and shrinking glaciers impact the operation of run-off-river as well as storage hydropower plants. On the other hand, higher ambient temperatures influence cooling processes, outages, efficiencies and effective power of thermal power plants. On the demand side, changing weather conditions result in different consumption for cooling and heating as well as different patterns of electricity use.

Since the electricity sector is characterized by strong international linkages, the impacts and adaptation options for Austria have to be investigated within the European context. The increasing power generation from fluctuating renewable sources, like wind power in the north of the Alps or solar power in the Mediterranean countries, requires additional capacities for electricity storage and control. Climate change is associated with rising cooling demand in Southern Europe and declining heating demand in the north. The power exchange between Austria and its neighbouring countries is thus expected to increase dramatically such that any future outlook has to take into account the European context of the electricity market. Another specific characteristic of electricity is its key role as an intermediate input in other sectors, particularly for energy intensive sectors, as well as in final demand. This necessitates not only a detailed analysis of the consequences for the sector itself but also an analysis of effects on the macroeconomy.

The aim of this project was to develop an integrated modeling framework to describe and analyze the requirement for and economic consequences of adaptation in the electricity sector in Austria on a time scale up to 2050. Due to the cross-cutting nature of the problem, an integration (or coupling) of different models is essential. The first focus of the project lies thus on the adjustment and integration of the different models employed. To depict the consequences of climate change for electricity, high-resolution climate change scenarios are used as input to the hydrological model to determine changes in hydrology relevant for hydropower generation and as input to the electricity sector models (temporal and spatial high resolution temperature, precipitation, river discharge, and wind data). The currently best available sectoral models for electricity are refined (in terms of temporal scale and adaptation detail): (i) techno-economic model of the electricity industry in continental Europe and (ii) econometric analysis to model the climate change impact on as well as adaptation options for the demand for electricity. The bottom-up electricity sector model is linked to a top-down, i.e. multi-country multi-sector, computable general equilibrium (CGE) model of Austria and other European countries to evaluate the sectoral and economy-wide climate change impacts and adaptation options for the electricity sector.

In addition to the development of an integrated modeling framework, we analyze uncertainties involved in the overall modeling approach, from uncertainties in climate scenarios (uncertainties in future greenhouse gas emissions, uncertainties due to the climate model's simplifications and errors) to uncertainties in economic modeling (assumptions on demographics, technological change, fuel prices).

## 2 Methodology

The aim of this project is to develop an integrated modeling framework to describe and analyse the requirement for and economic consequences of adaptation in the electricity sector in Austria on a time scale up to 2050. Due to the cross-cutting nature of the problem, an integration (or coupling) of different models is essential. The first focus of the project lies thus on the adjustment and integration of the different models employed, as indicated in Figure 1. To depict the consequences of climate change for electricity, high-resolution climate change scenarios are used as input to the hydrological model to determine changes in hydrology relevant for hydropower generation and as input to the electricity sector models (temporal and spatial high resolution temperature, precipitation, river discharge, global radiation and wind data). The currently best available sectoral models for electricity are refined (in terms of temporal scale and adaptation detail): (i) techno-economic model of the electricity industry in continental Europe and (ii) econometric analysis to model the climate change impact on as well as adaptation options for the demand for electricity. The bottom-up electricity sector model is linked to a top-down, i.e. multi-country multi-sector, computable general equilibrium (CGE) model of Austria and other European countries to evaluate the sectoral and economy wide climate change impacts and adaptation options for the electricity sector.

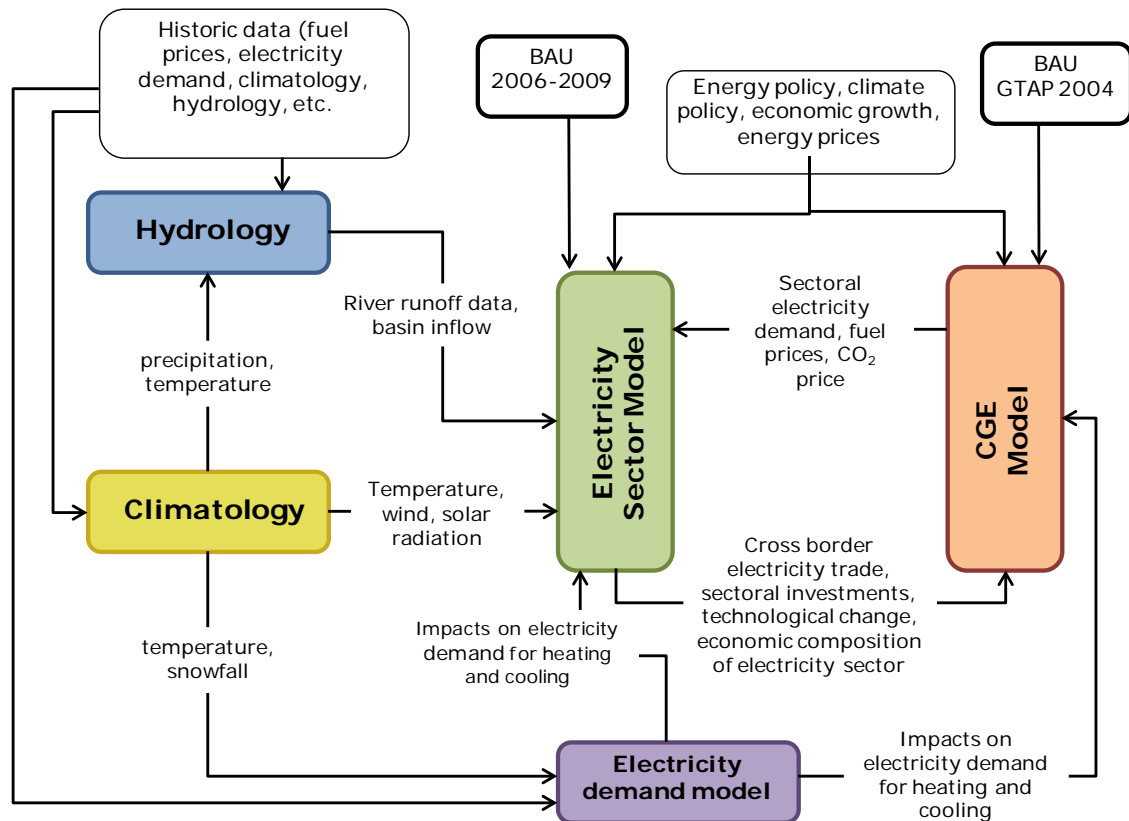


Figure 1: Overview of model linkage

## 2.1 Regional climate modeling

### 2.1.1 Data and study region

Based on the requirements of the electricity demand studies in EL-Adapt meteorological forcing in form of daily temperature, precipitation, wind speed and global radiation were needed between 1961 and 2050. Figure 2 illustrates the study area of EL.ADAPT which was approved by the project members. The study region was defined to cover the synchronous grid of Continental Europe including West Ukraine. Although the Scandinavian countries are members of ENTSO-E (European network of transmission system operators), they were not selected due to the minor physical connection to the continental European electricity system.

For model calibration as well as the error correction of regional climate models (RCMs), the E-OBS European gridded observational dataset (van den Besselaar et al., 2011; Haylock et al., 2008) was used in this study. E-OBS contains gridded daily time series of mean, minimum, maximum temperature and precipitation amount on a 25 km raster and is based on the most complete collection of station data over wider

Europe (Klok and KleinTank, 2009). A similar dataset for global radiation and wind speed does yet not exist for entire Europe.

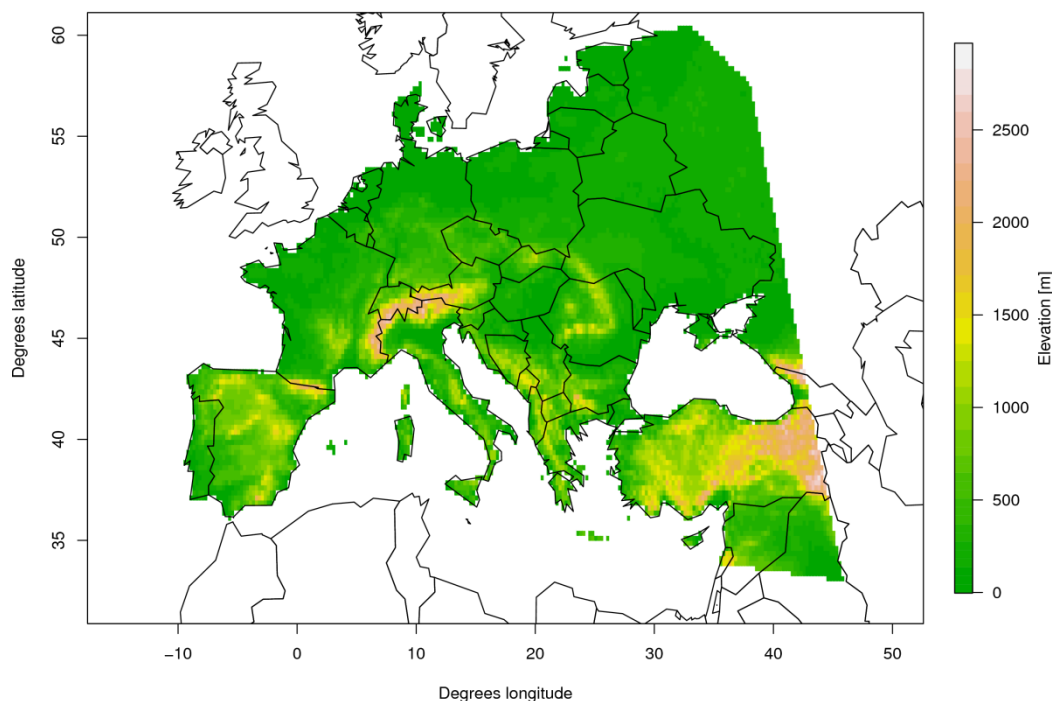


**Figure 2: The study region for the development of tailored climate information in EL.ADAPT.**

Concerning the provision of future climate scenarios, RCM simulations from the ENSEMBLES project (van den Linden and Mitchell, 2009) were used. ENSEMBLES contained a coordinated endeavor to produce regional climate scenarios for Europe and West Africa. Within ENSEMBLES 23 RCM simulation with a horizontal resolution of 25 km are available based on 8 GCM simulations. Thus, ENSEMBLES provides a well filled GCM/RCM matrix. Temporally the RCMs provide daily time series from 1951 to 2050. In EL.ADAPT climate scenario data which are based on the SRES greenhouse gas emission scenario pathway A1B (Nakicenovic et al., 2000) for the scenario period (2001-2050) are used. Furthermore, 19 out of 23 ENSEMBLES models entered the EL.ADAPT scenario selection process due to the availability of all needed parameters and time spans at the time of the model selection.

### **2.1.2 Climate scenario selection**

Based on 19 ENSEMBLES RCM simulations, four simulations have been selected in EL.ADAPT in order to cover the uncertainty spread within the available RCMs. All

considered meteorological parameters were taken into account in the selection process. The climate change signal (CCS) for the scenario selection was calculated between 1961-1990 and 2021-2050 on seasonal as well as annual basis but for different regions for the different parameters. The considered regions are shown in Figure 3 and have been defined according to the geographical distribution of the different energy production systems (e.g. wind power, hydro power,...)

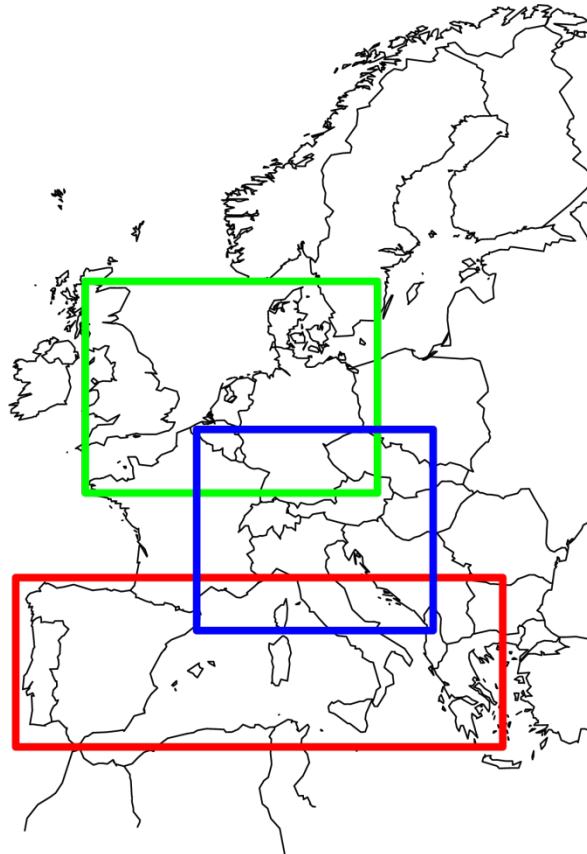


**Figure 3: Definitions of the geographical locations for the calculation of the CCS of temperature, precipitation (blue box), wind speed (green box), and global radiation (red box)**

In Tables Table 1 and Table 2 the respective climate change signals and the associated standard deviation of the 90 years time series from 1961-2050 are listed. For the calculation of the standard deviation, the daily time series were de-trended.

**Table 1: Mean climate change signal for temperature (air temp, °C), precipitation (prec, mm/day), windspeed (windsp, m/s) and global radiation (glob.rad, W/m<sup>2</sup>) and the standard deviation (sd) of the considered models for the winter season (December, January, February)**

Modell - WINTER	<i>air.temp m</i>	sd	<i>m/sd</i>	<i>prec m</i>	sd	<i>m/sd</i>	<i>windsp m</i>	sd	<i>m/sd</i>	<i>glob.rad m</i>	sd	<i>m/sd</i>
METO-HC_HadRM3Q0	2.406	1.201	<b>2.004</b>	0.045	0.540	<b>0.083</b>	0.017	0.460	<b>0.036</b>	1.918	4.476	<b>0.428</b>
METO-HC_HadRM3Q16	2.307	1.011	<b>2.282</b>	0.124	0.469	<b>0.265</b>	0.239	0.557	<b>0.429</b>	-0.923	4.005	<b>0.231</b>
ETHZ-CLM	2.065	1.271	<b>1.625</b>	0.077	0.484	<b>0.160</b>	0.047	0.405	<b>0.117</b>	0.654	4.386	<b>0.149</b>
METNOHIRHAM_HadCM3Q0	1.914	1.095	<b>1.748</b>	0.058	0.557	<b>0.104</b>	-0.186	0.398	<b>0.467</b>	1.831	6.684	<b>0.274</b>
METNOHIRHAM_BCM	1.422	1.060	<b>1.342</b>	0.179	0.492	<b>0.365</b>	0.101	0.381	<b>0.264</b>	1.642	5.209	<b>0.315</b>
ICTP-REGCM3	1.049	1.167	<b>0.899</b>	0.147	0.634	<b>0.231</b>	0.132	0.433	<b>0.304</b>	0.730	5.853	<b>0.125</b>
MPI-M-REMO	1.136	1.059	<b>1.073</b>	0.159	0.555	<b>0.287</b>	0.108	0.376	<b>0.288</b>	-0.537	3.993	<b>0.134</b>
C4IRCA3	2.297	1.107	<b>2.075</b>	0.295	0.465	<b>0.634</b>	-0.019	0.342	<b>0.055</b>	-1.379	3.444	<b>0.400</b>
CNRM-RM5.1	1.358	0.833	<b>1.630</b>	-0.240	0.542	<b>0.442</b>	0.015	0.442	<b>0.033</b>	0.447	5.637	<b>0.079</b>
CNRM-RM4.5	1.184	0.850	<b>1.392</b>	-0.162	0.552	<b>0.293</b>	0.085	0.589	<b>0.144</b>	0.086	5.081	<b>0.017</b>
DMI-HIRHAM5_ARPEGE	1.607	1.049	<b>1.532</b>	-0.215	0.583	<b>0.369</b>	-0.006	0.455	<b>0.013</b>	3.048	8.819	<b>0.346</b>
DMI-HIRHAM5_ECHAM5	0.919	1.099	<b>0.836</b>	0.176	0.646	<b>0.272</b>	0.119	0.440	<b>0.269</b>	-0.096	2.896	<b>0.033</b>
DMI-HIRHAM5_BCM	1.516	1.246	<b>1.217</b>	0.232	0.452	<b>0.513</b>	0.224	0.388	<b>0.577</b>	0.581	2.188	<b>0.266</b>
KNMI-RACMO2	1.162	1.121	<b>1.036</b>	0.262	0.582	<b>0.450</b>	0.165	0.423	<b>0.390</b>	0.080	3.316	<b>0.024</b>
SMHIRCA_BCM	1.251	0.953	<b>1.313</b>	0.079	0.510	<b>0.155</b>	0.307	0.350	<b>0.878</b>	0.056	2.494	<b>0.023</b>
SMHIRCA_ECHAM5-r3	1.010	1.089	<b>0.927</b>	0.202	0.615	<b>0.328</b>	0.112	0.355	<b>0.315</b>	-0.391	3.796	<b>0.103</b>
SMHIRCA_HadCM3Q3	2.234	1.398	<b>1.597</b>	0.142	0.444	<b>0.319</b>	-0.125	0.300	<b>0.418</b>	-1.596	3.827	<b>0.417</b>
UCLM-PROMES	2.145	1.350	<b>1.589</b>	0.012	0.501	<b>0.023</b>	0.019	0.518	<b>0.037</b>	6.228	5.462	<b>1.140</b>
VMGO-RRCM	2.033	1.123	<b>1.809</b>	0.437	0.547	<b>0.798</b>	-0.019	0.325	<b>0.057</b>	-0.828	1.901	<b>0.435</b>

**Table 2: Mean climate change signal for temperature (air temp, °C), precipitation (prec, mm/day), windspeed (windsp, m/s) and global radiation (glob.rad, W/m<sup>2</sup>) and the standard deviation (sd) of the considered models for the summer season (June, July, August)**

Modell - SOMMER	<i>air.temp m</i>	sd	<i>m/sd</i>	<i>prec m</i>	sd	<i>m/sd</i>	<i>windsp m</i>	sd	<i>m/sd</i>	<i>glob.rad m</i>	sd	<i>m/sd</i>
METO-HC_HadRM3Q0	2.787	1.519	<b>1.835</b>	-0.275	0.547	<b>0.503</b>	-0.001	0.211	<b>0.004</b>	3.876	4.004	<b>0.968</b>
METO-HC_HadRM3Q16	2.344	1.406	<b>1.667</b>	-0.034	0.442	<b>0.076</b>	0.007	0.222	<b>0.031</b>	1.026	3.449	<b>0.298</b>
ETHZ-CLM	2.400	1.042	<b>2.304</b>	-0.203	0.449	<b>0.452</b>	0.021	0.190	<b>0.110</b>	3.445	6.384	<b>0.540</b>
METNOHIRHAM_HadCM3Q0	2.184	1.177	<b>1.855</b>	-0.223	0.568	<b>0.392</b>	-0.041	0.215	<b>0.193</b>	9.995	11.916	<b>0.839</b>
METNOHIRHAM_BCM	0.611	0.892	<b>0.686</b>	0.107	0.455	<b>0.236</b>	-0.029	0.214	<b>0.137</b>	-0.430	7.783	<b>0.055</b>
ICTP-REGCM3	1.162	0.760	<b>1.529</b>	-0.022	0.366	<b>0.059</b>	-0.050	0.314	<b>0.161</b>	1.041	6.779	<b>0.154</b>
MPI-M-REMO	1.305	0.868	<b>1.503</b>	-0.154	0.328	<b>0.469</b>	-0.040	0.267	<b>0.150</b>	-0.990	4.509	<b>0.220</b>
C4IRCA3	2.023	0.748	<b>2.705</b>	0.171	0.265	<b>0.646</b>	-0.055	0.173	<b>0.319</b>	-3.458	4.803	<b>0.720</b>
CNRM-RM5.1	1.740	1.238	<b>1.405</b>	0.011	0.538	<b>0.021</b>	0.020	0.178	<b>0.113</b>	0.478	5.652	<b>0.085</b>
CNRM-RM4.5	2.115	0.898	<b>2.356</b>	0.144	0.362	<b>0.397</b>	0.016	0.218	<b>0.072</b>	6.181	4.906	<b>1.260</b>
DMI-HIRHAM5_ARPEGE	1.503	1.294	<b>1.162</b>	-0.051	0.323	<b>0.159</b>	-0.019	0.196	<b>0.098</b>	1.598	6.425	<b>0.249</b>
DMI-HIRHAM5_ECHAM5	0.866	0.942	<b>0.920</b>	0.061	0.475	<b>0.128</b>	-0.078	0.300	<b>0.260</b>	-0.863	5.008	<b>0.172</b>
DMI-HIRHAM5_BCM	0.474	0.796	<b>0.595</b>	-0.023	0.351	<b>0.064</b>	0.093	0.197	<b>0.470</b>	1.804	3.931	<b>0.459</b>
KNMI-RACMO2	1.441	0.796	<b>1.812</b>	-0.129	0.355	<b>0.365</b>	-0.001	0.275	<b>0.003</b>	0.529	4.821	<b>0.110</b>
SMHIRCA_BCM	0.711	0.591	<b>1.204</b>	-0.038	0.395	<b>0.096</b>	0.045	0.132	<b>0.339</b>	3.062	5.571	<b>0.550</b>
SMHIRCA_ECHAM5-r3	1.327	0.665	<b>1.994</b>	-0.149	0.375	<b>0.396</b>	-0.038	0.242	<b>0.155</b>	-1.281	4.877	<b>0.263</b>
SMHIRCA_HadCM3Q3	2.183	0.842	<b>2.592</b>	-0.164	0.409	<b>0.401</b>	0.048	0.217	<b>0.222</b>	2.197	7.665	<b>0.287</b>
UCLM-PROMES	2.436	1.080	<b>2.256</b>	0.049	0.425	<b>0.115</b>	0.056	0.262	<b>0.213</b>	10.891	9.082	<b>1.199</b>
VMGO-RRCM	2.082	0.650	<b>3.201</b>	-0.185	0.482	<b>0.385</b>	0.053	0.160	<b>0.333</b>	0.091	3.018	<b>0.030</b>

Due to the unequally distributed importance of the different meteorological parameters concerning the electricity system, weights were defined for the scenario selection process, which represent the impact of every CCS on the common electricity market of Germany and Austria. The values are given in Table 3.

**Table 3: Definition of weights for the considered meteorological parameters, which were applied in the scenario selection process.**

<b>Parameter</b>	<b>Weight</b>
<b>Air temperature</b>	0.5
<b>Precipitation amount</b>	0.21875
<b>Wind speed</b>	0.21875
<b>Global radiation</b>	0.0625

To find the weights, the expected amount of generation out of the appropriate renewable energy source (hydro, wind, photovoltaics), the expected electricity demand, which is mainly influenced by the temperature (Töglhofer et.al., 2011) as well as the corresponding standard deviations were taken into consideration.

In order to account for the uncertainty range in the climate scenarios regarding all four considered meteorological parameter, and balancing the work load for the subsequent climate impact estimations, a subset of RCMs was selected. For this purpose the CCSs were ranked according to their expected impacts on the energy sector, thus into best and worst scenarios. This classification was decided by the four participating working groups within WP1-3. Table 4 shows the scenario classification scheme where “+” represents positive impacts due to climate change for the electricity sector and “-“ indicates vice versa impacts. For example, an increasing mean of precipitation may lead to more river runoff and finally to more production of electrical energy in hydro power plants. To be precise, a positive CCS impact leads to a reduction of the residual load<sup>1</sup>, while a negative CCS impact results in an increase of the residual load.

---

<sup>1</sup> The residual load represents the customer electricity demand less the electrical energy produced from renewable energy sources, which must be supplied by conventional (thermal) power plants.

**Table 4: Influences on the electricity sector by changes of the corresponding meteorological parameter.**

	summer		winter	
	increase	decrease	increase	decrease
temperature	-	+	+	-
precipitation	+	-	+	-
wind speed	+	-	+	-
irradiance	+	-	+	-

**Table 5: Overview of the evaluated scenarios. "Best" and "worst" scenarios are marked with "X", colours indicate scenarios which were pre-selected by other drivers, too. Scenarios which finally have been selected are printed in bold.**

No.	Model Name	Best (Year)	Worst (Year)	Best (Summer)	Worst (Summer)	Best (Winter)	Worst (Winter)
1	<b>METO-HC_HadRM3Q0</b>				X		
2	METO-HC_HadRM3Q16					X	
3	ETHZ-CLM						
4	METNOHIRHAM_HadCM3Q0		X				
5	METNOHIRHAM_BCM						
6	ICTP-REGCM3						
7	MPI-M-REMO						
8	<b>C4IRCA3</b>						
9	CNRM-RM5.1						X
10	<b>CNRM-RM4.5</b>						
11	DMI-HIRHAM5_ARPEGE						
12	DMI-HIRHAM5_ECHAM5						
13	DMI-HIRHAM5_BCM	X		X			
14	<b>KNMI-RACMO2</b>						
15	SMHIRCA_BCM						
16	SMHIRCA_ECHAM5-r3						
17	SMHIRCA_HadCM3Q3						
18	UCLM-PROMES						
19	VMGO-RRCM						

In addition factors of special interest like unusual hydrological circumstances (scenarios 1 and 8, indicated by a blue background in Table 5) or significant temperature changes (scenarios 1 and 10 in Table 5) have been also taken into consideration.

Finally 4 RCM simulations have been selected. These RCMs feature the following characteristics and represent a large part of the associated uncertainty within the ENSEMBLES ensemble:

## EL.ADAPT

Model #1 (Meteo-HC HadRM3Q0): features a very warm and dry climate change signal in summer, mild conditions in winter. Furthermore the CCS of windspeed is slightly negative throughout the year. This scenario is considered to result in overall positive effects of the energy system, founded by a sharp decline of residual load in winter, although the residual load will slightly increase in summer. Thus model #1 was chosen as the "best case" scenario.

Model #2 (C4IRCA3): features a very wet and warm CCS both in summer and winter. Wind speed will slightly decrease again, while irradiation shows average changes. Due to its very wet characteristic and the large share of hydro power generation in Austria this scenario was considered to be worth investigating in the impact modeling chain.

Model #3 (CNRM-RM4.5): features the special case in the ENSEMBLES ensemble of a stronger summer than winter warming. It is selected due to its expected negative effects concerning increased cooling demand in summer, heating demand in winter and less energy production from renewable energy sources, which leads to a steep rise of residual load both in summer and winter. According to these effects, model #3 was selected as the "worst case" scenario.

Model #4 (KNMI-RACMO2): represents more or less an average realization of the considered RCM ensemble. Precipitation is shifted towards winter season, the overall precipitation during the year changes insignificantly. Furthermore it shows a slightly positive wind CCS in winter. This scenario was chosen as the "average" scenario, because it does not comprise any outstanding CCS.

Figure 4 displays the selected RCM scenarios in relation to the entire uncertainty space. The shown CCSs are given for the summer and the winter period and are weighted according to Table 3. Instead of normalizing to the maximum, the CCSs were fit in the same minimum-maximum range for a better view.

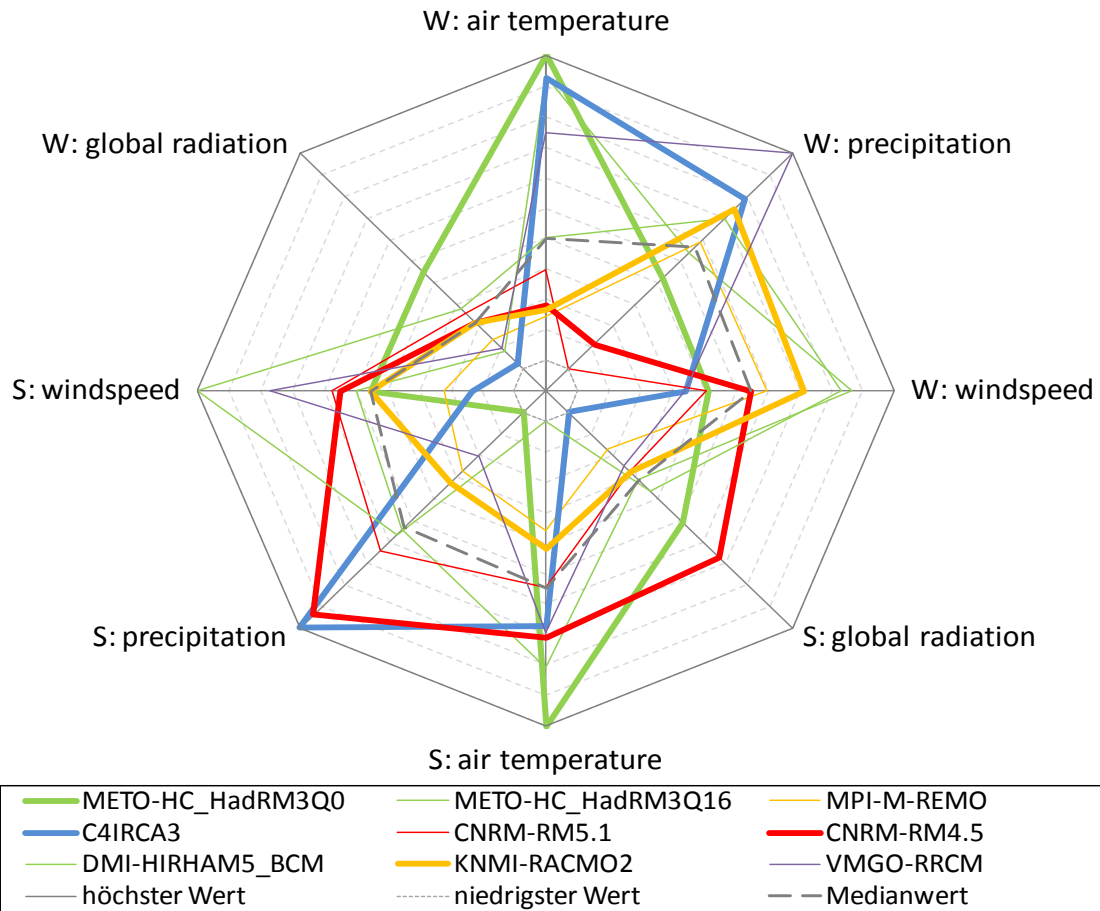


Figure 4: Overview of the pre-selected and finally selected scenario models.

### 2.1.3 Error correction of selected RCMs

The selected RCMs have then been further error corrected. Also RCMs have improved strongly over the last years and have already proofed their added value compared to coarser resolved GCMs, their direct use in impact models should be avoided, as suggested in the IPCC guidance for using RCM output (Mearns et al. 2003). This is firstly because daily precipitation statistics at a station or point are different from those averaged over a 20-km grid box (Boberg et al. 2010; Guo and Senior 2006). Rivington et al. (2008) evaluated the Hadley Centre's RCM with observed data from 15 meteorological stations in the UK for the period 1960-1990, and concluded that the generated daily data were unsuitable for detailed site-specific impact studies in their current form RCMs as they consistently over predict the number of wet days and light daily precipitation events. Secondly, it is well known that RCMs still feature systematic deficiencies in accurately predicting the main meteorological parameters as temperature and precipitation (e.g. Themeßl et al., 2011,2012) because e.g. small scale forcings as the orography are still too coarse but also because dynamical

processes as convection are not adequately resolved due to the RCMs too coarse resolution and computational limits. As a consequence it has become state of the art in recent years to combine RCMs with empirical statistical post-processing according to the concept of model output statistics (Wilks, 2006; Maraun et al., 2010). This post-processing is frequently called bias correction (e.g. Graham et al., 2007; Lenderink et al., 2007; Piani et al., 2010) but as these procedures do not only account for differences in the mean, but often also in the entire distribution, including the variance and extremes Themeßl et al. (2011) termed these post-processing techniques empirical statistical downscaling and error correction methods (DECMs). DECMs force RCM outputs in direction of observations, thus correct them assuming that the observations are an error free reference. If are applied on finer resolved observation data than modelled data, DECMs even perform an implicit downscaling step.

In EL.ADAPT, specifically, quantile mapping (QM) is applied for error-correction. The general procedure of QM is depicted in Figure 5 and described in addition in Equations 1-3. For further methodological information, interested readers should consider Themeßl et al. (2011; 2012). QM can be classified as distribution-based (calibrated on climatological distributions rather than on paired data), direct (predictor and predictand are the same parameters), and parameter-free (using empirical cumulative density distributions, *ecdfs*, rather than theoretical cumulative distribution functions). QM is applied on daily basis ( $t$ ) and for each grid cell ( $i$ ) separately resulting in a corrected time series  $Y^{cor}$  in Eq. 1 using a correction function ( $CF$ ) defined in Eq. 2.

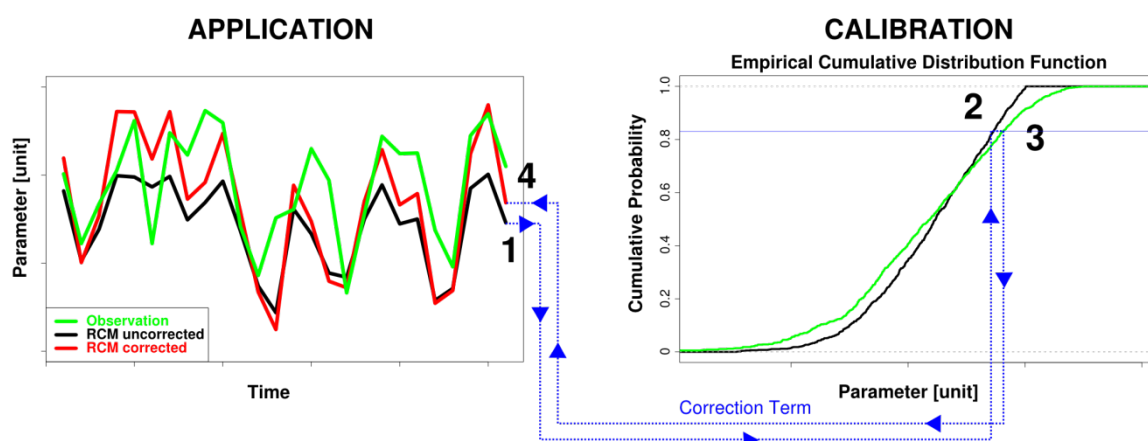


Figure 5: Scheme of QM. An RCM daily output (1) is associated with its probability in an ecdf of the calibration period (2). The difference between the modeled and observed ecdf at this probability is calculated as the correction factor in the calibration period (3) and added to the uncorrected ecdf to obtain a corrected value (4).

$CF$  represents the difference between the observed (obs) and the modelled (mod) inverse  $ecdf$  ( $ecdf^{-1}$ ) for the respective day of the year ( $doy$ ) in the calibration period (cal) at probability  $P$ .

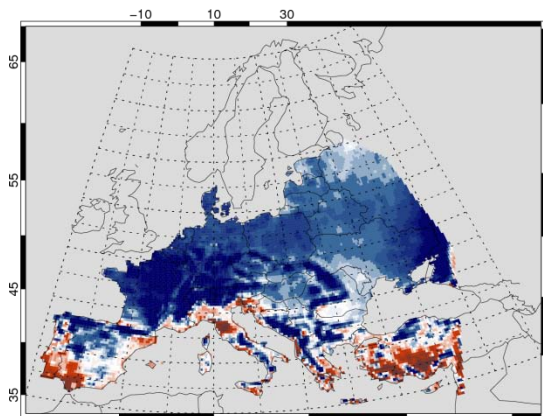
$$Y_{t,i}^{cor} = X_{t,i}^{raw} + CF_{t,i} \quad (1)$$

$$CF_{t,i} = ecdf_{doy,i}^{obs,cal^{-1}}(P_{t,i}) - ecdf_{doy,i}^{mod,cal^{-1}}(P_{t,i}) \quad (2)$$

$$P_{t,i} = ecdf_{doy,i}^{mod,cal}(X_{t,i}^{raw}) \quad (3)$$

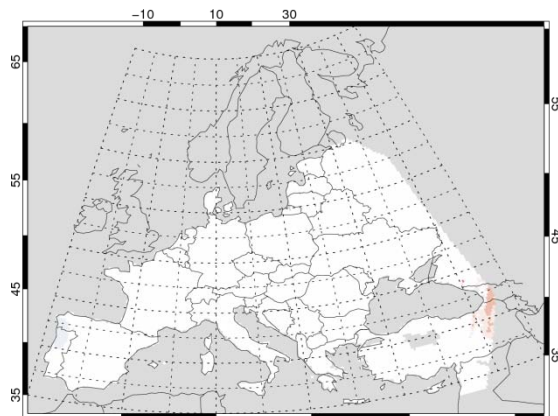
$P$  is obtained by relating the raw climate model output  $X^{raw}$  to the corresponding  $ecdf$  in the calibration period. For QM calibration,  $doy$  is centred within a 31 days moving window, which is used to construct an  $ecdf$  for each day of the year. This procedure also enables to generate new extremes outside the calibration range (compare Themeßl et al., 2012), which is one general restriction for any statistical model. This fact also increases QM's credibility for the application of future scenarios where e.g. in the case of air temperature new extremes are likely to occur due to global warming.

DJF uncorrected



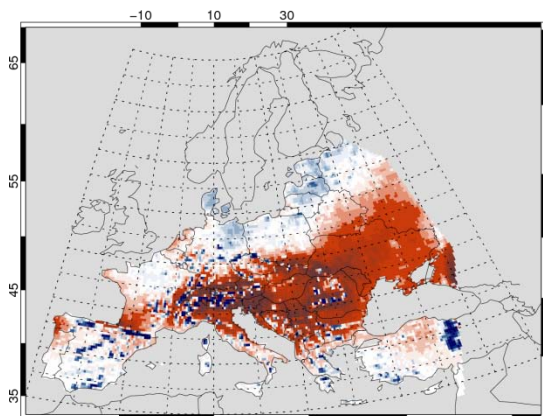
Mean: 0.9 Stand.Dev.: 1.0 Max: 11.4 Min: -3.4

DJF corrected



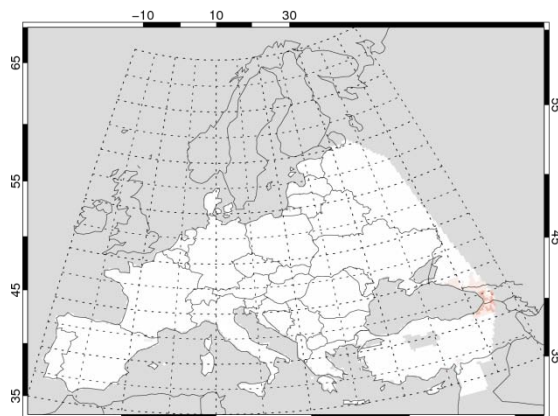
Mean: 0.0 Stand.Dev.: 0.0 Max: 0.2 Min: -0.5

JJA uncorrected



Mean: -0.4 Stand.Dev.: 0.8 Max: 8.8 Min: -4.1

JJA corrected



Mean: -0.0 Stand.Dev.: 0.0 Max: 0.1 Min: -0.5

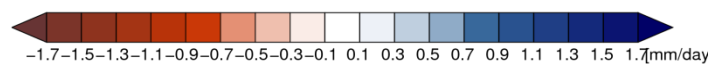
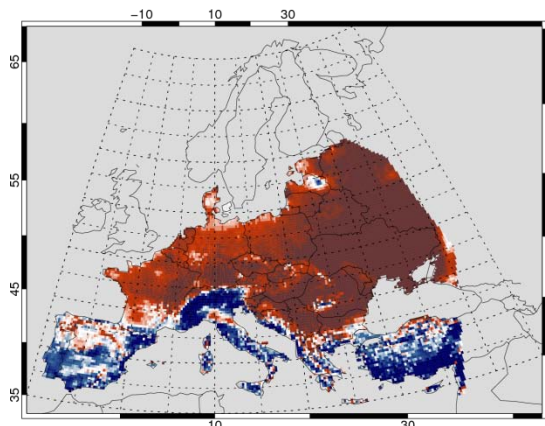


**Figure 6: Winter (DJF) and summer (JJA) biases of the C4IRCA RCM control run between 1961 and 2010 for precipitation amount compared to E-OBS (v4). Left panels show the uncorrected RCM; right panels show the corrected RCM.**

Figures Figure 6 and Figure 7 show the seasonal error characteristics of the selected C4IRCA RCM control simulation over Europe compared to E-OBS (v4) between 1961 and 2010 for precipitation and temperature respectively. For both parameters the uncorrected RCM yields biases throughout continental Europe and for all seasons. For precipitation amount the uncorrected RCM features an orographic bias dependence and thus a more scattered bias structure. In winter (DJF) the model mainly overestimated precipitation amounts

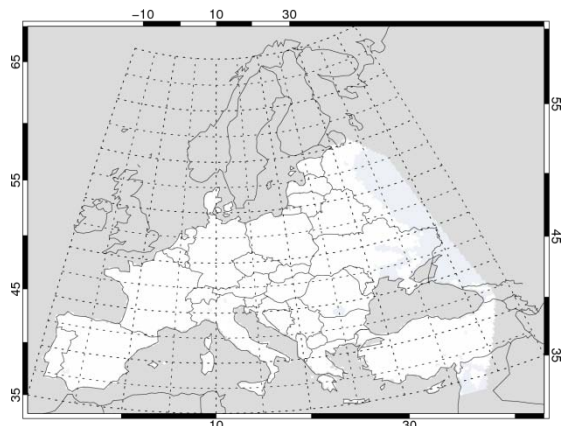
whereas in summer (JJA) the characteristic changes into a strong widespread precipitation underestimation. In autumn (SON) the C4IRCA results in a bi-polar structure with underestimation in the Mediterranean region and overestimation north of the Alpine crest (not shown).

DJF uncorrected



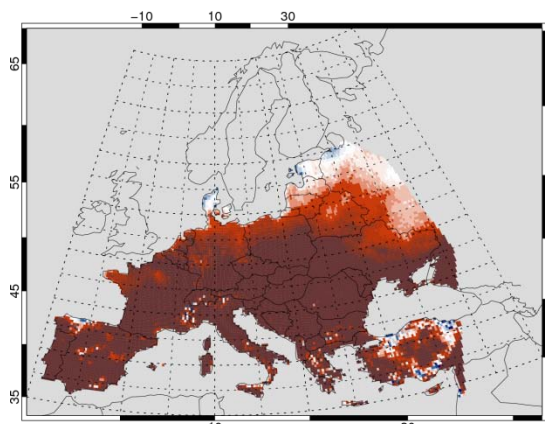
Mean: 0.9 Stand.Dev.: 1.4 Max: 4.8 Min: -6.8

DJF corrected



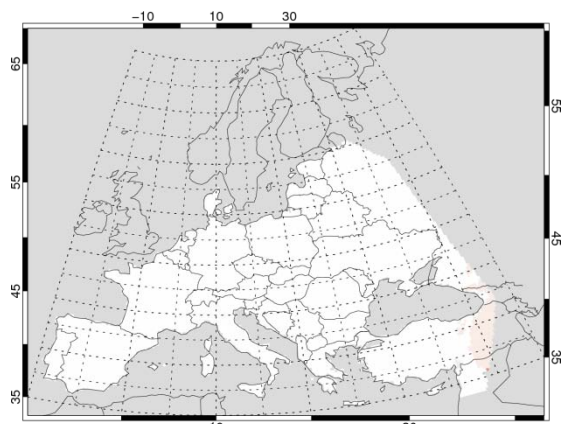
Mean: -0.1 Stand.Dev.: 0.0 Max: 0.1 Min: -0.2

JJA uncorrected



Mean: 2.0 Stand.Dev.: 1.3 Max: 7.9 Min: -2.0

JJA corrected



Mean: 0.0 Stand.Dev.: 0.0 Max: 0.7 Min: -0.4

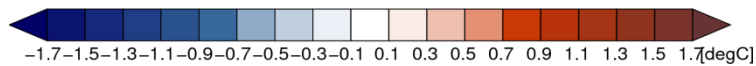


Figure 7: As in Figure 7 but for air temperature.

Concerning temperature, the uncorrected RCM overall features a warm bias, although the Mediterranean region as well as especially Turkey is e.g. strongly cold biased in DJF (compare Figure 7).

After QM, Figures Figure 6 and Figure 7 indicate that the regionally and seasonally varying biases for both precipitation amount and air temperature are in fact completely removed. Only small regions, especially in the most south-eastern parts of the study region show minor remaining biases, as here the underlying E-OBS observations are incomplete. In this example the calibration and validation period are the same, thus this nearly perfect error correction was expected. However, evaluations with cross-validation procedure Themeßl et al. (2011; 2012) and split sample tests (Wilcke et al. 2013) showed that the error correction potential of QM can be quoted by one dimension of the original uncorrected error for the mean as well as for extremes. The corrected time series may however feature stronger remaining errors for single short term periods due to natural variability.

In contrast to mean air temperature and precipitation amount, global radiation and 10 m wind speed are processed differently. In these cases QM cannot be applied as there are no daily observational data yet available for entire continental Europe. Thus, a delta approach is applied. The delta approach represents one common way to deal with model errors in climate change impact studies is the “delta change approach”, also called perturbation method (Déqué 2007; Graham et al., 2007). This method generates climate scenarios by adding the climate change signal (CCS) from a RCM simulation to daily or monthly observations. A CCS is defined as the difference of climatological means (e.g. monthly, seasonal, or annual) between the future (e.g. 2021–2050) and present or past (e.g. 1961–1990) of a climate variable. By taking the difference, systematic model errors are removed as long as they are similar in both periods, but any potential change in temporal variability is removed as well, since variability is inherited from the observations.

As in the case of wind speed the interesting height level for the electricity sector is between 75 and 100 m above ground, at the level of the wind turbines, empirical wind profiles have been used to upscale the 10 m winds to this level. In addition the CCS at 850 hPa was analyzed and compared to the respective 10 m CCS. It was found that the CCS strongly resembled each other in spatial patterns as well as in the overall sign of climate change, but the intensity of the CCS decreased from 850 hPa to 10 m. This, however, is expected due to surface roughness.

## 2.2 Hydrological modeling

The aim of the hydrological modeling is to estimate the impacts of climate change on the discharge characteristics of rivers at a monthly time step within the Greater Alpine Region focusing on Austria and the related changes in the power generation of hydro plants. Four

representative climate simulations from the ENSEMBLES project are chosen, that cover a bandwidth of possible climate changes from hot-dry over moderate to humid-warm based on the emission scenario A1B. A single consistent data set of air temperature and precipitation is available at a horizontal resolution of 25 km for the whole Greater Alpine Region. To simulate river runoff based on this data, an appropriate parsimonious, lumped-parameter rainfall-runoff model was identified, based on the GR2M monthly water-balance model (Makhlouf and Michel, 1994; Mouelhi et al., 2006), and extended by a temperature-based snow model (as proposed by Xu et al., 1996) and potential evapotranspiration (PET) computed based on temperature and extraterrestrial solar radiation (<http://www.cigar-csi.org>) only using the formula proposed by Oudin et al. (2005). Hence, temperature and precipitation are the only input data necessary (extraterrestrial solar radiation exhibits a seasonal variation but this is assumed to remain constant over the years). This model approach uses a spatial, temporal and conceptual lumping, which is believed to be a suitable model structure for the purpose of monthly rainfall-runoff-prediction due to its parsimony and the limited information content of discharge time series (Edijatno et al., 1999; Perrin et al., 2001; Gupta et al., 2005). Processes accounted for are snow accumulation and snow melt, evapotranspiration, soil storage, routing storage, and water exchange with neighboring catchments. The schematic model structure is shown in Figure 8. The four free (to be calibrated) parameters are a critical temperature ( $T_s$ ) below which snowfall begins, a critical temperature ( $T_m$ ) above which snow melt starts, the capacity of the production store ( $X_1$ ) and a water exchange term ( $X_5$ ), which accounts for water flow to neighboring catchments ( $X_5 < 1$ ) or flow from neighboring catchments ( $X_5 > 1$ ).

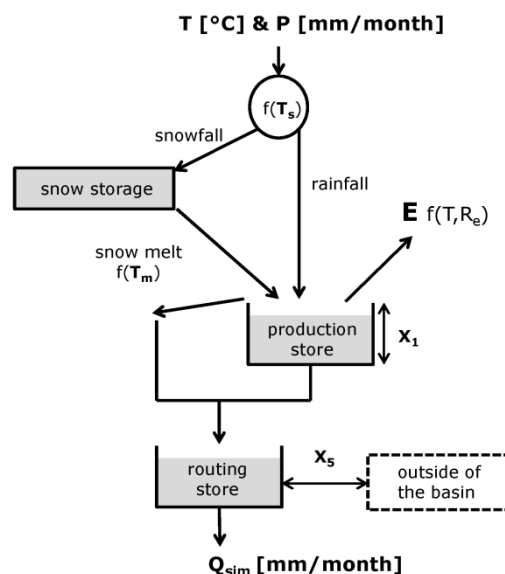


**Figure 8: Model structure of the rainfall-runoff model. The four free model parameters are  $T_s$ ,  $T_M$ ,  $X_1$  and  $X_5$ . Necessary inputs to the model are precipitation and temperature. The free model parameters are calibrated by minimizing the difference between simulated and observed river runoff data.**

Monthly temperature and precipitation (E-OBS observation data) from 1950 to 2010 provided by WEGC-ReLoCLim was used as forcing input for the hydrological modeling. Monthly discharge time series of 10-60 years provided by various organizations such as the “Hydrographische Dienst Steiermark” and the Global Runoff Data Centre (GRDC) (for a complete list see the acknowledgements) for a total of more than 100 gauging stations covering the whole GAR (Figure 9; finally 101 stations in AT, DE, CH, IT, FR and SLO were passed on to WP3) were used to calibrate and validate the model.

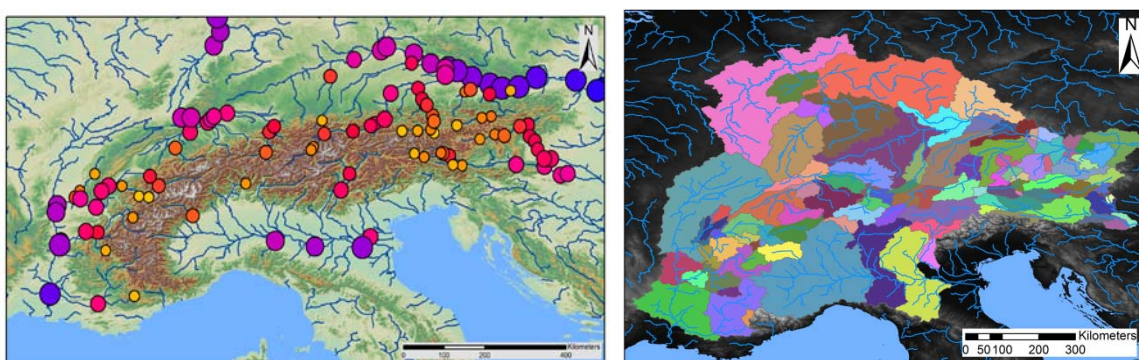


**Figure 9: Runoff measurement stations of the Greater Alpine Region used for the hydrological modeling. Color coding and size of the individual stations is related to the catchment sizes on the left panel; the right shows the individual catchments using a random coloring so that the individual catchments become obvious.**

The individual catchments range in size from less than  $500 \text{ km}^2$  to more than  $100,000 \text{ km}^2$ . The area-weighted mean values of precipitation and temperature for the individual catchments were computed based on the E-OBS data set. The hydrological model was calibrated for each catchment individually using the complete available historical discharge time series. Subcatchments were not considered for the calibration, although results from the (sub-) catchments along a river course were used to check for consistency and plausibility. The model parameters were calibrated using the maximum of the average of three efficiency criteria (in the following simply  $\overline{NSE}$ ), namely the classical Nash-Sutcliffe efficiency criteria (NSE; Nash and Sutcliffe, 1970), the log-transformed and the square-root-transformed Nash-Sutcliffe efficiency criteria. The classical NSE criteria optimizes with an emphasis on the peak flows, the log-transformed NSE with emphasis on the base flow and the square-root-transformed NSE gives an intermediate picture of the overall hydrograph fit (e.g. Oudin et al., 2006). NSE values can vary between 100% (perfect fit) and  $-\infty$  (minus infinity). Negative

values indicate that the average value of the observed time series would be a better estimate than the simulated time series. 0% corresponds to a minimally acceptable performance (Gupta et al., 1999) and values above 50% relate to a satisfactory performance (Moriassi et al., 2007).

To evaluate the predictive capability of the model, the model was calibrated using the first half of the data set and validated using the second half and vice versa (Klemes, 1986). At least one year of warm-up period was assigned to minimize effects of the initial conditions. Moreover, to check for parameter consistency or in a broader sense for the bandwidth of estimated river runoff due to different equally acceptable parameter sets (principle of equifinality; Beven, 1993); the efficiency criteria were applied individually (which will be discussed in more detail in section 3.2.3). As such, model validation was based on different efficiency criteria (multi-objective approach; trade-off in single efficiency criteria to have an overall consistency; the “closeness” of simulated and observed stream flow; Krause et al., 2005), visual inspections of the hydrographs, and split sample tests. In addition, the simulations per gauging station were compared to each other along a river course and changes in model parameters from one to another gauging station were checked for consistency and plausibility. If the model was able to reproduce the observed discharge time series for all these tests in an acceptable manner, it is believed to be suitable to compute future runoffs.

The calibrated and validated hydrological models for the individual stations along the various rivers were then used with the four selected climate scenarios as input to simulate runoff for the two periods 2011-2030 and 2031-2050. Using the predicted area-weighted average temperature and precipitation data of the individual catchment, an estimated runoff under the conditions proposed by the respective climate change scenario is provided. The comparison of the predicted future mean monthly runoff with runoff simulated for the reference period 1961-1990 yields the expected change in monthly runoff for each of the 4 climate change scenarios. For each of the four climate scenarios and for each catchment analyzed, the mean monthly changes in runoff and the related standard deviations were passed on to WP3 and the hydropower modeling.

For the run-of-river hydro plants which are not necessarily located next to the gauging stations (or vice versa), a correction for the different catchment sizes between measurement station and power plant were applied. Moreover, for power plants in Austria intra-monthly changes were taken into consideration. Not only was the mean monthly change in runoff taken in to account, but also the standard deviation (“sigma”). It is assumed that a change in the shape of the flow duration curve on a daily basis can be estimated by the change in the

## EL.ADAPT

mean and the standard deviation of the monthly runoff data. This is an approach that allows taking possible changes in the flow duration curves (steeper or flatter) into account, which is of interest for the discharge capacity of run-of-river hydro plants. At stations outside Austria only the changes in mean monthly runoff of the nearest measurement station was used. For a more detailed description of the hydro power modeling see section 2.4.2).

Besides estimating changes in river runoff for run-of-river hydro plants, the influence of climate change related to the natural inflow to storage reservoirs of storage power plants was considered in a different, more simplified way. The hydrological model applied for run-of-river plants is not applicable for this purpose. On the one hand, the climatic forcing parameters (temperature and precipitation) were available for the complete GAR only on a coarse grid (25 km horizontal resolution) which is not representative for such small catchments feeding individual storage power plants at high elevations. On the other hand, a similar hydrological model as used for the computation of river runoff only yields reliable data, if historical rates of inflow would be known to calibrate the model. This data were not at our disposal. In addition, inflow from nearby glaciers might become relevant in these settings. An additional glacier model (or module) would be necessary to simulate runoff from glaciers due to changes in precipitation and temperature including an existing glacier inventory. Because of the limited data and resources available a simple approach assuming that the change of the climatic water balance (precipitation minus potential evapotranspiration) provides a rough estimate of the expected change of the natural inflow to the storage power plants was employed.

The climatic water balance was computed for four subregions of the GAR located above 1000 m a.s.l. (Figure 10). These subregions were based on a cluster analysis of historical precipitation data by Leuprecht and Gobiet (2010). Area-weighted averages of monthly precipitation minus area-weighted averages in potential evapotranspiration (based on temperature and the same formula of Oudin et al. (2005) as used in the hydrological model presented above) were computed. Then, the annual climatic water balance was computed as the annual difference between precipitation and PET. Average annual values of the climatic water balance for the time periods 1961-1990, 2011-2030 and 2031-2050 were finally compared to each other for the 4 subregions and the 4 climate scenarios to get an idea of possible changes for energy production of storage power plants with natural inflow (basin inflow). This approach has to be seen as a rough estimate to assess the change in basin inflow at elevations above 1000 m a.s.l. and moreover to get an idea of how different scenarios might influence the basin inflow to individual storage power plants. Each of the storage power plants considered will either increase or decrease its energy production related to natural inflow based on the region they are located in and the general change in

the climatic water balance computed for that region and a specific scenario. These changes are included in the further model steps of WP3.

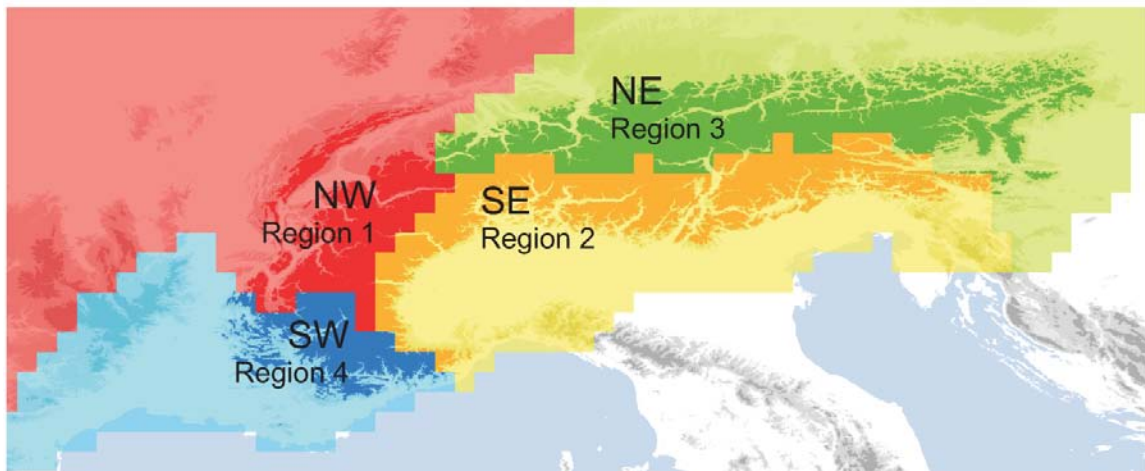


Figure 10: The 4 subregions of the Alpine region above 1000 m a.s.l. in the dark colors to compute an area-weighted climatic water balance for the different climate scenarios.

### 2.3 Households' electricity demand modeling

For Europe, recent studies have provided an overview on the likely impacts of temperature change on electricity use for heating and cooling using econometric regression models (Pilli-Sihvola et al. 2010; Eskeland and Mideksa 2010). The present study seeks to further contribute to this issue by (1) using four different spatially and temporally highly resolved climate scenarios, which helps to provide impacts for a range of possible temperature changes, (2) doing calculations for altogether 16 Continental European countries (AT, BE, BG, CZ, FR, DE, HU, IT, NL, PL, PT, RO, SK, SI, ES, HR), which enables to study different regional response patterns, and (3) working with daily electricity data, which allows to examine the non-linear relationship between temperature and electricity demand by the means of advanced statistical techniques such as smooth transition regression (STR) models, recently also applied in Moral-Carcedo and Vicéns-Otero (2005) and Bessec and Fouquau (2008).

This combined use of sophisticated regression models and high frequency load data allows to study heating and cooling electricity demand in better detail than approaches which determine temperature impacts by regressing cumulative heating and cooling degree days (HDD and CDD) on monthly loads. On the one hand, STR allows to model the slow transition from temperatures where heating is needed to temperatures where cooling is needed, rather

than arbitrarily choosing one exact threshold value for HDD and CDD. On the other hand, the use of daily data makes it possible to describe well-observed cooling effects for moderate-temperated countries such as Austria or Germany, while when using monthly data more pronounced effects like summer holidays may superimpose comparatively small but not negligible cooling effects for these countries.

From a methodological point of view we proceed in the following way: First, we create national temperature indices, which summarize both observational meteorological data (EOBS - Haylock et al. 2008) as well as climate scenario data (ENSEMBLES - van der Linden and Mitchell 2009) in such a way, that the population distribution within a country is accounted for. For that we use both Corine Land Cover data (EEA 2010) and NUTS-3 population data (Eurostat 2011).

Second, we correct daily national electricity load for non-climatic effects, such as the effects of public holidays and bridging days, Christmas time and summer holidays, weekdays as well as variations in economic activity. Overall, the effectiveness of these different ways to correct the original load data for the purpose of estimating load-temperature models strongly differs between countries. For Austria the smoothing of summer holiday effects has the largest influence on the load data and is certainly fruitful for estimating the respective load-temperature relationship. For other countries however, in particular those hit hardest by the financial and economic crisis in 2009 and 2010, the industrial production index and additional annual dummies are necessary to correct for these non-temperature related changes in load levels. Therefore, while it is not possible to have one single procedure for all countries to correct for different non-temperature related effects on load, it seems to be a good idea to apply the statistical modeling of the load-temperature relationship to all of the different datasets obtained from smoothing and correcting loads, and finally let a statistical criterion decide on the best model.

Third, we estimate the statistical relationship between temperature indices and the corrected load and estimate the effects of changing climate conditions. To estimate the statistical relationship we use the so called Smoothed Transition Regression Models (STR). As literature (Moral-Carcedo and Vicéns-Otero 2005) shows the transition from cooling to heating is a gradual not a sudden process. Therefore, it makes sense to model the transition accordingly. In our case this means that the corrected load data  $y_t$  is described via two straight lines modeling the heating and cooling respectively, and then multiplied with a transition function  $F(TMP_t, c, \gamma)$ .

$$y_t = (\alpha_1 + \beta_1 TMP_t)(1 - F(TMP_t, c, \gamma)) + (\alpha_2 + \beta_2 TMP_t)F(TMP_t, c, \gamma) + \varepsilon_t \quad (4)$$

In (4)  $TMP_t$  stands for the temperature at time  $t$  and  $\varepsilon_t$  is an independent and identically distributed random variable with expectation  $\mathbb{E}[\varepsilon_t] = 0$  and variance  $\text{var}(\varepsilon_t) = \sigma^2$ , while  $\bar{\alpha}$ ,  $\bar{\beta}$ ,  $\gamma$  and  $c$  describe the parameters which will be estimated thereafter. Moreover the transition function is in our work represented by a probability distribution function to be precise the logistic distribution function

$$F(TMP_t, c, \gamma) = \frac{1}{1 + e^{-\gamma(TMP_t - c)}}.$$

The parameter  $c$  characterizes the threshold where the change of state occurs, while the parameter  $\gamma$  describes the pace at which the transition takes place.

To estimate the parameters in (4) we use a Nonlinear-least-squares approach, which requires the computation of starting values. For this a grid search is used, which means that for each value of  $c$  in the sequence of natural numbers from 9 to 20 and each value of  $\gamma$  in the sequence from 0.5 to 2.5 with step size 0.5 the transition function can be computed and the parameters  $\bar{\alpha}$  and  $\bar{\beta}$  can be estimated via a linear regression model. In this way we get for each  $c$  and  $\gamma$  estimates for the  $\alpha_i$ 's and  $\beta_i$ 's in (4). Thereafter, the estimate for the mean depending on the temperature is calculated. In a next step the sum of squares of the difference of the load-data and the calculated mean for each given  $c$  and  $\gamma$  is computed

$$SQ_{c,\gamma} = \sum_{t=1}^n (y_t - \mu_t)^2.$$

Now the starting values for the Nonlinear-least-squares-estimation are those parameters who compute the least sum of squares. With the computed starting values the estimation of the model via Nonlinear-least-squares represents no further problem. We use the nls-function, which is implemented in R, see R Development Core Team (2011), and is based on the Gauss-Newton-algorithm. Another possibility would have been to assume that the  $\varepsilon_t$  in (4) are normally distributed and estimate the model via a Maximum-Likelihood-estimation. But this approach would in the case of normally distributed residuals lead to the same solution as the minimization of the sum of squares.

In Figure 11 the process of model estimation is shown at the Austrian example. On the x- and y-axis of the plot the daily mean temperature and the daily filtered electricity load can be observed. Therefore, each black dot corresponds to one data point and the green and red lines are in accordance with the different steps in the process of model estimation. While the green line represents an interim stage (result from the grid search), the red one stands for the final model fit. While a heating effect is very distinct for Austria in Figure 11, the cooling

effect is comparatively small. The transition from heating to cooling takes place around 17°C and is a gradual not a sudden one.

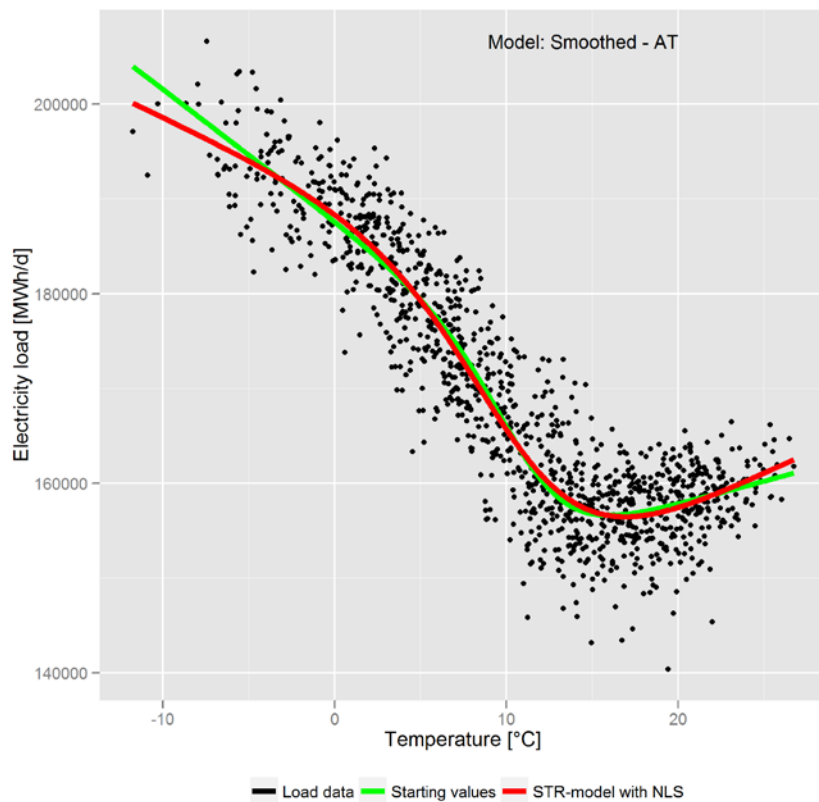


**Figure 11: Temperature impacts on electricity load in Austria on working days.**

In order to analytically separate the impacts of temperature change from socio-economic developments, we did calculations under the strong assumption that consumers will react to temperature changes in the future in the same way as they currently (period 2006-10) do. This assumption is helpful, as the extent of future heating and cooling electricity consumption will heavily depend on uncertain future energy policy and consumer behavior. However, the assumption is relaxed in a further step of modeling, see 3.3.2.

## 2.4 Electricity sector model ATLANTIS

ATLANTIS is a techno-economic model of the electricity industry in Continental Europe (former area of the UCTE) – a synchronous area with a net installed capacity of about 750 GW by the end of 2011 and annual consumption of approximately 2,600 TWh in 2011 (ENTSO-E, 2012). A major part of the scenario model is a database of the most important facilities and companies in the investigated area.

Based on the comprehensive database, ATLANTIS is a simulation model which is close to reality in technical matters but is also able to give an explanation of the economic behavior of electricity markets. The technical part of the model includes all necessary elements of the physical system like the synchronous transmission grid (400 kV and 220 kV levels), about 20.000 individual power plants as well as demand of consumers geographically downscaled to grid nodes. The economic part of the model covers electricity trade by using market models like net transfer capacity (NTC) based zonal pricing and a European-wide market coupling between states, as intended by the European Union. Major European power producers are described by simplified balance sheets and income statements.

Figure 12 shows the flow chart of a scenario simulation. Based on the predefined scenario, the calculations are performed on an annual and, respectively, monthly base. Every month is furthermore divided into a number of peak and off-peak periods. The monthly load duration curve is discretized by the means of the corresponding periods. At the beginning of every simulated year, the calculation starts with a system adequacy check for winter and summer peak load, which also considers physical load flow restrictions. The physical load flow is calculated using a DC-OPF (DC optimal power flow) algorithm. In this initial step, the model proves whether the simulated electricity system is able to handle the annual peak load hour. If not, the model automatically builds a new gas-fired CHP plant to cover the missing generation capacities. This step is repeated until the amount of generation capacities is sufficient, and no lines are overloaded.

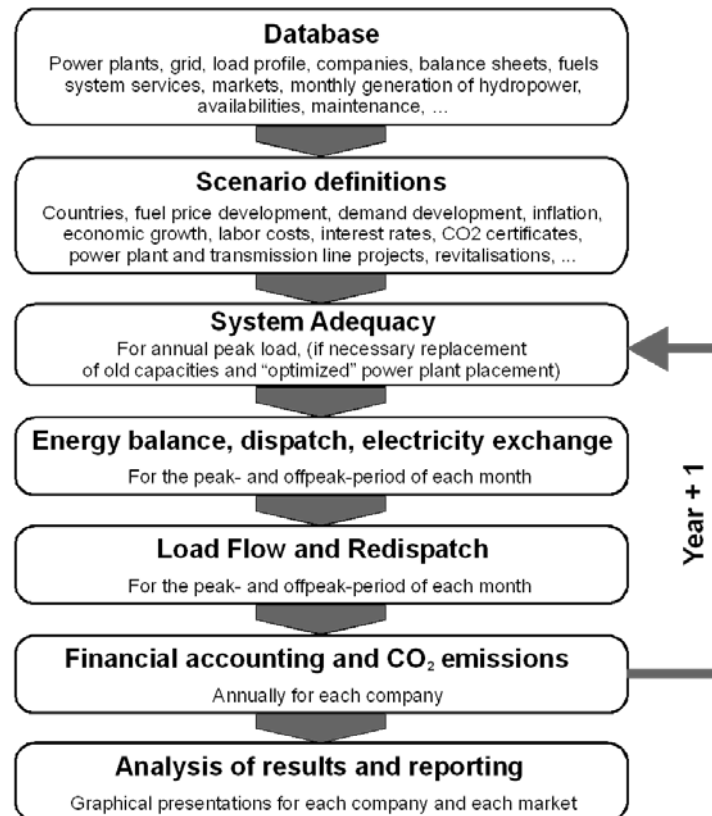


**Figure 12: Flow chart of the ATLANTIS scenario model (Gutsch et al., 2010).**

In the next steps, the dispatch of power plants is calculated by minimizing the total generation costs, using different market models. More precisely, a zonal pricing algorithm under consideration of net transfer capacities (NTCs) at cross border lines is applied, followed by a DC-OPF calculation to proof whether the market results can be realized without violating the (n-1) criterion. In case of a violation, power plants are re-dispatched to resolve the limiting congestions, still trying to keep the total generation costs as close to the optimal dispatch as possible.

Fluctuating generation like hydro power or wind power is considered by the long-term average generation in the particular month. A power exchange where the modeled companies trade generation surpluses is calculated parallel to the dispatch. When the utilization of the power plant park is determined, fuel demand and CO<sub>2</sub> emissions of each period are calculated.

Finally, the required retail price of electricity for each country is calculated considering “second best” regulation. The dynamic simulation of different scenarios over time shows the effects of changing climatic conditions on power production, electricity exchange and network utilization.

For more information on the model ATLANTIS and recent developments, see Stigler et al. (2012), Gutschi et al. (2010), Gutschi & Bachhiesl (2009) or Huber et al. (2009).

#### **2.4.1 Model improvements within the project focus**

To answer the research questions asked within EL.ADAPT, certain model adaptations and improvements are needed. This chapter is intended to offer an overview of the improvements made.

##### Investment and operation costs

In order to estimate future electricity generation costs of a power plant, it is necessary to take technological progress in terms of cost reduction into consideration. Technological progress takes place in various fields and sectors.

It is necessary to break down overnight (investment) costs<sup>2</sup> (OC) at a component level for each power plant technology as well as transmission/distribution grid system, in order to determine necessary values within the social accounting matrix (SAM, see section 0) correctly. Within the SAM only three aggregated sectors – construction and real estate (CRE), electronic equipment and machinery (MPE) and other services and utilities (SERV) – will be considered in terms of investment costs of the electricity sector. Therefore, the components were reassigned to one of those sectors in a second step.

Costs for operation and maintenance (O&M) for both technologies – power plants as well as transmission/distribution grid systems – have to be broken down at a similar level. Again O&M need to be subdivided into the three considered sectors: CRE, MPE and SERV.

##### Technological progress and experience curves

Technological progress takes place in various fields. Firstly, a decrease in investments costs caused by an increased production can be illustrated and forecasted with experience curves. Secondly, an improvement in power plant efficiency levels reduces primary energy demand and also leads to economical as well as environmental benefits.

Experience curves describe a shift in overnight costs of a specific power plant technology over time as production increases (in terms of building units of this specific technology) and the costs of the components decrease. Technologies pass through several development phases according to the level of experience gained from already installed power plants.

The final implementation of this kind of technological learning in ATLANTIS is shown in Figure 13 for a selection of power plant technologies. The horizontal axis represents the total installed cumulative capacity of a power plant technology in GW, whereas total overnight costs (in € per MW) are applied to the vertical axis. To illustrate the different development

---

<sup>2</sup> Usually the construction of power plants and transmission lines takes a long time, especially if approval procedures or planning phases - already incurring costs - are taken into consideration. As a simplification, the total costs are added up and presented as overnight costs, assuming that the construction was completed „over night“.

phases of a technology, a logarithmic representation for both axes was chosen. Photovoltaics, solar thermal (CSP) and offshore wind generation will pass through all three stages within the next years. Already mature technologies like (large) hydro power plants or combined cycle power plants show hardly any reduction in costs due to their very low learning rates. The different learning phases are illustrated by the example of photovoltaics; period 2 is represented by the red dashed regression line, period 3 by the red dashed and dotted regression line.

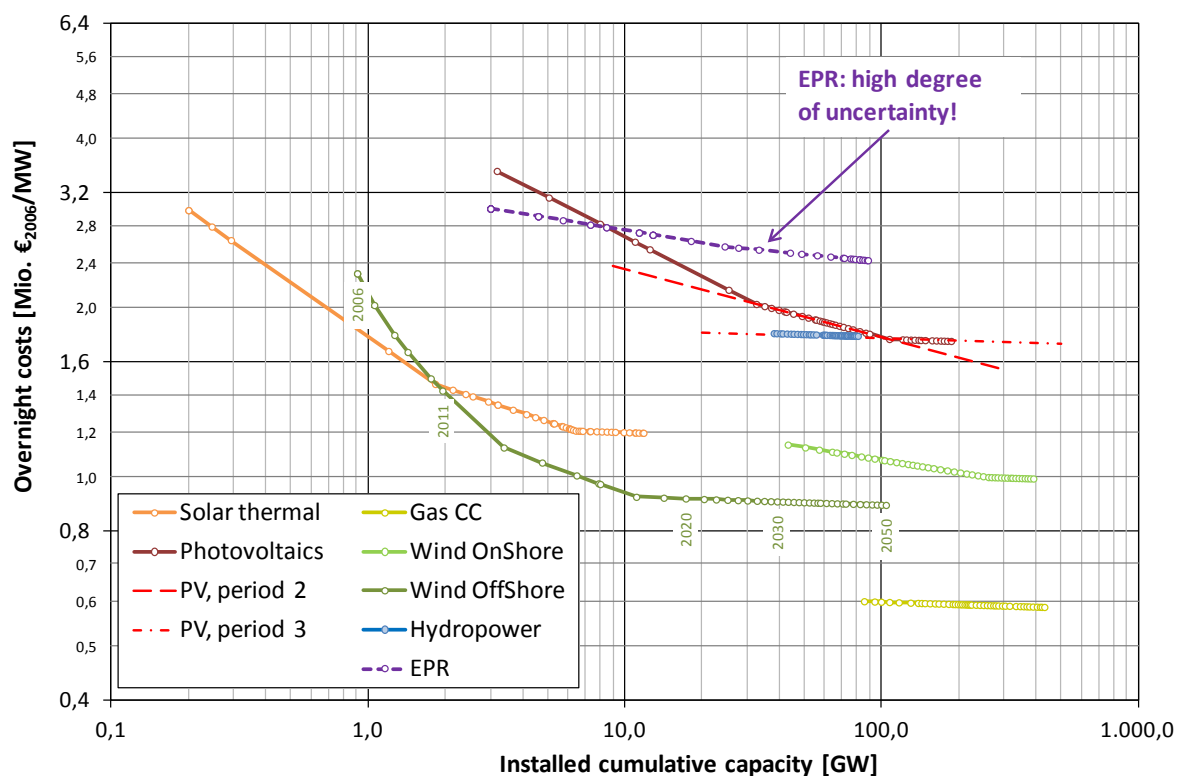
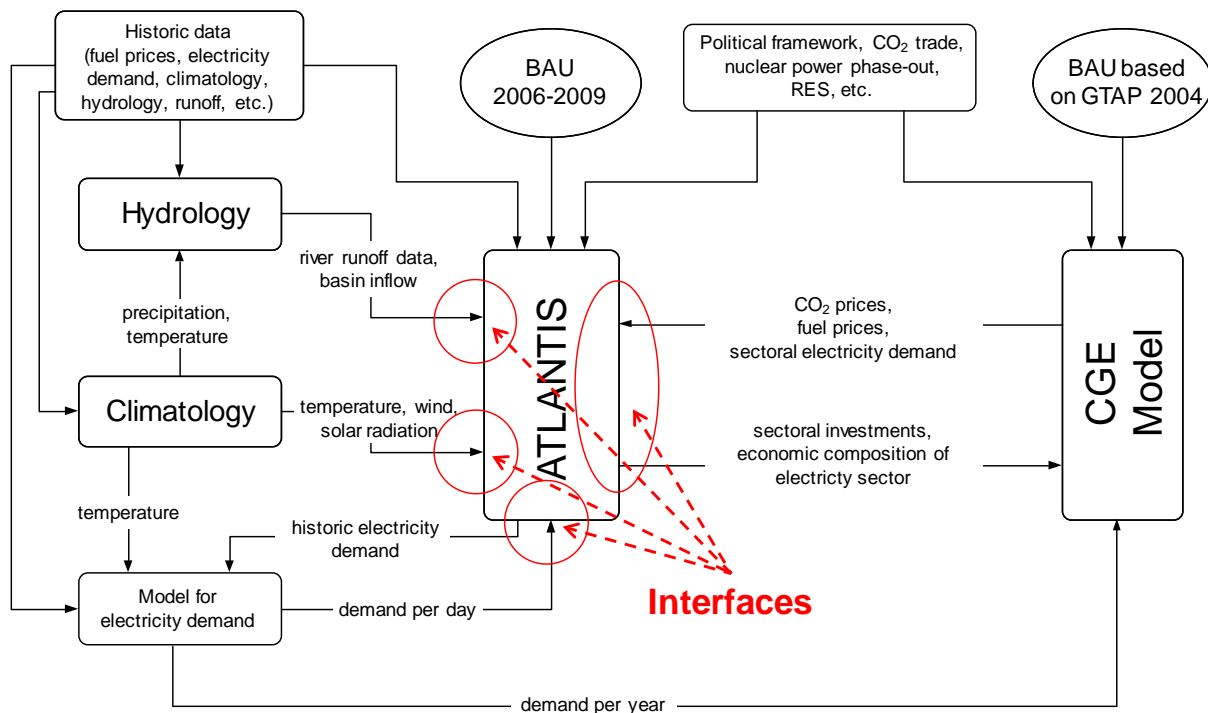


Figure 13: Technological learning for a selection of power plant technologies (DoE, 2010)

### 2.4.2 Implementation of interfaces to other models

In order to meet some new requirements caused by the EL.ADAPT project, ATLANTIS had to be modified and extended properly. Figure 14 shows all four defined interfaces between ATLANTIS and the models of climatology and hydrology, electricity demand and the multi-regional, multi-sectoral general equilibrium model (computable general equilibrium: CGE).



**Figure 14: New ATLANTIS interfaces introduced within EL.ADAPT**

*Interfaces with climate models and hydro model (“model chain”)*

Climate and hydro models provide detailed information about the changes in renewable energy power plants, in particular for hydro, photovoltaics as well as wind power plants. In order to estimate the impacts caused by the climate change, all simulations have been run until 2050. In addition, the simulation period has been subdivided into two climate change periods (2011-2030, 2031-2050), in which each climate change period is affected by different climate change signals. Hydro power plants are affected by a change in the water supply (river runoff, basin inflow), photovoltaic power plants due to a change in global radiation and wind power plants due to a change in local wind speed.

To feed the climate change signals into ATLANTIS, conversion models<sup>3</sup> were used to derive changes in standard capacity and monthly characteristics from climate and runoff change signals. In the case of hydro power in Austria, an existing, more detailed model was used, cf. Schüppel (2010). The model uses historic runoff data to calculate hydro power generation on a daily basis for a single power plant. Under consideration of known technical parameters, e.g. hydraulic head, maximum inflow, maximum capacity and standard capacity, the model is calibrated by variation of the efficiency factor. For EL.ADAPT, the model was enhanced to support a catchment area correction included in the calibration process that allows considering differences between catchment areas of the gauge and the power plant (see also chapter 3.4.4.1). Furthermore the power plant model was adopted to handle the runoff change signals of the hydrological model.

<sup>3</sup> These models are not part of the ATLANTIS model, but developed separately.

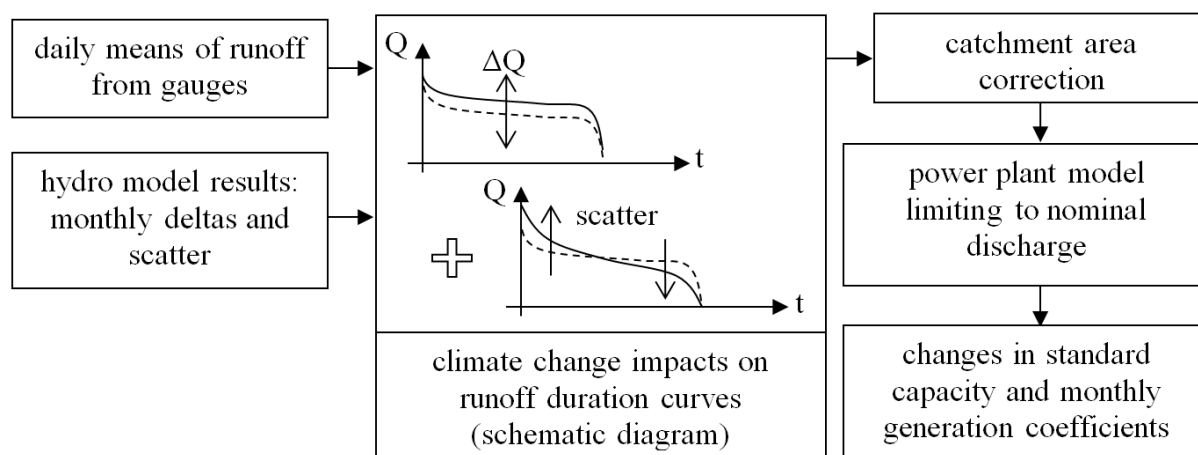


**Figure 15: Flow chart of the hydro power model chain for hydro power plants in Austria**

Figure 15 shows the complete flow chart starting with results from the hydro model. In the second step, these results are applied on historic runoff data (duration curves), which are then fed into the power plant model including the catchment area correction. The resulting changes in standard capacity and generation coefficients are directly imported into ATLANTIS. For hydro power plants in other countries (Italy, Switzerland, Germany and France), a less detailed linear approach was used, mapping the monthly change signals of runoff directly to standard capacities. For all hydro power plants, the corresponding gauge was assigned by using geographical information system (GIS) software.

Regarding photovoltaics, it was shown that a linear approach to model electricity generation will be sufficient for long-term studies, cf. Pattis (2012). Thus, climate change signals of global radiation are directly mapped to the standard capacity of photovoltaics, concerning the location of the generation units and the average climate change signal at NUTS-2 level. For wind power, a similar, but nonlinear approach was used. Due to the fact that monthly means of wind speed are insufficient for a more detailed model, an empirical approach was used to estimate standard capacities from average wind speed.

$$W_{el} \approx w \cdot \bar{v}^c$$

where:

$W_{el}$	monthly standard capacity
$w$	weighting factor
$\bar{v}$	monthly average of wind speed
$c$	constant

By using known parameters like the current standard capacity (without considering climate change), historical average wind speeds and historical feed-in data of wind turbines, the empirical parameters  $w$  and  $c$  can be found and wind power characteristics can be derived on NUTS-2 level.

The impacts of these applied climate change signals result in a change in production of a specific power plant. Within the simulation process in ATLANTIS, three types of changes

need to be considered, in order to provide accurate simulation results. Firstly, the standard capacity of these power plant technologies are changing due to climate change and need to be applied for both time periods, 2011-2030 and 2031-2050. Secondly, due to modified environmental conditions caused by climate change, production in several months of a power plant may slightly shift<sup>4</sup>. As a result of that, modified monthly production factors need to be applied as well. Finally, at the end of their operational period, hydro power plants will be renewed (refurbished) automatically. These refurbishments include an increase in energy capacity of 5 % of that specific power plant and therefore need to be considered during the appliance of the modified standard capacities.

#### Interface with the electricity demand model

Changes in electricity demand are caused by an increase in global temperature. An appropriate model approach calculates these changes in electricity demand caused by modified temperatures. These daily demand change values need to be further processed and integrated into the simulation process of ATLANTIS. Depending on the type of simulation (coupled with/uncoupled from the CGE model) ATLANTIS expects either monthly shifts or annual changes in terms of electricity demand.

#### Interface with the CGE model ("model coupling")

For information on the interface with the CGE model, please refer to chapter 2.6.

## **2.5 Multi-country multi-sector modeling**

In order to analyze the economic effects of changing climatic conditions on the electricity sector a static, multi-region, multi-sector computable general equilibrium (CGE) model is developed. Methodologically, the model is based on Bednar-Friedl et al. (2012) and contributes to the literature on multi-sector, multi-regional CGE models analyzing climate and energy policy (e.g. Babiker and Rutherford 2005; Paltsev 2001; Böhringer 2000).

On a regional level the focus lies on continental Europe, thus aggregates of 9 European regions and further 9 regions representing the rest of the world (ROW) are constructed (see Table 16 in the Annex). The regional aggregation within Europe reflects similarities in the electricity production and networks, similarities in their economic performance and their vulnerability and exposure to climate change. The rest of the world is aggregated in major world regions according to regional proximity, stage of development and their relevance for energy markets.

---

<sup>4</sup> i.e. the production of a hydro power plant decreases in April, but increases in March due to a change in precipitation and snowmelt

On a sectoral level, we differentiate 19 sectors, consisting of the electricity sector itself (ELY), representing production, collection and distribution of electricity, additional six electricity intensive sectors (e.g. pulp and paper), and 11 non electricity intensive sectors which are differentiated according to their importance as intermediate suppliers for ELY or other sectors in the economy (Table 6). Furthermore it's crucial to separate sectors which are using natural resources, as their production function differs from non-resource using sectors. Table 6 is summarizing all economic sectors.

**Table 6: List of economic sectors**

	Aggregated Sectors	Model Code
1	Electricity	ELY
	Electricity intensive sectors	EIS
2	Manufacture of paper products and publishing	PPP
3	chemical industry	CRP
4	manufacture of other non-metallic mineral products	NMM
5	Other mining	OMN
6	manufacture of basic iron and steel and casting	I_S
7	precious and non-ferrous metals	NFM
	Non-Electricity intensive industries	NEIS
8	Coal	COA
9	Crude Oil	OIL
10	Refined oil products	P_C
11	Natural Gas	GAS
12	Transport	TRN
13	Agriculture	AGRI
14	Forestry and Fishery	FOF
15	Construction, real estate	CRE
16	Machinery, fabricated metal products	MPE
17	Other services and utilities	SERV
18	Capital Goods	CGDS
19	Other non-electricity intensive industries (textiles, food, tourism etc.)	NEII

Figure 16 gives a diagrammatic overview of the CGE model structure (for more details see Bednar-Friedl et. al. 2012). The so called “Regional household”, which is endowed with labour ( $L_r$ ), capital ( $K_r$ ) and natural resources ( $R_r$ ), represents final demand of all households (private and public) in each region ( $r$ ). Within a region labour, capital and natural resources are mobile among economic sectors ( $i$ ), but immobile between regions. All of the regional household’s endowments are used for domestic production ( $Y_{ir}$ ), with different production technologies for (i) resource extracting sectors, (ii) process emission related sectors, (iii) the electricity sector and (iv) other sectors. If not stated otherwise all production activities are constant multilevel nested elasticity of substitution (CES) production functions and do not differ across regions.

In our model production induced emissions can be classified into (i) emissions through combustion ( $CO_2$ ) and (ii) process emissions ( $ProcessCO_2$ ). The former are produced as a fixed share of fossil fuel input in production. This share varies across used fossil inputs depending on its carbon content. Next to emissions due to combustion, process emissions are arising in three sectors (I\_S, NMM and CRP), thus at the top level of their production function process emissions (regionally and sectorally differentiated) are added with an elasticity of zero (see Figure 71 in the Annex).

For regional aggregates of continental Europe (AUT, WEU, GERL, ITA, ESP, EEU) the production structure of ELY is treated differently than all other sectors, as its technology is given exogenously by ATLANTIS (see section 2.4). The ELY production sector of the linking regions (LR, which are GERL, AUT, EEU, ITA, ESP and WEU) is constructed as a top level Leontief production function (fixed input shares). In all other regions the ELY sector has the same structure as described in Figure 71 (except for the process emissions on the first level of the nesting).

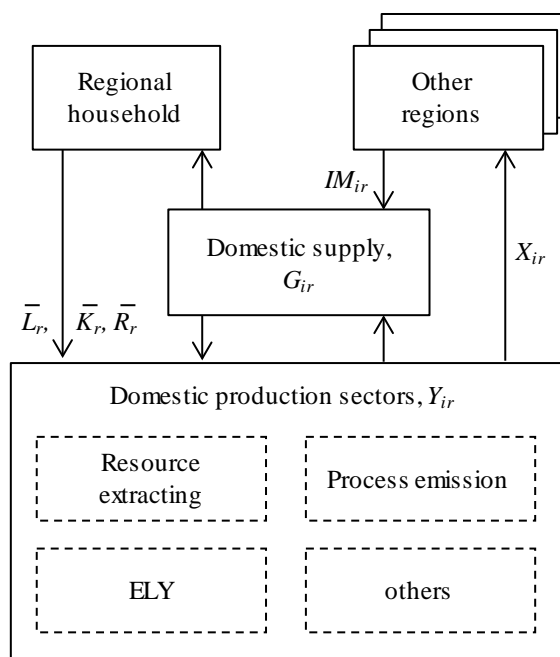


**Figure 16: Diagrammatic overview of the CGE model**

According to Figure 16, domestic production ( $Y_{ir}$ ) is either used in its home country or is exported to other regions ( $X_{ir}$ ) to satisfy final and intermediate demand. According to Armington (1969) commodities produced in different regions are not perfectly substitutable, thus every region treats its imports and goods ( $IM_{ir}$ ) from domestic production ( $Y_{ir}$ ) differently. The corresponding Armington elasticities ( $te/a$ ) specify the degree of substitutability between imports and domestically produced commodities. Then, the “Armington aggregate” ( $G_{ir}$ ) corresponds to actual domestic supply, which is used either as intermediate production input or as consumption good of private and public households. Furthermore regarding international trade, all imports per region (i.e. all exports to this specific region) are traded off at a given – sectorally differentiated – elasticity of substitution. Regarding final demand, the regional household receives factor income, which states the constraint for utility maximization by consuming goods and services. Consumption of private households is modeled as a nested CES function trading off between material consumption goods and an energy bundle, whereas consumption of public goods is implemented as a top level Leontief function.

Another important feature of the CGE model is the implementation of climate policy. For the purpose of our research we implement binding CO<sub>2</sub> targets for all member-regions of the EU (the targets differ by region). The remaining European and world regions do not experience climate policy targets. Furthermore, in terms of the EU, we allow trade of CO<sub>2</sub> emission permits on a single market, with a resulting price for CO<sub>2</sub> emission permits. Since CO<sub>2</sub> can be traded on the EU-wide permit market regions with less carbon-intensive production (CO<sub>2</sub>

emissions are below the region-specific target level) are able to sell their permits and hence gain revenues.

### 2.5.1 Model calibration

In principal, the CGE model is calibrated to the Global Trade Analysis Project database, GTAP7, for the reference year 2004. This database contains bilateral trade information, transport and production linkages for 113 regions and 57 commodities in US Dollar. In order to account for the characteristics of the electricity sector in Continental Europe, the CGE model deviates from the GTAP 7 database in several ways because there are limitations: Firstly, the expenditure structure of the electricity sector does not depict reality in European regions well. Secondly, for global consistency reasons (among all 133 regions), import and export flows of ELY in GTAP7 do not reflect natural conditions and boundaries (e.g. Europe imports ELY from Australia and China). We therefore replaced expenditure data of ELY in Continental Europe regions by data from ATLANTIS; moreover, we used data from EUROSTAT (2012) to adjust and correct ELYs' trade relations. To ensure balanced social accounting matrices for the affected regions, we used a balancing routine (based on Robinson et al. 2001) to incorporate the modified production structure as well as the updated trade-flow for the electricity sector. The incorporation of these data was also necessary to ensure data consistency between the CGE model and the electricity sector model ATLANTIS.

## 2.6 Iterative coupling of CGE model and ATLANTIS

In order to ensure consistency between ATLANTIS and the CGE model, we iteratively link both models in 5-year intervals. For each time step we carry out two iterations where ATLANTIS provides detailed information on the cost and structure of power generation in the various European regions, while the CGE model provides macro indicators for ATLANTIS, namely economy wide electricity demand, fossil fuel prices and the CO<sub>2</sub> price. As above mentioned, in the CGE model the production technology of ELY is exogenously given by ATLANTIS. Thus, the CGE model employs a top level Leontief cost function (fixed input shares from ATLANTIS) for ELY and is given by:

$$C_{ELY,r} = \left( \sum_j \alpha_{ELY,j,r}^Y (p_{j,r}^G (1 + \bar{t}_{j,r}^G)) + \sum_f \alpha_{ELY,f,r}^Y (p_{f,r}^F (1 + \bar{t}_{f,r}^F)) \right) Y_{ELY,r}$$

where:

$j$  intermediate input  
 $f$  primary factors (capital and labor)

## EL.ADAPT

$r$	region
$p_{r,j}^G$	price of intermediate input $j$ in region $r$
$p_{f,r}^F$	price of factor $f$ in region $r$
$\bar{t}_{j,r}$	tax rate on commodity $j$ in region $r$
$\bar{\alpha}_{j,r}$	share of production input $j$ in region $r$
$Y$	activity level of sector
$C$	production costs

In particular, ATLANTIS provides the value share of each intermediate input  $j$   $\alpha_{ELY,j,r}^Y$  as well as of each factor  $\alpha_{ELY,f,r}^Y$  in the production of ELY for all linking regions in  $r$ . Acknowledging the fact that electricity production is changing over time, input values change accordingly for each 5-year time-step; again derived from ATLANTIS. Thus it is possible to include the exogenously given technology shift, depending on the regarded point in time and climate policy scenario. The CGE model also accounts for investments in the ELY sector in order to ensure capacity and production volume of certain technologies, mainly due to expansion of renewable energy sources.

To be able to link the CGE model with ATLANTIS, a variety of new functions had to be introduced in ATLANTIS. Before working on EL.ADAPT, the implementation of ATLANTIS was a “one shot” simulation model, starting with its base year 2006 and running continuously until the simulation finishes the specified final year. Due to data exchange and the need of standby time while the CGE model calculates its results, ATLANTIS had to be enhanced to support interrupts and continuations as well as (automated) restarts of simulations at a specified year later than the base year.

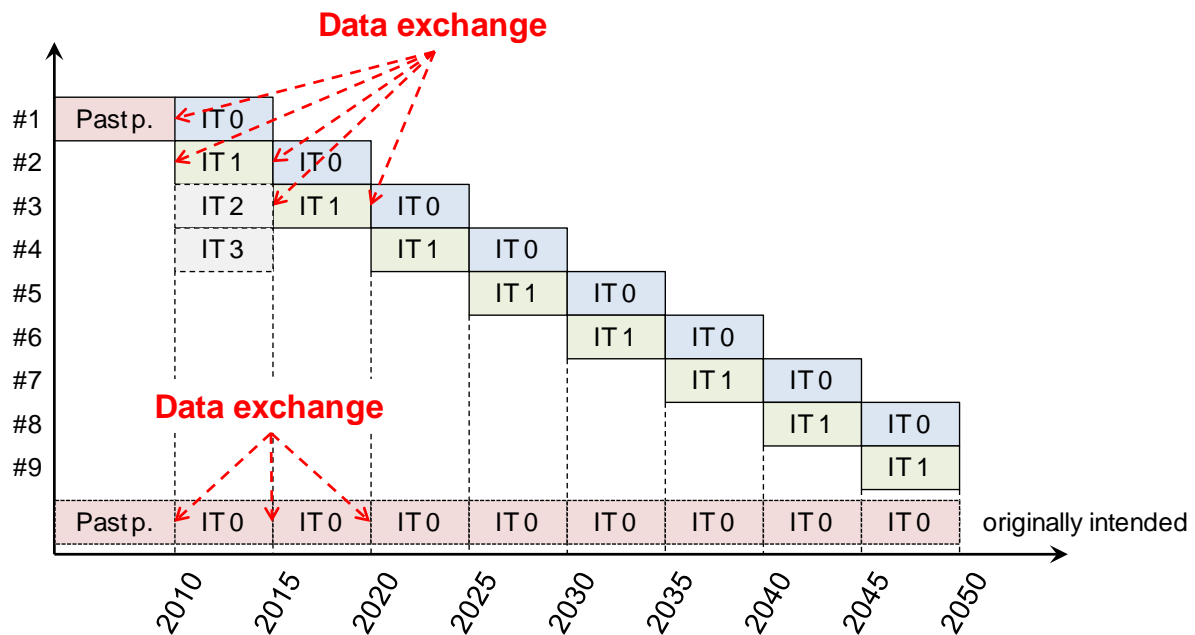


**Figure 17: Data exchange during the simulation process**

Figure 17 compares the finally implemented interface between ATLANTIS and the CGE model and the originally intended one. In the beginning of the EL.ADAPT project, only one data exchange per period (2010-2015, etc.) was considered. Due to the consideration of feedback effects in terms of additional iterations for each simulation period (in order to prevent some sort of oscillating results, see the Appendix for details), the number of data exchanges increased depending on the number of iterations of each simulation period. That implementation of iterations resulted in a dramatically increased duration of the overall simulation process. Now, a simulation until 2050 needs at least one week compared to a simulation duration of 2-3 days before the modification. Furthermore, within ATLANTIS a continuous simulation process considering feedback effects covers in total nine separated but interconnected simulations (#1 - #9), in contrast to only one simulation as originally intended.

The data exchange between both models is based on the so-called “social accounting matrix” (SAM), a table that is similar to an input-output table, representing all economic transactions of a given country for a specific year. Every economic sector has its row and column within the SAM. The row of the electricity sector represents the electricity demand of all other sectors, which are represented by columns. Hence, the SAM row elements of the electricity sector are used by ATLANTIS to calculate e.g. the changes in electricity demand. The SAM column elements – showing all the needed inputs for a sector’s production and therefore representing its technology – are provided by ATLANTIS to continue the simulation process of the CGE model (see the description of the cost function above for further details). Additionally, the CGE model provides price indices for oil, gas and coal as well as CO<sub>2</sub> emission certificate prices, which are imported into ATLANTIS.

## EL.ADAPT

The intermediate production covers several entries concerning the electricity sector and fuel costs. The intermediate production of the electricity sector itself (ELY) consists of ancillary services (e.g. control reserves) and the transmission losses. Fuel costs are categorised by the different types of power plants, including waste combustion power plants (NEI), coal fired power plants (COA), oil fired power plants (P\_C), gas fired power plants (GAS) and biomass as well as biogas power plants (EXT).

The production factors comprise of capital (CAP), capital tax (Capitaltax), labor (LAB) and labor tax (Labortax). Capital consists of the depreciation of all existing and additionally built power plants as well as the profit reduced by the capital taxes. The capital taxes reflect the capital gains tax on retained profits and dividends. Labor includes all labor costs without national insurance contribution, which is part of Labortax entry<sup>5</sup>. The product tax<sup>2</sup> covers the associated employer outlay. Due to missing information all other tax entries will be set to zero or left empty.

The costs for operation and maintenance for power plants as well as transmission and distribution grid systems are subdivided into three major components: construction and real estate (CRE), electronic equipment and machinery (MPE) and other services and utilities (SERV). Additionally, information about new investments for these power plants and grid systems are disclosed separately, but are subdivided into these three major components as well (INV\_CRE, INV\_MPE, INV\_SERV).

In order to give an overview of total produced CO<sub>2</sub> emissions by the electricity sector (CO2\_Emissions) as well as CO<sub>2</sub> emissions produced separately by coal fired (\_COA), gas fired (\_GAS) and oil fired (\_P\_C) power plants will be provided as well. These values are represented in tons of emitted CO<sub>2</sub>.

Since electricity demand is exogenously given in ATLANTIS in standalone simulations, but a crucial parameter when it comes to climate policy and climate change impacts, the linkage with the CGE model enables an endogenous response. In order to transform the demand signals given by SAM row entries for intermediate inputs and demand of private households, an import routine was implemented in ATLANTIS. This routine converts the CGE model results for electricity demand (given in €) using electricity price indices of the CGE model - separated in wholesale and retail market - into changes in physical demand (given in GWh) for the next simulation period.

The CGE result set provides three different fuel price indices for coal, gas and oil. Only the oil price index will be used in ATLANTIS and is fed into a fully integrated econometric fuel-price model. The econometric model estimates regional different fuel prices for coal, gas,

---

<sup>5</sup> "Labor" and "Labortax" will be provided for Austria only

light and heavy oil, which mainly depend on transportation costs, derived from the crude oil price<sup>6</sup>.

## **2.6.1 Baseline**

### 2.6.1.1 Policy assumptions and calibration

In terms of economic growth, the CGE model draws on GDP growth rates from IEA (2010) for 2004 to 2035. More precisely, for all EU regions average annual growth between 2004 and 2035 is 1.6%. Beyond 2035 we adopt GDP growth rates from OECD (2012) to generate a continuous growth path until 2050. Fossil fuel prices are not endogenously determined but exogenously given. To ensure consistency with economic growth assumptions IEA's (2010) fossil fuel price forecast (new policies scenario) for coal, oil and gas is taken as a guideline. Following IEA (2010), prices for oil and gas are assumed to have the same relative growth rates, whereas prices for coal follow a different relative growth path. However, an exact adoption of IEA price forecasts is not possible, as for future periods certain necessary equilibrium conditions are not fulfilled if they were implemented without any adaptation. Thus assumed fossil fuel prices for the CGE model are mostly higher as IEA (2010) suggests. Autonomous energy efficiency improvement (AEEI) is assumed to be 1% p.a. (Graus et al., 2010) reflecting a slight dampening in electricity demand of private households in EU regions.

To get specific CO<sub>2</sub> reduction targets for all EU regions reduction paths from 2004 (base year in CGE model) to 2050 are constructed. The EU meets its "EU 2020 emission reduction targets" of -20% CO<sub>2</sub> emissions compared to reference year 1990 (European Commission, 2008). As the base year of the CGE model is 2004, reduction targets are "updated" to the reference year of 2004, additionally taking into account actual CO<sub>2</sub> emissions from 1990 to 2004 (UNFCCC, 2011). Beyond 2020 the "current policy path" of the EU Roadmap 2050 (European Commission, 2011) is adopted meaning -40% CO<sub>2</sub> emissions compared to reference year 1990.

The EU targets concerning the share of renewable generation in the generation mix are considered in the development of generation capacities implemented in ATLANTIS, which are exogenously defined. This development of the generation mix is mainly based on the World Energy Outlook 2010 (IEA, 2010), as well as the National Renewable Energy Action Plans (NREAPs) of the EU member states. The EU 20 % renewable target is well met in the

---

<sup>6</sup> The econometric model assumes that gas and coal prices are coupled with the crude oil prices, though showing a certain delay. This effect can be observed until the beginning of 2011. Thus, it was not foreseeable in the project planning phase that oil and gas prices will separate from each other.

assumed development. Figure 18 shows the assumed net electricity generation capacities in Continental Europe over time.

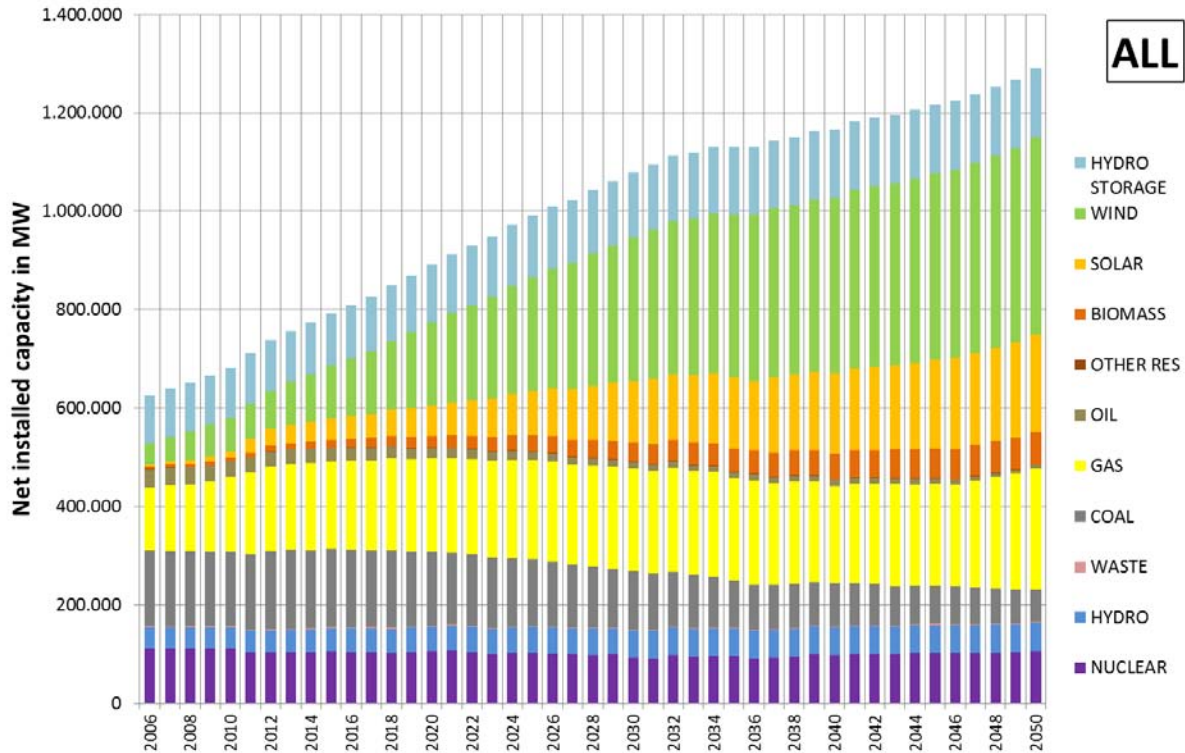


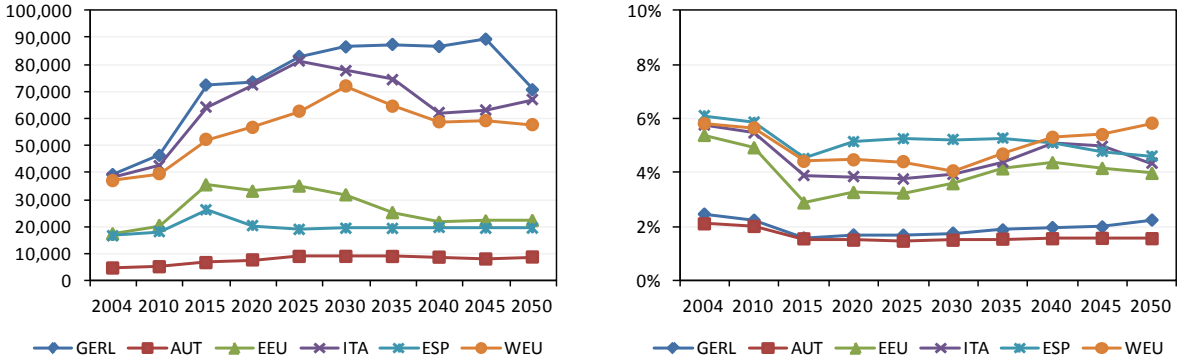
**Figure 18: Assumed development of net installed electricity generation capacity in Continental Europe in the baseline scenario.**

### 2.6.1.2 Scenario results

Climate change impacts are illustrated relative to a non-climate change baseline scenario until 2050. Drawing on the iterative linking of the CGE model and ATLANTIS and based on the above mentioned assumptions on regional growth rates, climate and energy policy we lay out the main findings of the Baseline scenario.

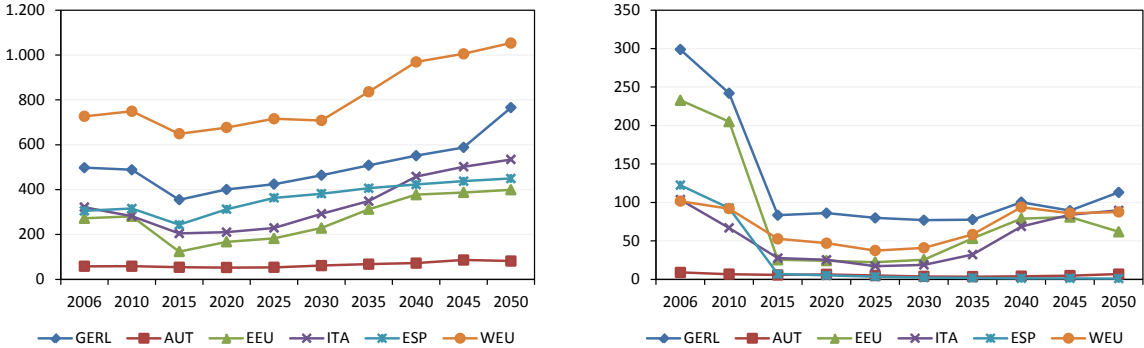
We find that aggregate electricity demand of industries, measured as expenditures on electricity by all sectors, is rising over time. However, regarding specific regions there are different effects in electricity demand. Whereas demand is rising in many regions, it's stagnating in ESP and even falling in EEU and WEU in later periods (see Panel 1, left figure). These results are mainly driven by climate policy induced price effects. At the beginning until 2015 electricity prices are high and demand in physical quantity falls. However, the considerable price increase implies that electricity demand in value terms rises. In contrast, from 2015 onwards where climate policy gets stronger (hence higher CO<sub>2</sub> prices) we observe

a shift from fossil fuels to electricity in intermediate production of economic sectors. Due to climate policy, the relatively higher prices for fossil fuels strengthen competitiveness of the electricity sector in energy demand. Thus electricity demand is rising considerably, also in physical quantities. The findings on a climate policy induced increase in electricity demand are also backed up by the electricity use per unit output (electricity intensity). As reported in Panel 1 (right figure) the intensity of electricity is increasing between 2015 and 2050 in most regions. Further results indicate that the rise is much stronger in electricity intensive sectors (EIS).



**Panel 1: Expenditures on electricity by all sectors (= value of electricity demand in Euros; left figure) and electricity intensities (= electricity use per unit of output) by all sectors (right figure).**

Regarding electricity generation – which has to meet electricity demand – physical units in terms of GWh are of importance (see Panel 2, left figure). Caused by the assumed stringent climate policy, CO<sub>2</sub> intensive generation technologies are heavily reduced within the first period from 2010 to 2015. Thus, notably high CO<sub>2</sub> prices compared to real trading results lead to high electricity prices, followed by a reduction of electricity demand expressed in physical units in the first years, reaching a minimum in 2015 (Panel 2, left figure).



**Panel 2: Electricity demand in TWh (left figure) and resulting CO<sub>2</sub> emissions in million tonnes (right figure)**

The resulting reduced demand leads to a reduction of produced energy between 2010 and 2015, as shown in Figure 19. Due to the high CO<sub>2</sub> price, mainly the electricity generated by coal power plants is affected, especially in countries showing a high share of coal power plants, e.g. EEU. The development of CO<sub>2</sub> emissions in the baseline scenario is illustrated in Panel 2 (right figure). We can see clearly, the strong effects of the implementation of CO<sub>2</sub> reduction targets in the first years.

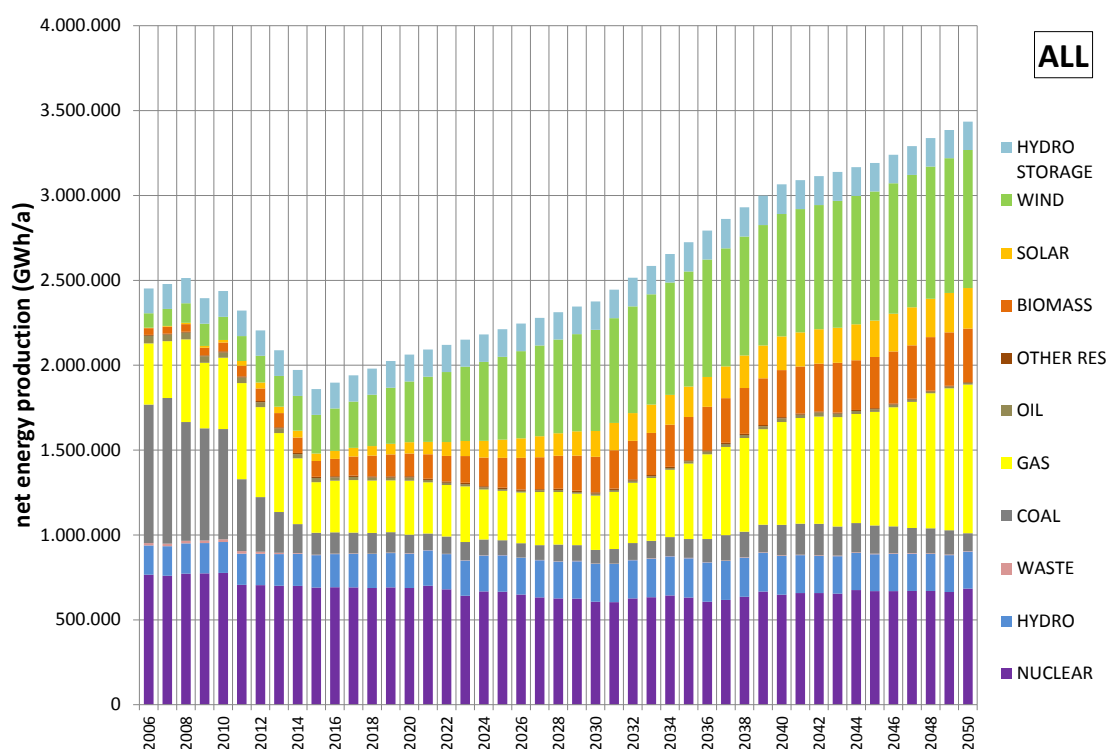
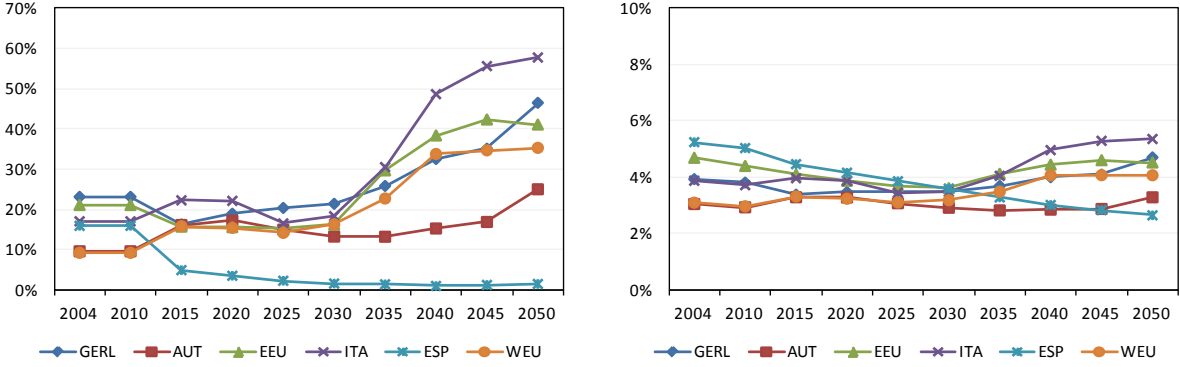


**Figure 19: Simulated annual energy production (GWh) of Continental Europe (baseline scenario)**

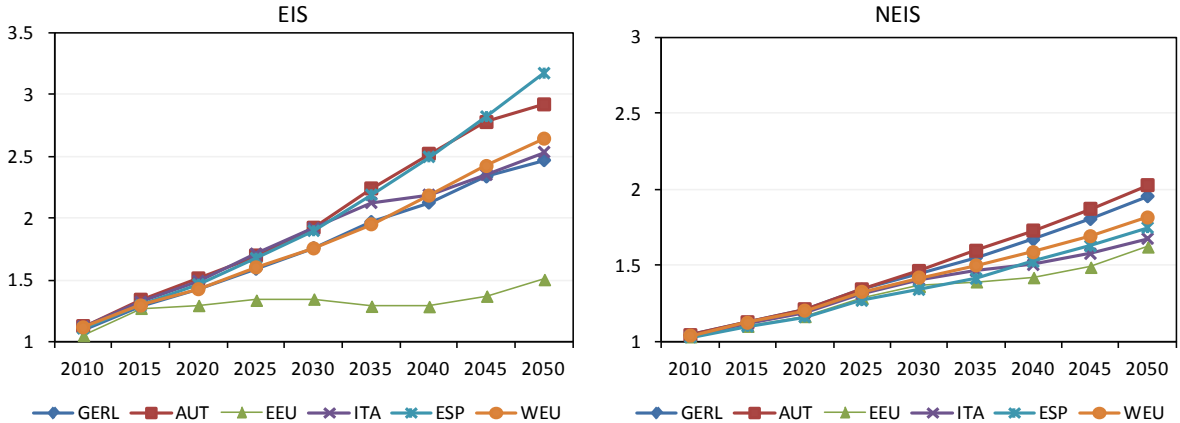
As Figure 19 illustrates, until 2030 the share of renewables (especially wind) in electricity production is rising to meet the RES policy targets, which arises from substitution processes in industry and private consumption. Nevertheless, in later periods the CO<sub>2</sub> price is putting more and more pressure on the whole economy (to meet the CO<sub>2</sub> reduction targets), amplifying the substitution of fossil inputs with electricity. Therefore from 2030 onward additional electricity demand has to be produced by fossil fuels (especially gas) as the capacities of renewable technologies cannot meet the risen demand. This reliance on gas starting in 2030 can also be seen in Figure 19 where net energy production of many technologies remains nearly constant whereas the share of gas rises constantly. Therefore from 2030 onwards in some regions fossil-fuel intensity is rising. Following these results on power generation mix, Panel 3 (left figure) shows fossil fuel use per unit of output of electricity (fossil-fuel intensity) for every region; provided by ATLANTIS. Especially GERL, ITA and EEU show a high degree of fossil fuel use in the end of the second period. ESP

hardly uses fossil fuels in the electricity generation. Panel 3 (right figure) shows how the electricity sector is influencing the fossil fuel intensity of the whole economy, as it is a relatively large sector in terms of production value. For example the high share of fossil fuel inputs in ITA in electricity production is reflected in a high overall share in the economy; vice versa for ESP.

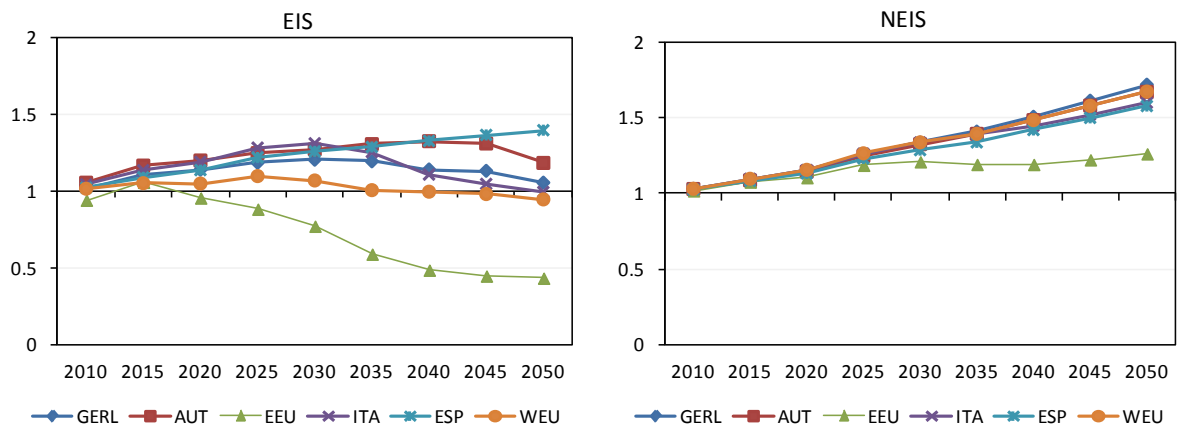


**Panel 3: Fossil fuel intensity [in %] in electricity sector by country (left figure) and in aggregate economic production (right figure)**

Overall, on a sectoral level we find that output of economic sectors in value terms is rising constantly over time. As illustrated in Panel 4 the increase of EIS is more strongly than that of NEIS. However, in terms of quantity (output volume) we find a different picture (see Panel 5). There output of EIS sectors is falling, especially from 2030 onwards. In terms of sectoral feedback there is a shift from EIS to NEIS in Continental Europe. We also find substantial differences between the regions. While EIS output in quantity terms is falling strongest in EEU, ESP experiences a continuous output growth of EIS. The reason for the rise in ESP is the relatively low price for electricity due to clean power generation with a high share of renewable energy. Summarizing, the strong differences in price and quantity effect trace back to the relatively high electricity prices as well as overall energy prices as a result of a sharp rise in the CO<sub>2</sub> price over time.



**Panel 4: Output growth of EIS and NEIS in value terms (2004=1)**



**Panel 5: Output growth of EIS and NEIS in quantity terms (2004=1)**

The shift in output volume from EIS to NEIS also impacts CO<sub>2</sub> emissions. Figure 20 shows that in all countries emissions are reduced. GERL and EEU experience the highest emission reduction. For EEU we find on the one hand the above mentioned shift in economic structure from EIS to NEIS and on the other hand a switch in fossil fuels from a high share of COA to mainly GAS combined with a fall in energy consumption.

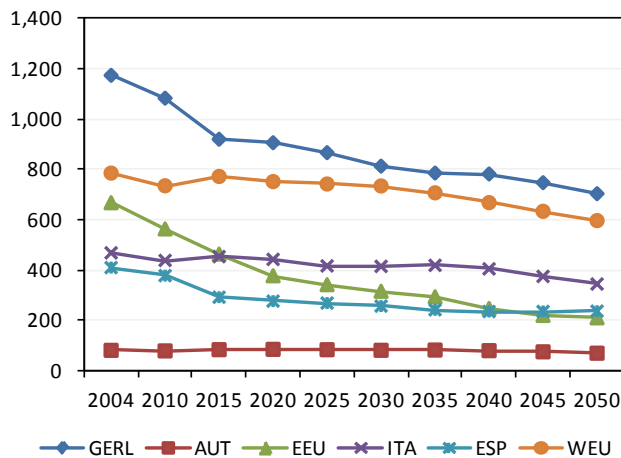


**Figure 20: Overall CO<sub>2</sub> emissions by country**

## 2.7 Uncertainty and reliability assessment

The uncertainty in the meteorological forcing data was analyzed based on the multi-model dataset from the ENSEMBLES project. This dataset covers large part of model uncertainty, but is based on only one emission scenario. However, for the period before 2050, it is expected that the effect of different emission scenarios on climate will be largely similar. Remarkable differences are expected in the second half of the 21st century, however. The uncertainty analysis took care of ensuring that the four simulations selected for EL.ADAPT are representative for the uncertainty range spanned by the entire ENSEMBLES dataset and therefore provide pairs of wet or dry and hot or cool simulations.

The uncertainty of the hydrological model was analyzed by applying the principle of equifinality, where various different “equally like” parameter sets were used to compute runoff estimates. The difference in runoff due to the different parameter sets is compared to the difference in runoff due to the different climate change scenarios. Interestingly, the difference of the former is rather small, although not negligible compared to the difference of the latter. Also a sensitivity analysis of the four free (to be calibrated) parameters has been conducted. The capacity of the production store ( $X_1$ ) was found to be the most sensitive parameter (see the Appendix). However, even changing the parameters by +/-20%, changes in runoff show a narrower bandwidth than produced by the four different climate scenarios.

Regarding the economic and technological uncertainties, uncertainties were assessed by either running ATLANTIS and the CGE model separately or jointly. In the stand-alone simulations with ATLANTIS, the influence of the share of RES generation on the change of standard capacity was investigated. In a similar vein, two simulations are contrasted in the CGE model in its standalone version: one with and one without climate policy to see how strong the effect of climate change impacts is relative to the effects of climate policy. Moreover, the sensitivity of model results with respect to alternative parameter specifications (foreign trade elasticities; elasticities of substitution for electricity) was assessed.

To give an idea on the uncertainty of the results of the coupled simulations, we compared results between simulations using ATLANTIS coupled with the CGE model and uncoupled (stand-alone simulations). In the latter, direct influence of climate change on e.g. CO<sub>2</sub> emissions, market prices etc. are assessed but follow-up effects between economic sectors are not taken account of. As an example, the comparison shows that the climate change itself will lead to reduced CO<sub>2</sub> emissions in the electricity sector, independent of simulated climate scenarios, while in the coupled simulations these emissions may rise due to industry sectors substituting e.g. electrical energy for fossil energy sources.

### 3 Results and conclusions

#### 3.1 Regional climate change across Europe and uncertainties involved

Regarding meteorological forcing for the project EL.ADAPT, four representative regional climate scenarios have been selected to ensure to cover the uncertainty range of expected climate change.

The parameter range covered by the selected RCMs covers a large part of the entire RCM ensemble. Furthermore, the selected RCMs show different characteristics: Meteo-HC HadRM3Q0 being a hot and dry realization, C4IRCA3 being a warm and wet realization, KNMI-RACMO2 being a moderate realization and CNRM-RM4.5 representing a special case, which show stronger summer than winter warming. The climate change signals between 1961-1990 and 2021-2050 of the selected models are summarized in Table 7 and Table 8. Based on the selected simulations, we expect changes ranging from +1.2°C to +2.8 °C for temperature, -0.27 to +0.3 mm/day for precipitation, -3.46 W/m<sup>2</sup> to +6.81 W/m<sup>2</sup> for global radiation and no remarkable change for mean wind speed.

**Table 7: Mean climate change signal for temperature (air temp, °C), precipitation (prec, mm/day), windspeed (windsp, m/s) and global radiation (glob.rad, W/m<sup>2</sup>) for the winter season (December, January, February)**

Model - WINTER	<i>air.temp m</i>	<i>prec m</i>	<i>windsp m</i>	<i>glob.rad m</i>
METO-HC_HadRM3Q0	2,406	0,045	0,017	1,918
C4IRCA3	2,297	0,295	-0,019	-1,379
CNRM-RM4.5	1,184	-0,162	0,085	0,086
KNMI-RACMO2	1,162	0,262	0,165	0,080

**Table 8: Mean climate change signal for temperature (air temp, °C), precipitation (prec, mm/day), windspeed (windsp, m/s) and global radiation (glob.rad, W/m<sup>2</sup>) for the summer season (June, July, August)**

Model - SOMMER	<i>air.temp m</i>	<i>prec m</i>	<i>windsp m</i>	<i>glob.rad m</i>
METO-HC_HadRM3Q0	2,787	-0,275	-0,001	3,876
C4IRCA3	2,023	0,171	-0,055	-3,458
CNRM-RM4.5	2,115	0,144	0,016	6,181
KNMI-RACMO2	1,441	-0,129	-0,001	0,529

## 3.2 Change in water availability in the GAR and uncertainties involved

Based on the hydrological model presented in Section 2.2 the model performance, the model application taking the four climate scenarios into account and an estimate of uncertainties involved in this modeling step are provided. Uncertainties related to the hydrological model are discussed by analyzing different sets of model parameters considering the principle of equifinality. Moreover, comparisons to previously published studies are made.

### 3.2.1 Calibration and Validation

At first, the hydrological model was calibrated and validated using the available historical data (precipitation, temperature and runoff at a number of gauging stations). If the model is able to reproduce the observed streamflow and moreover, if the model calibrated on one part of the time series is able to simulate another part of the historical time series, the model is considered to be functional for simulating future runoff (Klemes, 1986). An example of a calibrated hydrograph including a split sample test is shown in Figure 21. It is noteworthy that if the model is calibrated using the first half of the time series (1661-1985;  $\overline{NSE}$  of 74.9%), it is able to simulate the runoff for the second half (1986-2010) rather good ( $\overline{NSE}$  of 79.1%), even the low flow during the drought period in 2003.

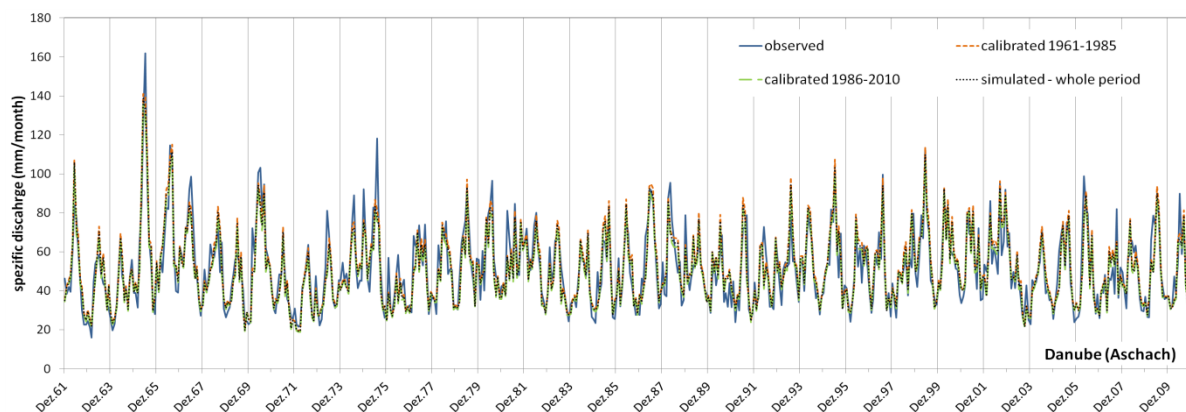


**Figure 21: Hydrograph of the gauging station Aschach (Danube River, 78190 km<sup>2</sup>): observational data (blue line), calibration using the whole time span (black dotted line; 77.2%  $\overline{NSE}$ ), calibration using the first half of data (orange dashed line; 74.9%  $\overline{NSE}$ ; validation on 2nd half: 79.1%  $\overline{NSE}$ ) and calibration using second half (green dashed line; 80.0%  $\overline{NSE}$ ; validation on 1st half: 74.2%  $\overline{NSE}$ ). Note good fit of drought period 2003 even for the model calibrated using the first half of the date (1961-1985).**

This evaluation was done for the whole data set of 101 measurement stations. The average of the three efficiency criteria ( $\overline{NSE}$ ) for all the stations yielded  $78.9 \pm 6.8\%$  when calibrated

EL.ADAPT

for the whole time period,  $75.1 \pm 8.5 \%$  and  $76.1 \pm 9.0 \%$  when validated on the half of the time series after calibrating it on the other half of the time series, respectively. An overview of the model efficiency is shown in Figure 22 and Figure 23.

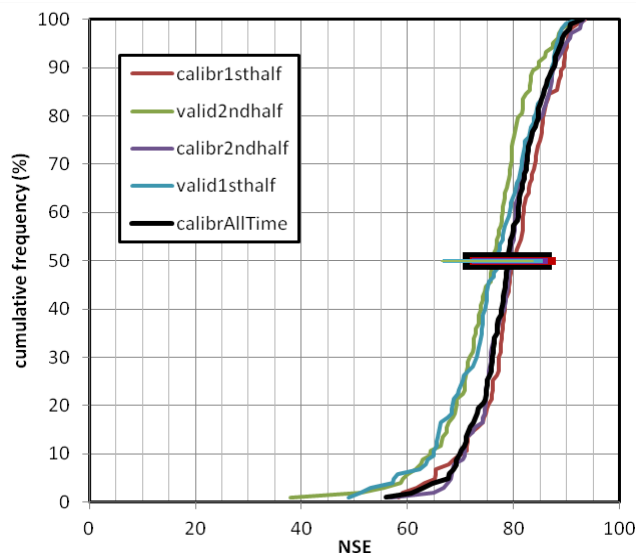


**Figure 22: Cumulative frequency distribution of model efficiency ( $\overline{NSE}$ ) for all catchments considered in the hydrological modeling. Even in validation the model efficiency is for the most part in acceptable ranges ( $\geq 65\%$ ) or even good ( $\geq 80\%$ ).**

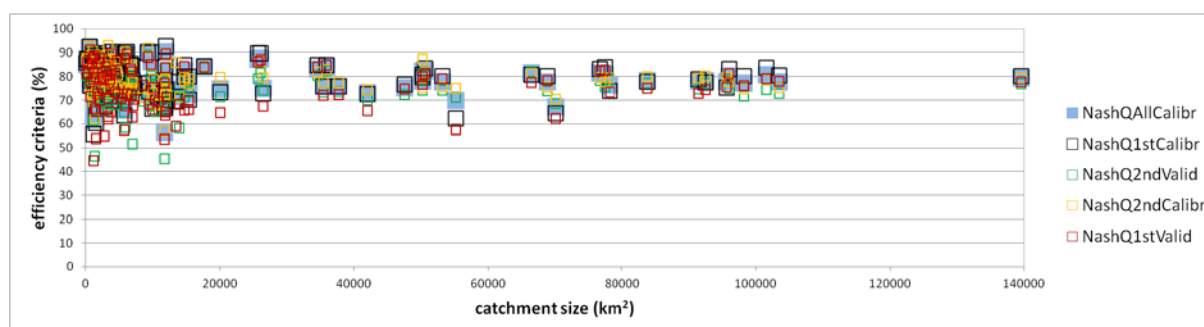


**Figure 23:  $\overline{NSE}$  efficiency criteria in % versus the catchment size of the individual catchments. The blue boxes show the efficiency when the model is calibrated on the whole time series of the individual catchments; the black boxes when the model is calibrated on the first half of the available time series, the green boxes when validated on the second half of the time series using the calibrated model of the first half; the yellow boxes when the model is calibrated on the second half of the available time series, the red boxes when validated on the first half of the time series using the calibrated model of the second half.**

In addition to the acceptable efficiencies illustrated above, the model results were compared to published results of other models on the one hand for future estimations (shown in section

3.2.3) and on the other hand for historical data (e.g. Kling et al., 2011; Stanzel and Nachtnebel, 2010; Klein et al., 2011; Kranzl et al., 2010; Pöhler et al., 2010; ZAMG/TU-Wien Studie, 2011). As an example, the model performance to simulate observed runoff for the two gauging stations Passau-Ingling (26084 km<sup>2</sup>) and Golling (3555.7 km<sup>2</sup>) at the rivers Inn and Salzach respectively are shown in Figure 24 compared to the simulations by Pöhler et al. (2010), which used the physically based catchment model WaSiM-ETH at a daily time step. A general agreement between observed data, the published simulated data and the simulations from the parsimonious model used herein increases the confidence in the appropriateness of the simple model (structure).

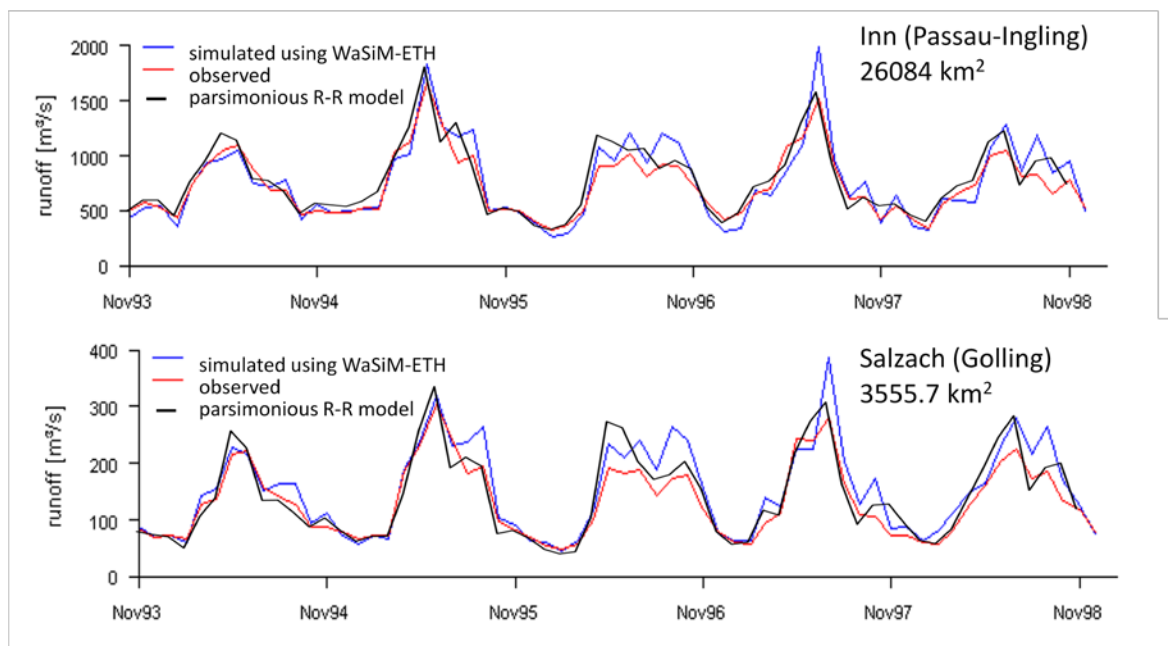


**Figure 24: Observed and simulated runoff data for two Austrian stations. The red lines are the observed hydrographs; the blue lines are the simulated data using the physically based catchment model WaSiM-ETH as reported in Pöhler et al. (2010) and the black lines are the simulated runoffs using the parsimonious lumped-parameter model used for this work.**

### 3.2.2 Runoff estimates based on four climate scenarios

Using temperature and precipitation input from the choice of four climate scenarios, the calibrated and validated hydrological model is used to simulate a range of possible runoff estimates for the two periods 2011-2030 and 2031-2050 in relation to the reference period 1961-1990 for all 101 catchments. As an example, Figure 25 shows for each of the four climate change scenarios the predicted seasonal change of the mean monthly runoff of the river Danube at the station Kienstock in the two time periods 2011-2030 and 2031-2050. The comparison of the predicted future mean monthly runoff with runoff simulated for the

EL.ADAPT

reference period 1961-1990 yields the expected change in monthly runoff for each of the 4 climate scenarios (Figure 26). The overall annual changes for the two periods 2011-2030 and 2031-2050 related to the reference period 1961-1990 are shown on the very left of Figure 26.

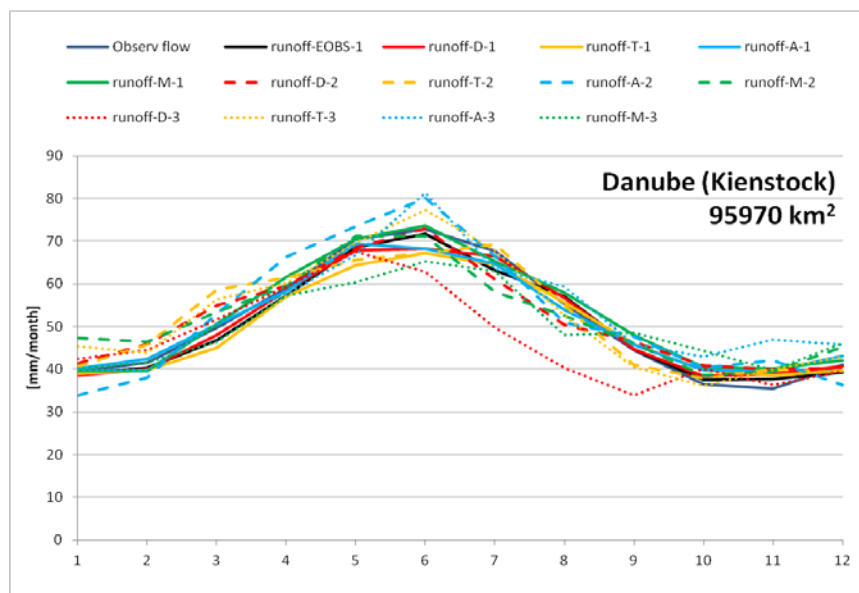


Figure 25: Seasonal change of the mean monthly predicted runoff of the station Kienstock (Danube River). The color coding of the lines is based on the different scenarios. Red and the letter D (“Desert”) represents the hot and dry scenario (Meteo-HC HadRM300); orange and T (“Tropic”) the warm and wet scenario (C4IRCA3); blue and A (“AirCondition”) the scenario with stronger summer than winter warming (CNRM-RM4.5); green and M (“Moderate”) the moderate scenario (KNMI-RACMO2). 1, 2, and 3 in the legend are related to the time periods 1961-1990, 2011-2030 and 2031-2050.

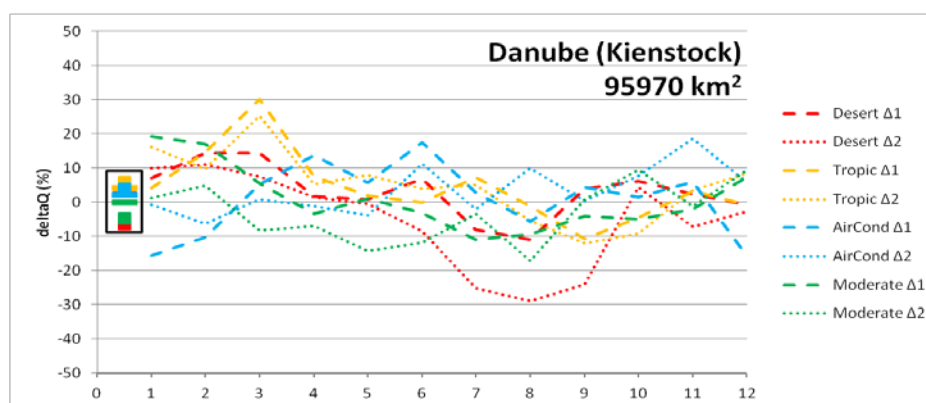
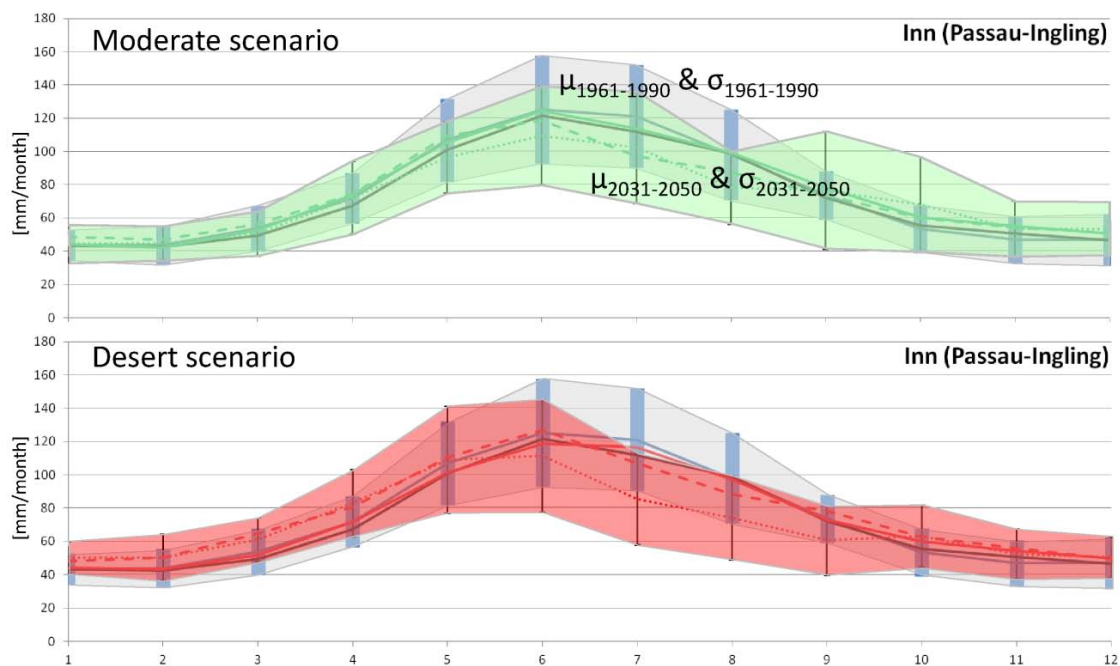


Figure 26: The difference per month of the runoff for the two time periods 2011-2030 vs. 1961-1990 ( $\Delta 1$ ) and 2031-2050 vs. 1961-1990 ( $\Delta 2$ ). Note that small increases in the runoff during periods of low flow (e.g. in winter) might give the impressions of large changes (up to 100% and more; see e.g. Figure 15); however, these do not have a great influence on the difference in the overall annual runoff indicated by the bars (period 1) and rectangles (period 2) at the left side of the plot (in the black box).

Mean monthly runoffs ( $\mu$ ) as shown e.g. in Figure 25 and their standard deviations ( $\sigma$ ) for each catchment, each month and each scenario for the two time periods 2011-2030 and 2031-2050 versus the reference period 1961-1990 were computed to get a bandwidth of possible runoff changes in the near future (as an example see Figure 27). Each result from the different climate scenarios was passed on to the next modeling steps in WP3.



**Figure 27: Range of runoff for the Inn River at the station Passau-Ingling (26084 km<sup>2</sup>) for historical data and the estimated ranges of future runoffs for the Moderate (top) and the Desert (bottom) scenario.**

Depending on the climate scenario used, there is a certain variation in the change in runoff for all the catchments analyzed and moreover for the two periods 2011-2030 and 2031-2050 compared to the reference period 1961-1990. In general the variations in runoff are within +10 and -15% (Figure 28). Interestingly, for the Desert scenario a positive trend in runoff change is observed for the period 2011-2030 whereas a strong decrease (of up to -35% in Southern France and Northern Italy) is estimated for the period 2031-2050. However, this is not surprising, as the precipitation patterns already show such a behavior.

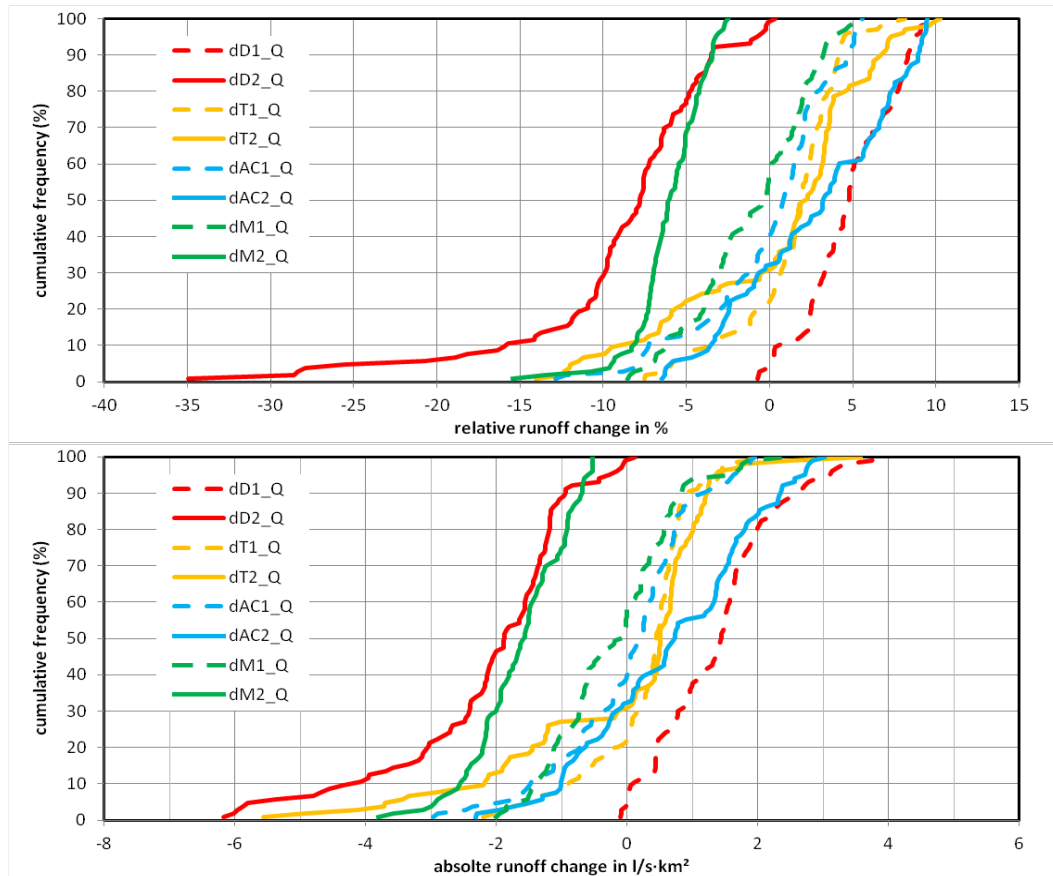


**Figure 28: Cumulative frequency of relative (in %) and absolute (in l/s.km<sup>2</sup>) runoff change for all the analyzed catchments of the GAR. Red lines represent the changes in runoff for the Desert scenario, orange ones for the Tropic scenario, blue ones for the Air Condition scenario and green ones for the Moderate scenario. Dashed lines relate to the difference in runoff for the time period 2011-2030 versus 1961-1990 and the solid lines to the period 2031-2050 versus 1961-1990.**

As Figure 28 allows no spatial differentiation between individual regions, Figure 29 a-h shows the spatial distribution of the mean annual runoff changes in % for all the considered catchments of the GAR individually for the four scenarios and the two time periods.

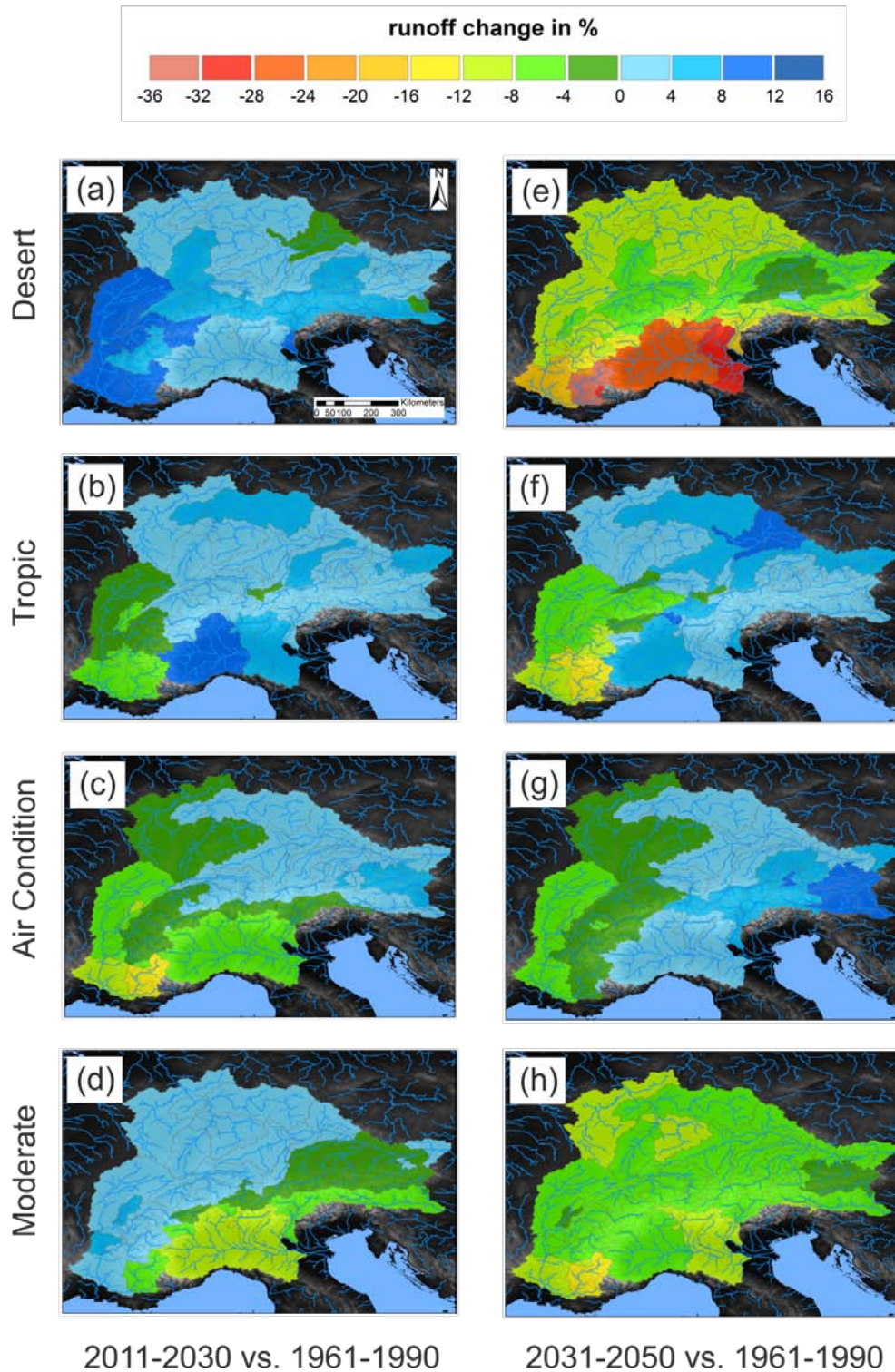


**Figure 29:** The computed changes in runoff for the considered catchments of the GAR. Changes are in percent (%) of 2011-2030 vs. 1961-1990 (a-d) and 2031-2050 vs. 1961-1990 (e-h) for the 4 climate scenarios (a & e: Desert scenario; b & f: Tropic scenario; c & g: Air Condition scenario; d & h: Moderate scenario). The computed changes are related to the outlets of the actual catchments, but the color coding of smaller sub-catchments is superposed on the corresponding larger catchments.

Eight different catchments of various size and runoff regimes are shown in Figure 30 and Figure 31 to indicate likely monthly changes that are not covered in Figure 28 and Figure 29.

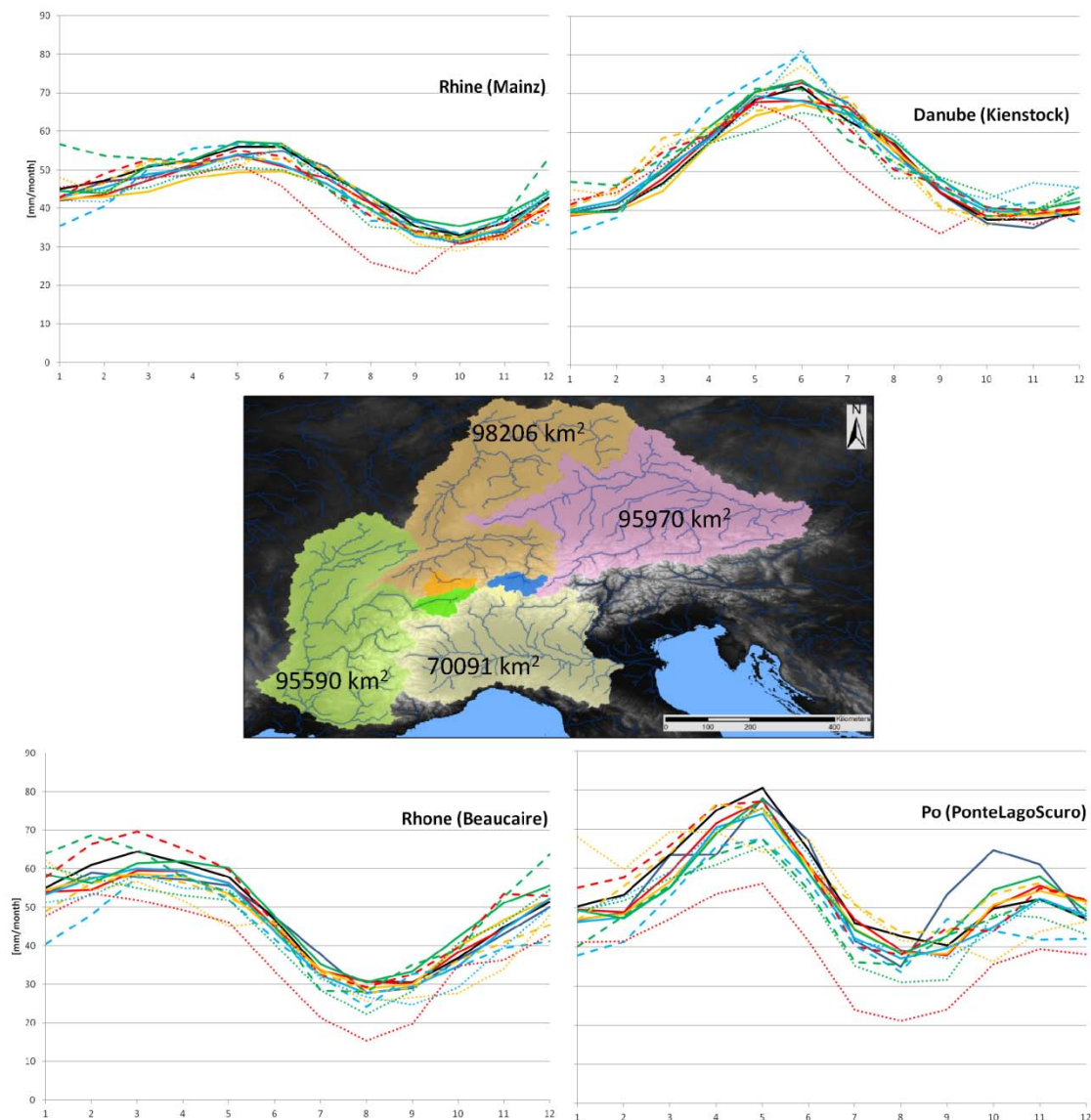


**Figure 30: The estimated average monthly runoff for the time periods 2011-2030 and 2031-2050 compared to the period 1961-1990 for four larger catchments draining the whole Alpine region. The color coding is identical to Figure 8. The smaller catchments in the middle of the figure are the ones shown in detail in Figure 14.**

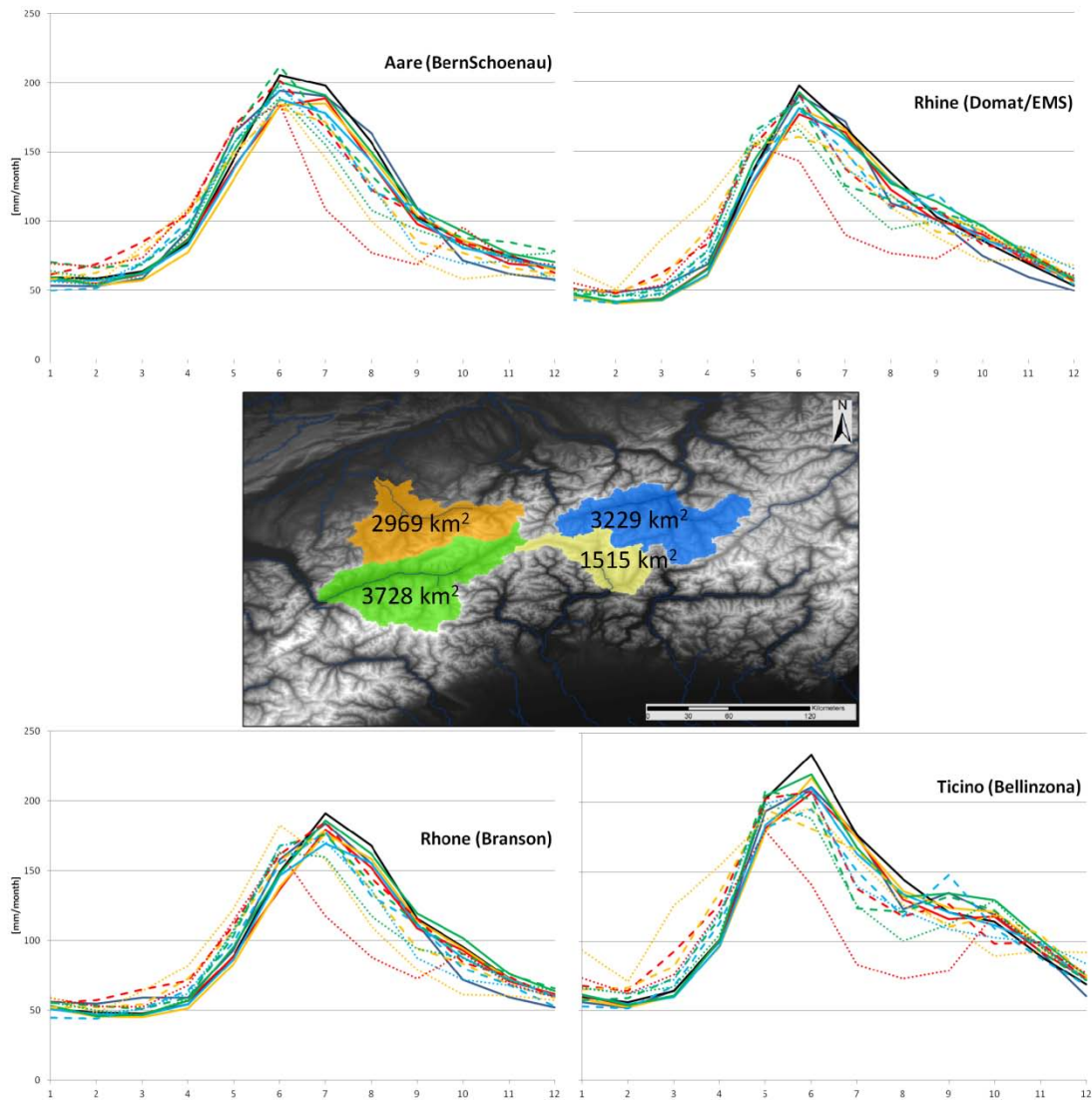


**Figure 31: The estimated average monthly runoff for the time periods 2011-2030 and 2031-2050 compared to the period 1961-1990 for four smaller catchments draining a central part of the Alpine region. Their locations are indicated in Figure 13.**

Especially for the smaller catchments a shift towards earlier runoff and a decrease in the summer months is observable. Monthly variations are up to +190% due to seasonal changes and a shift towards earlier runoff (especially in March and April) related to a warming trend observed in all climate scenarios. The largest decreases of up to -70% are observed in the summer months of July and August. An example where both of these effects are observable is shown for the River Inn at the station Imst in Figure 32.

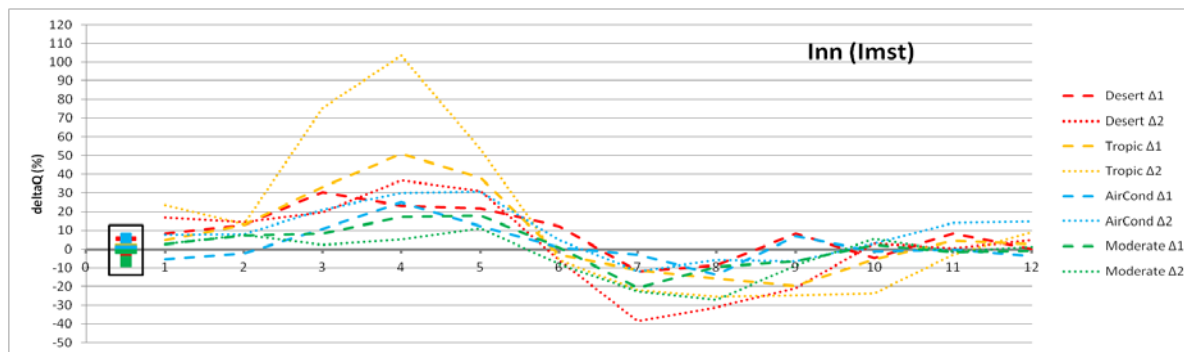


**Figure 32:** The estimated changes in runoff for the river Inn at the station Imst (3842 km<sup>2</sup>). Note the increase in runoff early in the season (March, April and May) and a decrease in the summer months (July and August). Color coding is as in Figure 9.

### 3.2.3 Uncertainties involved

To take the uncertainty in climatic input data into account, four different climate scenarios have been used to cover a wide range of possible future changes based on the parameters temperature, precipitation, wind and global radiation; only the former two are used for the hydrological modeling. To assess the uncertainty in the hydrological modeling itself, various parameter sets that lead to a similar acceptable fit (a “sufficiently accurate” simulation) of the historical data (principle of equifinality; Beven, 1993) are used to compute runoff changes for the future. Different “equally like” parameter sets due to equally acceptable fits to observed historical runoff data might lead to different future runoffs for the individual climate scenarios. However, this difference is shown to be small compared to the difference due to different climate scenarios. As there is a single hydrological model applied and as such only a single model structure used, some results were compared to published data to endorse the applicability of it.

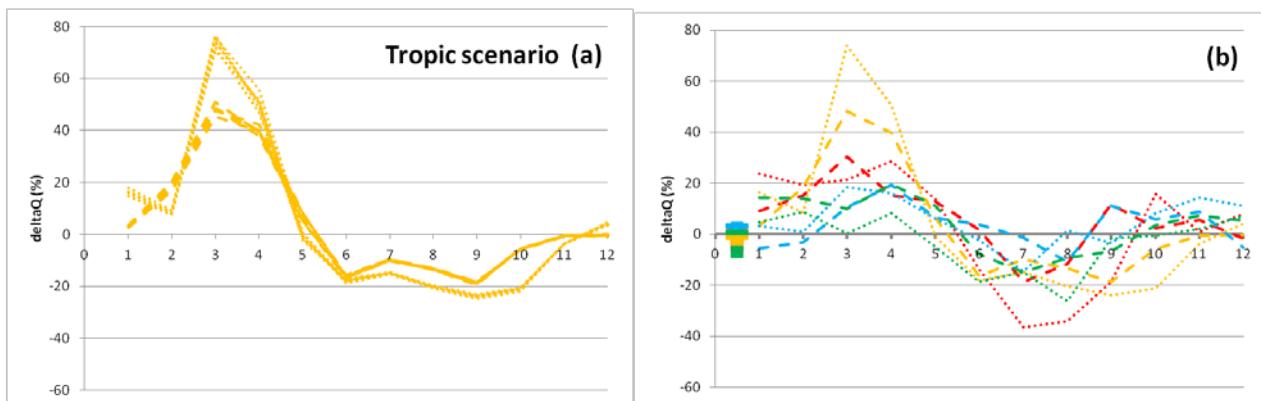
In the following the difference in runoff estimates due to different parameter sets and due to the 4 different climate scenarios is evaluated. Based on this analysis, a range of possible runoff estimates was passed on to the electricity sector model of WP3. Moreover, the results of the simple, parsimonious hydrological model are compared to published data to be able to document the models ability to simulate future runoff sufficiently.

#### 3.2.3.1 Uncertainty in parameter set

The optimal parameter set for a single measurement station was computed by optimizing a certain efficiency criteria for a certain time period of the discharge time series, where observed and simulated runoff are compared. On the one hand, there might be different parameter sets of equally good fits (i.e. equifinality; Beven, 1993), on the other hand the

optimization can be performed with different efficiency criteria or a combination of multiple efficiency criteria and the time period for which the model is calibrated can be chosen differently.

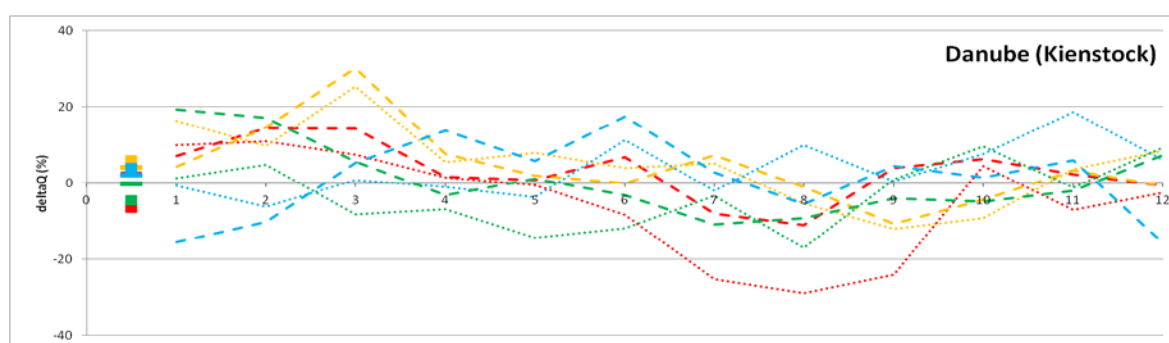
Here we used three different Nash-Sutcliffe efficiency criteria (NSEs) individually and a combination thereof and computed them for the whole and for the first and the second half of the available discharge time series. All these different calibrations result in possible (~equally likely) runoffs. These different results can be compared to each other and to results from different climate scenario inputs. From Figure 33a it can be seen that different “equally likely” parameter sets lead to comparable (but admittedly different!) monthly runoff changes for a single climate scenarios. Here, the difference in runoff for the periods 2011-2030 and 2031-2050 compared to the reference period 1961-1990 are shown. However, the difference due to the different parameter sets is usually (much) smaller than the difference in runoff due to the different climate forcing, the different climate scenarios (Figure 33b).



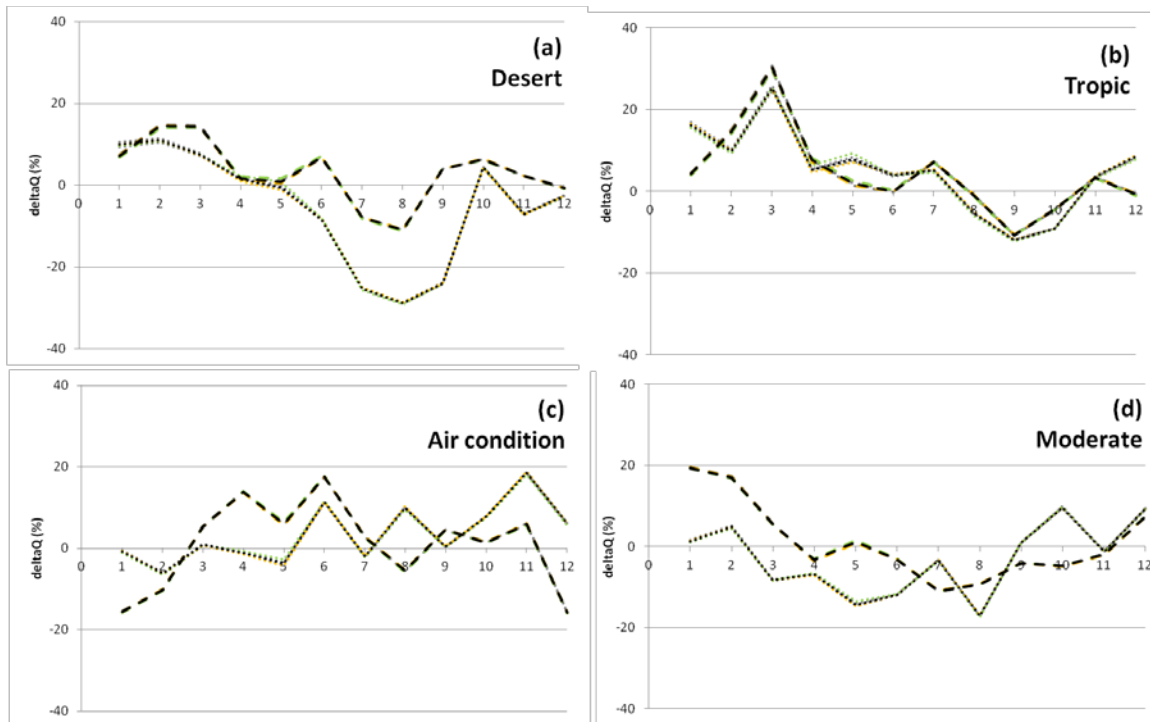
**Figure 33: Monthly change in runoff for the measurement station Gisingen at the River Ill. a) changes in the average runoff for the period 2011-2030 versus 1961-1990 and the period 2031-2050 versus 1961-1990 (the dashed and dotted lines respectively) due to different “optimal” parameter sets and the “Tropic” climate scenario as forcing input. b) Changes in the average runoff due to four different climate scenario inputs: “Desert” in red, “Tropic” in orange, “Air condition” in blue and “Moderate” in green. Note the large differences of runoff at a monthly timescale due to different climate scenarios (b) compared to the small differences from using various “optimal” parameter sets for a particular climate scenario (a).**

Figure 34 shows the changes in runoff at the station Kienstock (95970 km<sup>2</sup>) for the 4 different climate scenarios. Figure 35 a-d shows the various changes due to 6 different “optimal” parameter sets for the individual climate scenarios. The 6 “optimal” parameter sets are computed using different efficiency criteria or all of them for the calibration. First, the classic NSE criteria (Nash and Sutcliffe, 1970) is used for optimization; second, the square root

transformed NSE; third the log-transformed NSE and fourth, a combination of all these three criteria ( $\overline{NSE}$ ). All these are done for the full available time series (excluding a warm up period of 1 year). Moreover, the  $\overline{NSE}$  is used for calibration only for the first and only for the second half of the available time series. Using these 6 different “optimal” parameter sets the bandwidth of the simulated output can be considered. Note that there is hardly a difference in the simulated change in runoff due to the 6 different parameter sets for the station Kienstock along the Danube river (Figure 35 a-d individually), whereas the difference due to the different climate scenarios is obvious (Figure 35 a-d compared to each other).



**Figure 34: Change in monthly runoff for the measurement station Kienstock at the Danube River with a catchment size of 95970 km<sup>2</sup>. Changes in the average runoff for the period 2011-2030 versus 1961-1990 and the period 2031-2050 versus 1961-1990 (the dashed and dotted lines respectively) are displayed. The four different climate scenario inputs are “Desert” in red, “Tropic” in orange, “Air condition” in blue and “Moderate” in green.**



**Figure 35: Change in runoff for the measurement station Kienstock at the Danubue River using 6 different optimal parameter sets. The dashed and dotted lines in Figure 18a-d represent the time periods 2011-2030 versus 1961-1990 and 2031-2050 versus 1961-1990. Figure 18 a, b, c and d show separately the changes in runoff due to the 6 different “optimal” parameter sets for a single climate change scenario; a for “Desert”, b for “Tropic”, c for “Air condition” and d for “Moderate”. Note that the different parameter sets for this particular catchment yield almost identical changes in runoff as all 6 dashed and all 6 dotted lines nearly overlap each other.**

On the one hand, this shows the bandwidth of possible runoff estimates due to different parameter sets (for this particular catchment almost identical), on the other hand it gives confidence in the outcome, as the difference in runoff due to different optimal parameter sets is (usually) small compared to the differences due to different climate scenarios. In the following, a subset of measurement stations are used as examples of how different parameter sets influence the runoff estimates that are used to come up with changes in runoff in the Greater Alpine Region (Figure 36). The range of these runoff estimates is compared to the changes due to different climate change scenarios.

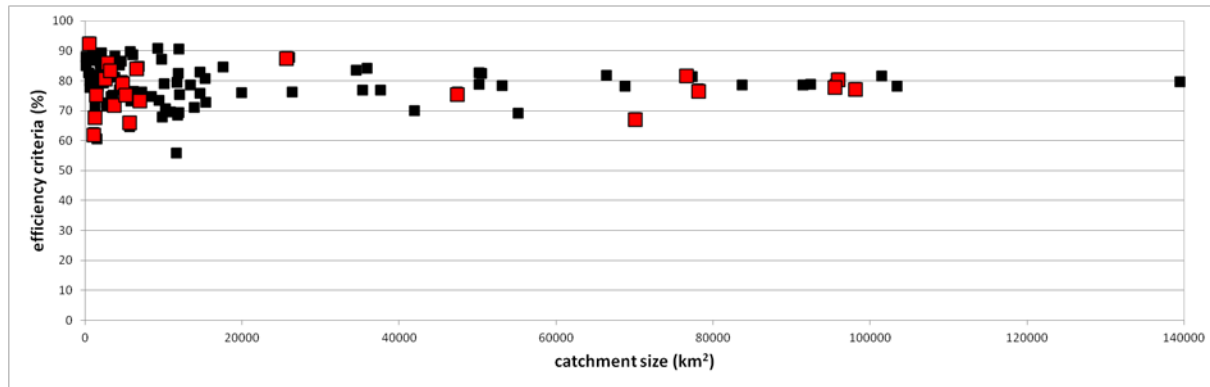


**Figure 36: The  $\overline{NSE}$  criteria and the catchment sizes of the subset of 21 measurement stations that have been analyzed in detail for the consequences of different “optimal” parameter sets on the monthly runoffs as red boxes. The black boxes are the complete data set used in the hydrological modeling.**

Interestingly, stations that resulted in high  $\overline{NSE}$  values are not necessarily the ones where different parameter sets result in small differences in the simulated runoffs. The station Mittersill along the Salzach river gave  $\overline{NSE}$  values above 90%, however the different changes in runoff due to the different “optimal” parameter sets resulted in a rather large bandwidth for a specific climate scenario at specific months; especially in March, April and May (the Tropic scenario or yellow lines in Figure 37 and especially Figure 38). However, the difference is again small compared to the differences due to the different climatic forcings: the 4 different climate scenarios (Figure 37 and Figure 38).

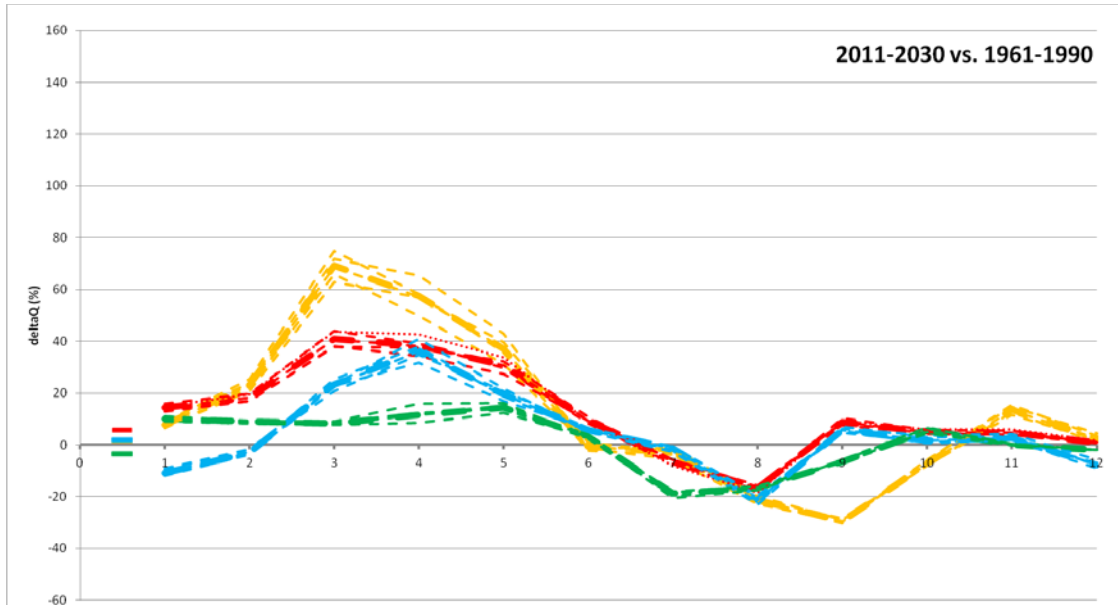


Figure 37: The change in runoff for the station Mittersill along the Salzach river for the period 2011-2030 versus 1961-1990 for all 4 climate scenarios and different optimal parameter sets. Note that the difference in the climate scenarios are of more significance than the difference due to different optimal parameter sets for a specific climate scenario. The four different climate scenario inputs are “Desert” in red, “Tropic” in yellow, “Air condition” in blue and “Moderate” in green.

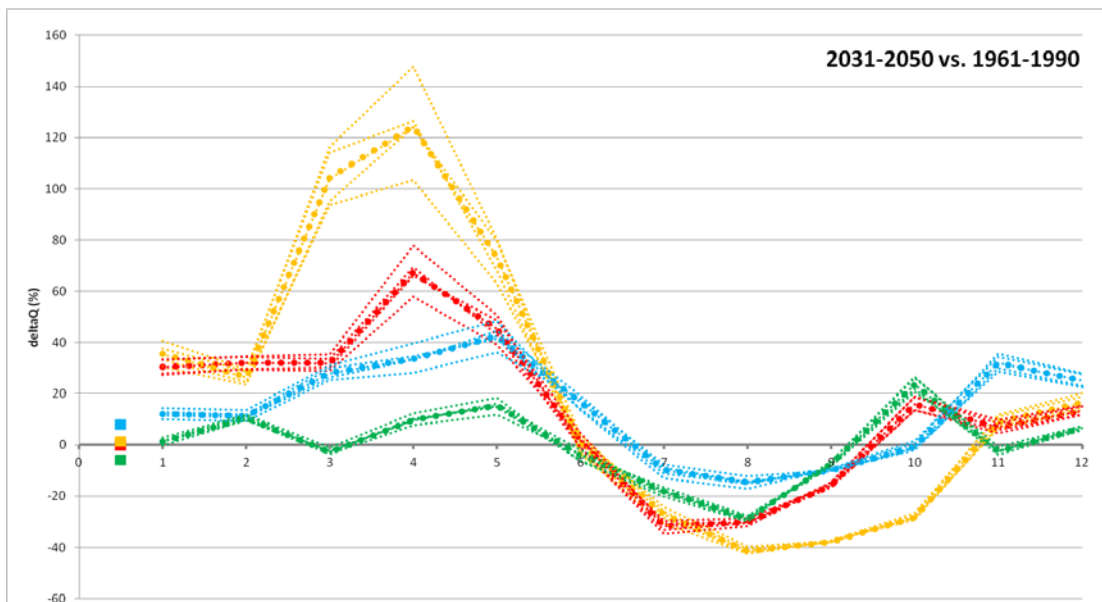
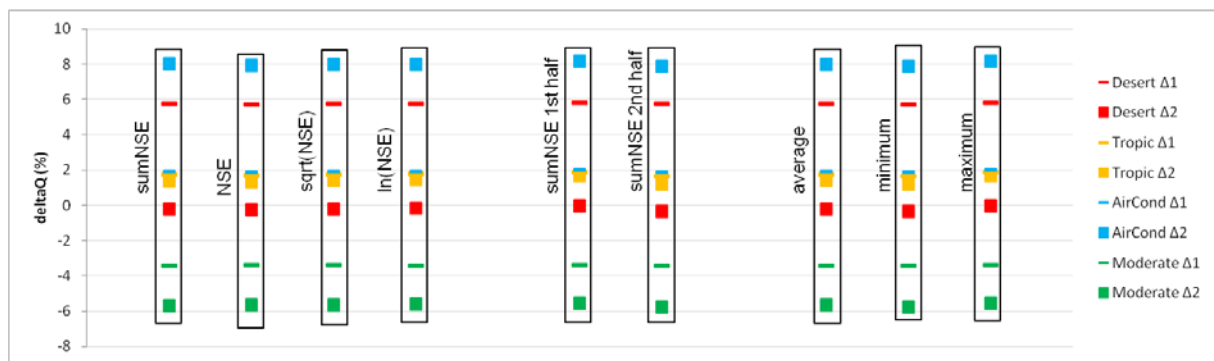


Figure 38: The change in runoff for the station Mittersill along the Salzach river for the period 2031-2050 versus 1961-1990 for all 4 climate scenarios and different optimal parameter sets. Note that the differences in runoff due to different optimal parameter sets are increased especially for the Tropic scenario and the months March, April and May. However, still the changes due to the different climate scenarios are clearly separated from each other. The four different climate scenario inputs are “Desert” in red, “Tropic” in yellow, “Air condition” in blue and “Moderate” in green.

The difference in runoff changes for the different optimal parameter sets becomes even less pronounced if the annual changes are displayed, although the differences due to the different climate scenarios are obvious (Figure 39).



**Figure 39:** The annual change in runoff for the station Mittersill along the Salzach river for 2011-2030 versus 1961-1990 ( $\Delta 1$ ) and 2031-2050 versus 1961-1990 ( $\Delta 2$ ) shown as bars and boxes, respectively using different optimal parameter sets. The first 4 columns show the differences in runoff in percent for the optimal parameter set using the  $\overline{NSE}$ , the classical NSE, the square-root transformed NSE and the log-transformed NSE, respectively. Column 5 and 6 show the results of using the optimal parameter sets when calibrating only for the first and only for the second half of the data set (using  $\overline{NSE}$ ). The last 3 columns show the mean, minimum and maximum values of runoff difference of the 6 optimal parameter sets. Even though the different optimal parameter sets result in somewhat different runoff estimates on a monthly basis, the annual changes are very similar.

Moreover, the change in runoff (shown here as the difference in percent between the future period 2011-2030 and the reference period 1961-1990 and the future period 2031-2050 and the reference period 1961-1990) can also be computed by using the parameter sets from neighboring stations. This resembles a proxy basin test, but Figure 40 uses parameter sets from measurement stations along the same river, so strictly speaking this is not a real proxy basin test. Nevertheless, also this approach shows that the difference in change in runoff due to these parameter sets is still small compared to changes due to different climate change scenarios. In addition such a test builds confidence in the model, as each of the stations along a river is computed separately. Only the same input data of precipitation and temperature for the overlapping area is common.

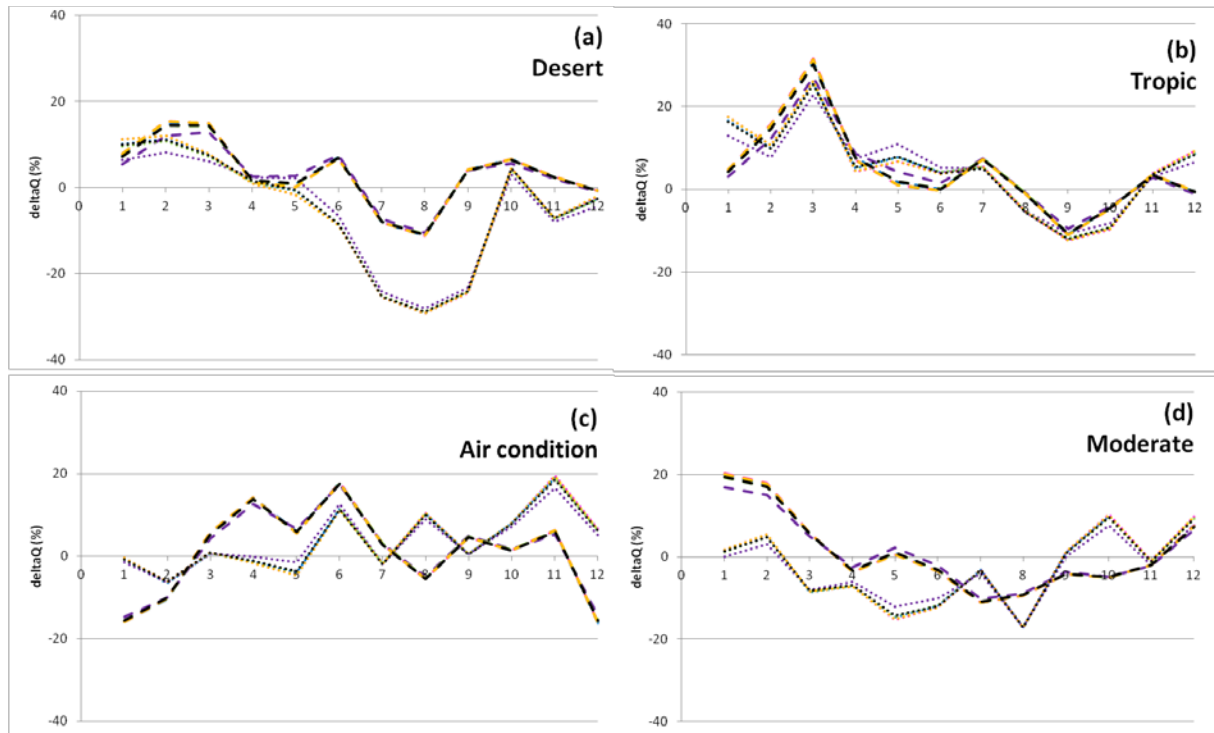


**Figure 40: Change in runoff for the measurement station Kienstock at the Danubue River using the optimal parameter sets from other measurement stations along the Danube river: Wallsee (91461.3 km<sup>2</sup>) in green, Korneuburg (101536.6 km<sup>2</sup>) in orange, Ybbs (92464.2 km<sup>2</sup>) in dark blue, Wildungsmauer (103992.7 km<sup>2</sup>) in pink and Achleiten (76653 km<sup>2</sup>) in violet compared to the optimal parameter set of the actual station (Kienstock, 95970 km<sup>2</sup>) as black lines. Figure 40 a-d are the different climate scenarios Desert, Tropic, AirCondition and Moderate, respectively. Although there is some noticeable difference (especially for the Tropic scenario), still the differences in runoff estimates due to the climate change scenarios are more of importance.**

Due to the fact that only a limited number of possible runoff scenarios can be passed on to the electricity sector model of WP3 (a simple time constraint), it has been decided that the changes in runoff due to the 4 different climate change scenarios will be used, and only a single optimal set of parameters from the hydrological model will be considered: The optimal parameter set was computed for the individual measurement stations by i) considering the whole available time series (minus a warm-up period of 1 year to reduce the influence of initial conditions) and ii) optimizing for  $\overline{NSE}$  (a maximum of the classical Nash-Sutcliffe efficiency (NSE) criteria and its two modified versions: the square-root transformed and the log transformed NSEs and the constraint that all NSEs have to reach at least 60%).

### 3.2.3.2 Uncertainty in the model structure

As there is only a single hydrological model applied and as such only a single model structure used, the results are compared to published data found in the literature. This is not

EL.ADAPT

straightforward though, as published data is usually referring to other reference periods or other future periods, used other downscaling methods or other discharge time series data. However, this approach has been chosen to demonstrate that the parsimonious rainfall - runoff model used herein is capable of reproducing possible changes that are observed with other more complicated model structures.

Figure 41 shows exemplarily that the model applied here yields reasonable runoff estimates for historical as well as future time periods. Compared to other model structures, the simple model is able to estimate runoffs adequately at the monthly time step.

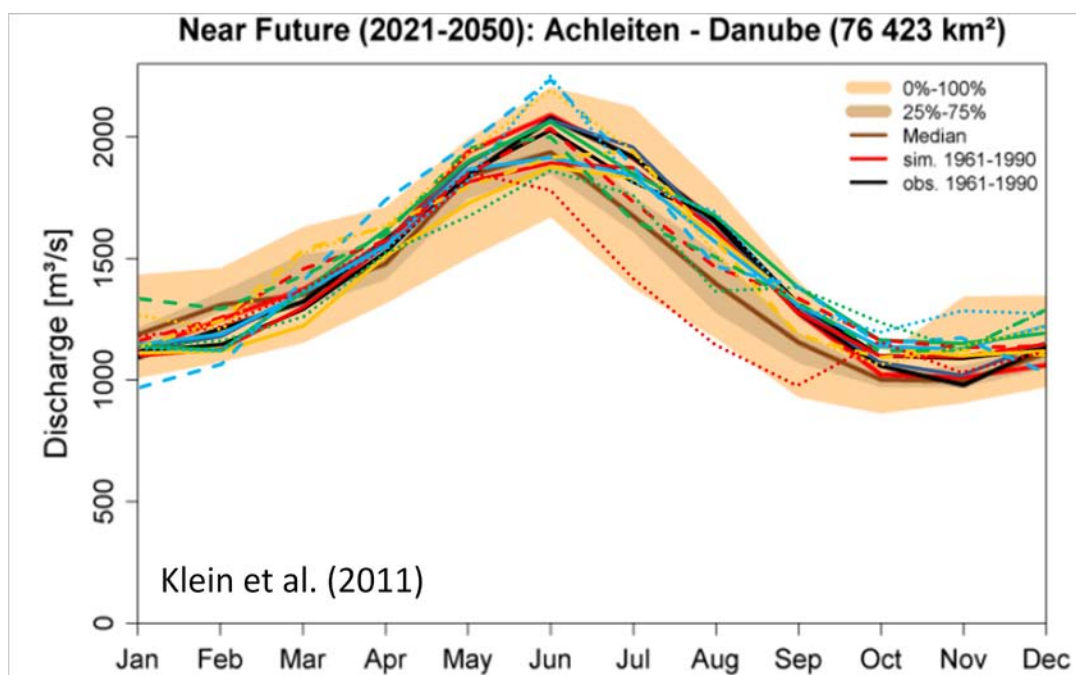


**Figure 41: Runoff computed for the station Achleiten along the Danube river. The “background” data are taken from Klein et al. (2011) and on top, the estimates from this work are displayed. For color coding of the data, refer to e.g. Figure 8. Note that the historical reference time period is the same for both studies (1961-1990). However, the future periods are different. The study of Klein et al. (2011) show the range of runoff estimates based on the whole ENSEMBLES scenarios available for the future period 2021-2050. In this work, we use the future periods 2011-2030 and 2031-2050 and the estimates are only based on 4 different climate scenarios. No range of runoff based on these 4 scenarios is computed as for this project all 4 different climate scenarios are used in further computations individually. However it is interesting to note that these estimates are to a great extent within the estimates from Klein et al. (2011) which give confidence in the simple, parsimonious model structure, that the major processes are covered and the model results are within a range of possible future runoff values.**

### 3.2.3.3 Uncertainty in the measured data (the observed runoff at individual stations)

Various discharge time series (data sources) were integrated into this analysis. More than 100 stations were used in this study, covering small, medium and large catchments all over the Greater Alpine Region (Figure 9). The discharge time series had various time periods from 10 to 60 years and were provided from various countries / services and in different file formats. All these measured data are not error free.

Although the data has been checked for outliers and plausibility, the authors cannot be aware of all the stations peculiarities or individual problems. However, as the hydrological model is a lumped-parameter model and runoff is computed based on the area-weighted catchment average of forcing parameters (temperature and precipitation), each station along a river is analyzed separately. This allows comparing the stations along a river and changes in runoff from station to station can be checked for plausibility (e.g. a change in the calibrated parameter set due to inflow from a major tributary). If changes in measured runoffs from one station along a river to the next station were noticeable, but no obvious explanations were found, the data set was not considered any further (e.g. the measurement station Landeck Perjn (3,503.1 km<sup>2</sup>) along the Inn river, where mean observed streamflow is only about half of what the stations up- and downstream show: 34.4 mm/month compared to 81.1 mm/month and 75.9 mm/month for the stations Prutz (2,461.5 km<sup>2</sup>) and Imst (3,842 km<sup>2</sup>)).

### 3.2.3.4 Summary concerning uncertainties in the hydrological modeling

To summarize, it was shown that the simple model structure seems to be sufficient to cover changes in runoff estimates for future climate scenarios on a monthly basis. The range of possible runoff estimates (“uncertainties”) arising from different equally like parameter sets is rather small (although not always negligible) compared to the range of runoff estimates due to different climate scenarios as forcing input. The estimated changes in runoff were passed on to the hydro power plant model (see section 3.4.4.1) by considering all four climate scenarios and a single optimal parameter set of the hydrological model only.

## 3.2.4 Concluding remarks

Estimates of changes in runoff for a large number of catchments covering the Greater Alpine Region were computed using a parsimonious lumped-parameter rainfall-runoff model. The calibrated and validated hydrological model has been used for simulating future runoff using precipitation and temperature input from four selected climate scenarios. Changes in the seasonality and a shift towards earlier runoff are observable in all four scenarios to some

extend and related to a warming trend. However, changes in precipitation are diverse for different scenarios (and time periods) and as such, a general trend in runoff for certain regions is not obvious. There are both positive and negative changes estimated. This can be related to the bandwidth (or uncertainty) of the different climate models/scenarios applied.

The effects of the four climate scenarios on runoff for the individual catchments is further translated to an estimate of future hydro power generation in WP3 taking every scenario into account separately. In general, the shift to increased runoff in the winter and spring months due to increases in temperature for all the four climate scenarios might indicate a positive effect on the power production, however the overall change remains more uncertain due to the precipitation patterns in the climate scenarios being more ambiguous.

### **3.3 Climate change impacts on households' electricity demand across Europe**

Summarizing the impacts of temperature on annual heating and cooling electricity demand for the climate reference period 1961-90 compared to the scenario periods 2011-30 as well as 2031-50 for Austria, clearly show the dominance of the effects of a decreasing heating electricity demand relative to the effects of an increasing cooling electricity demand (Figure 42). While in relative terms the temperature induced change in consumption for the period 2011-50 compared to the reference period 1961-90 lies, dependent on the climate scenario, between -7% and -14% for heating and between +37% and +144% for cooling, in absolute terms the decrease in heating is 4 to 20 times stronger than the increase in cooling. Assuming current consumption patterns, the net effect accounts for -270 GWh/a to -670 GWh/a, which equals -0.5% to -1.2% of the current level of total electricity consumption.

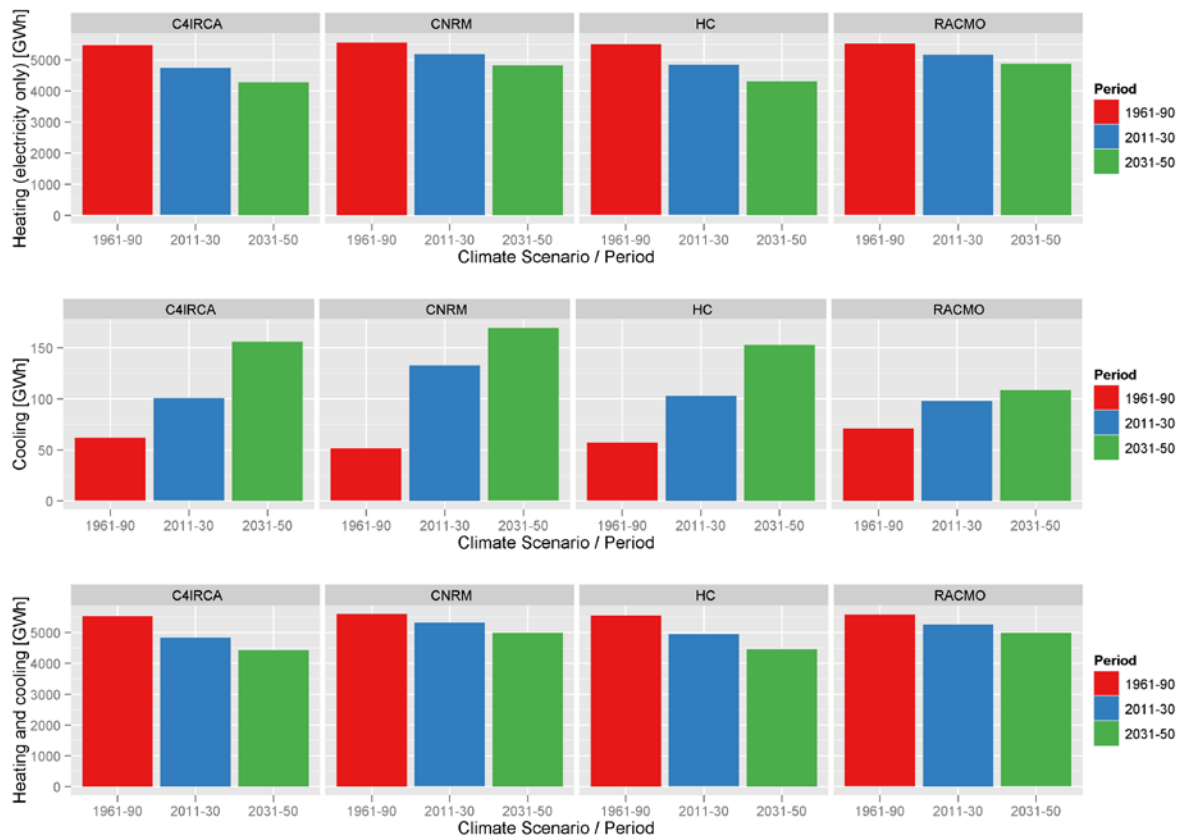


Figure 42: Climate induced change in electricity use for heating and cooling services in Austria

### 3.3.1 Cross-country comparison of heating and cooling electricity demand

While we have illustrated the statistical modeling results for Austria before, we now compare these results between countries. We begin with analysing results both for current climate conditions and for the current heating and cooling system.

As can be seen in Figure 43, in general less heating electricity is needed in countries with higher winter temperatures and more cooling electricity is needed in countries with higher summer temperatures, although the relationship is not straightforward. Even if we do not consider the special case of France, per capita heating electricity demand varies by more than a factor 3. The same is true for cooling electricity demand in countries with moderate temperatures. This again demonstrates very clearly that temperature is only one of many influencing factors.

Furthermore, it can also be seen that, while for most countries cooling electricity demand is only a small fraction of heating electricity demand (different y-axis scales!), it seems to grow exponentially at summer temperatures of around 23 °C. While the share of cooling electricity demand is currently less than 20 % of heating electricity demand in most countries, it is 35%

EL.ADAPT

in Spain and 80% in Italy, albeit cooling electricity consumption is observed on fewer days than heating electricity consumption.

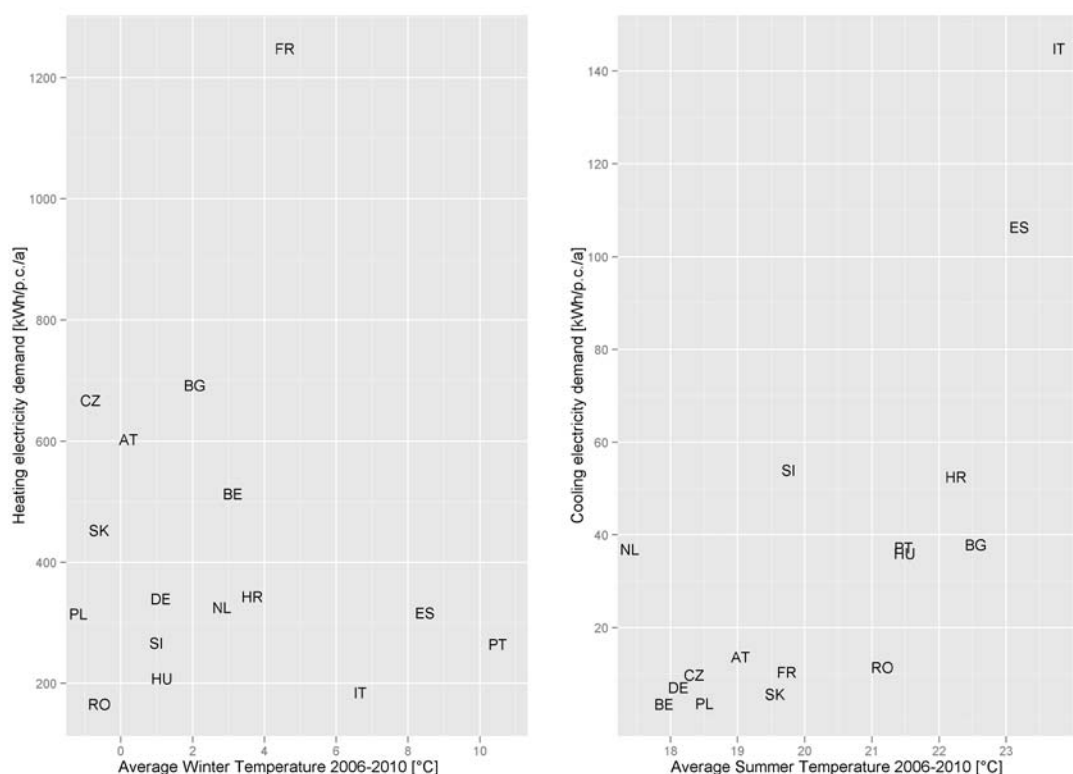


**Figure 43: Current winter/summer temperature compared to the annual per-capita heating/cooling electricity demand**

One particular way to illustrate modeling results for changes in temperature conditions is to compare average annual temperatures with the estimated current transition point temperatures (Figure 44). As can be seen, for most European countries, and therefore also for the Continental European average (*ALL*), temperature change even under the scenarios with the highest increase does not mean that the average temperatures will be above transition points. This means that until 2050 for these countries (except IT, ES, PT) heating will be an issue rather than cooling on the majority of days.

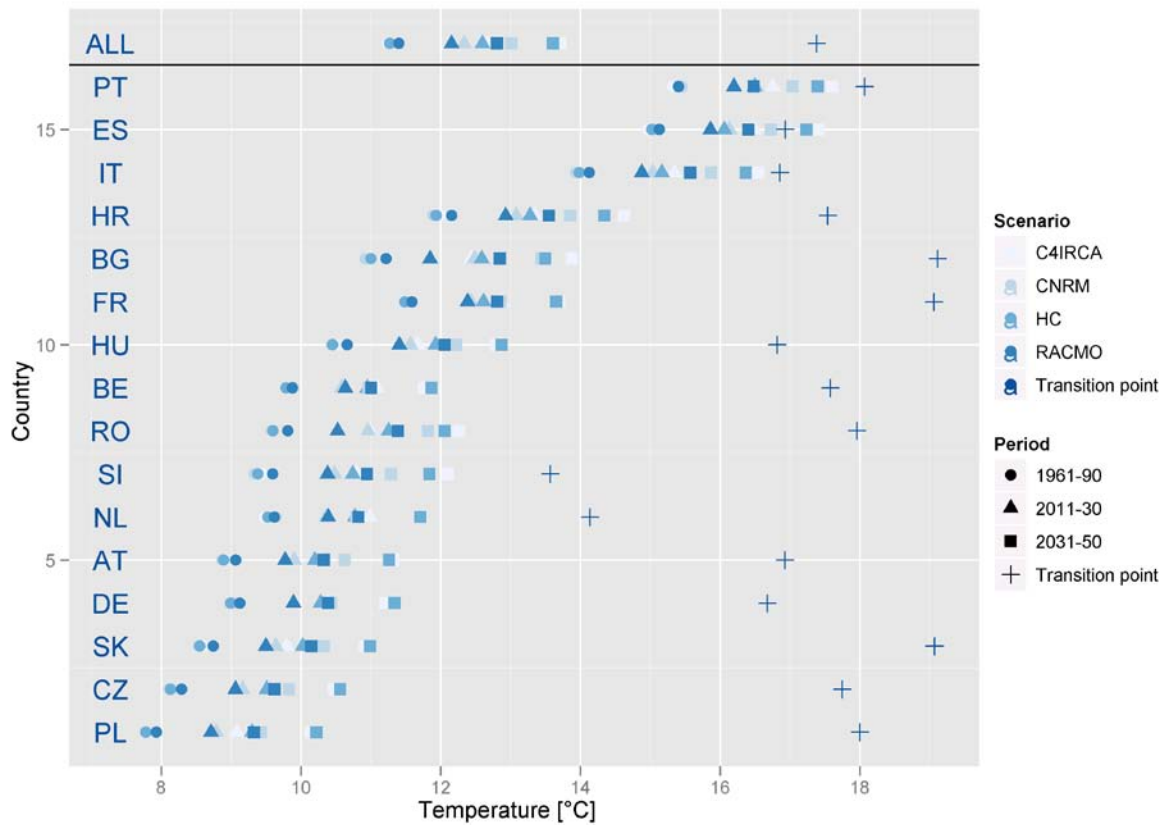


**Figure 44: Current transition points compared to the average temperature in the reference and scenario periods**

For our sample of 16 Continental European countries the absolute climate induced change of the four climate models reveals some very interesting patterns. Overall, warmer annual temperatures reduce the total electricity consumption in Continental Europe (Figure 45). While this effect is not as clear as described for Austria before, the ratio between the absolute decrease in heating and the absolute increase in cooling electricity demand is still 2:1 to 6:1, depending on which climate scenario is considered.

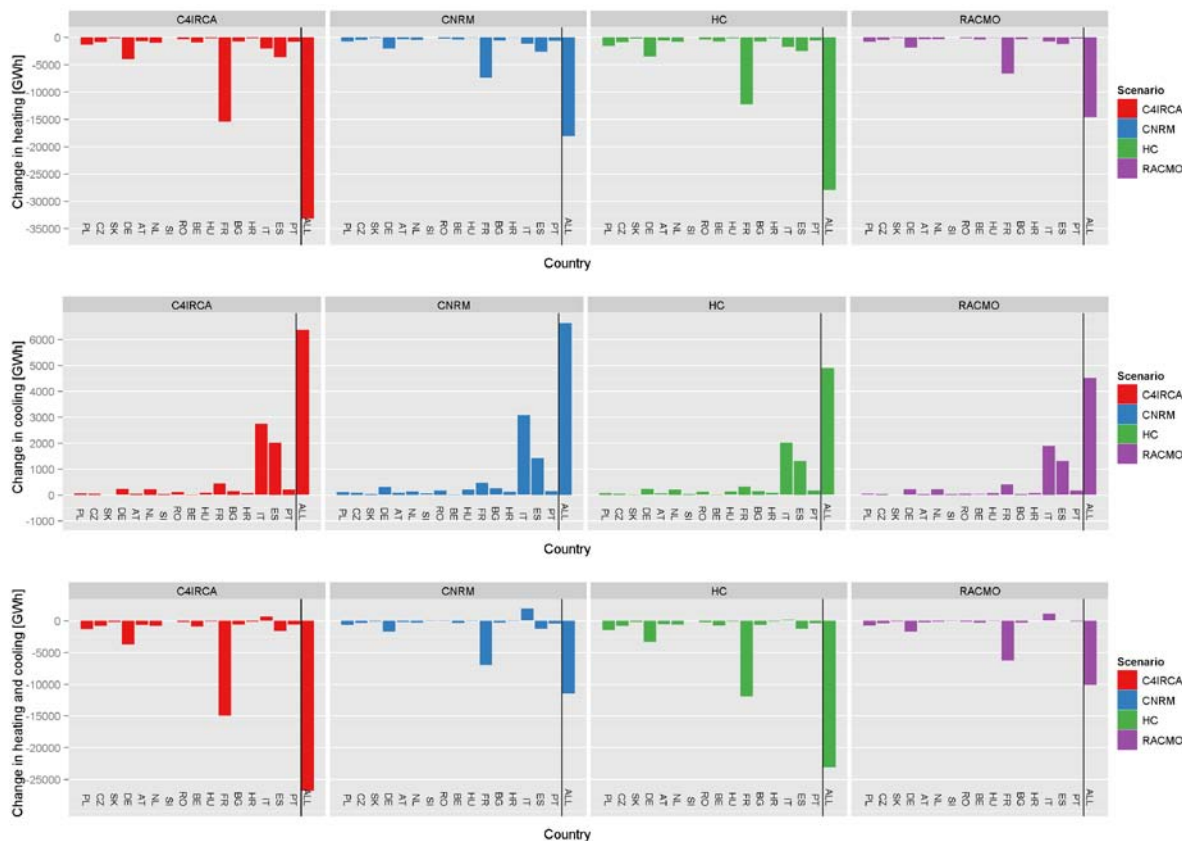


**Figure 45: Average climate-induced change in annual heating and cooling electricity demand compared between the reference period 1961-90 and the scenario period 2011-50**

In particular, this dominance of changing heating electricity demand can be explained by French energy policy, where electric heating has been strongly promoted since the 1970s. Due to this policy, the reductions in heating electricity demand in an unusually warm winter in France alone more than outweigh the additional demand for cooling in an unusually warm summer observed in the 16 Continental European countries for which calculations are done. In addition, other moderate-temperated countries like Germany and to a lesser extent also warmer-temperated countries like Italy and Spain face reductions in heating electricity demand due to milder winter temperatures.

However, even if overall heating effects dominate, cooling effects are not negligible for some countries with warmer summer temperatures. In particular, in Italy even nowadays annual cooling electricity demand almost equals annual heating electricity demand, but is potentially more threatening to network reliability due to its concentration to fewer peak days. Notably, for Italy the increase in cooling electricity demand is predicted to be stronger than the decrease in heating electricity demand for all climate scenarios, while for other countries with comparatively warm summer temperatures (Spain, Hungary, Croatia) overall effects do not point in a clear direction and differ strongly between climate scenarios. On the other hand, in

all other countries (12 out of 16!) cooling effects are estimated to be relatively small compared to heating electricity effects, even if some of these countries exhibit warm summer temperatures (Portugal or Bulgaria).

Putting these climate-induced reductions in heating electricity demand and increase in cooling electricity demand in relation to current total electricity consumption reveals that effects of these long-term climate changes are comparatively small compared to other potential driver of electricity demand (Figure 46). The overall long-term reduction for Continental Europe is -0.4 % to -1.1 % of total electricity use. To provide a comparison, this amount roughly equals the growth in electricity consumption in the EU-15 which was observed on average every 3 to 6 months in recent decades. However, in some countries with major electric heating or cooling activities climate induced changes are of course more pronounced, like up to -3 % in heating-dominated France and up to +0.6 % in cooling-dominated Italy.

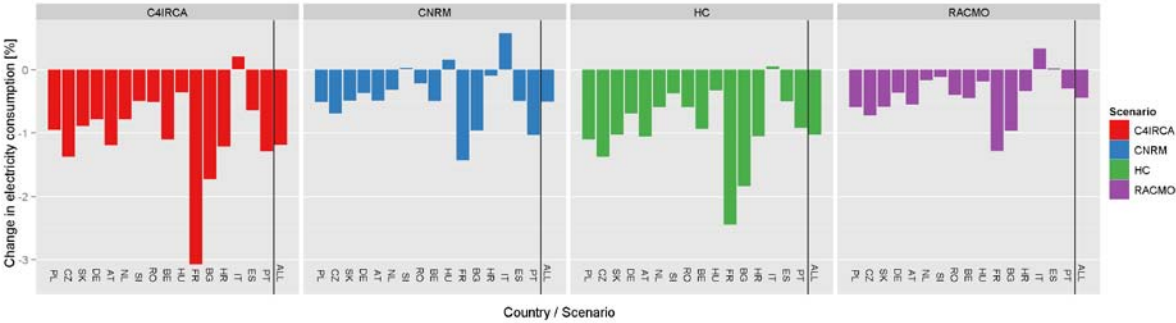


**Figure 46: Share of the climate induced change in heating and cooling electricity demand on total electricity demand**

To sum up the considerations on temperature-induced changes in heating and cooling electricity demand in this project, we draw the following conclusions:

- Unless Europe will switch to a very cooling intensive lifestyle or will abandon electric heating, climate change until 2050 will very likely have positive effects on electricity demand in the sense that overall less electricity will be demanded.
- In most (12 out of 16) countries for which calculations are done current cooling electricity demand is estimated to be relatively small compared to heating electricity demand, and climate change will lead to a reduction of electricity consumption. While in several countries with comparatively warm summer temperatures (Spain, Hungary, Croatia) the size and seasonal distribution of the climate change signal might determine the direction of the effect, for Italy the increase in cooling electricity demand is predicted to be stronger than the decrease in heating electricity demand for all climate scenarios. This increase in Italy might have major implications for the Austrian electricity system.

- In accordance with other studies it needs to be highlighted that, compared to the potential impacts of changes in income, demography, prices and technology, these effects of climate change will be small. The amount of electricity used for heating and cooling purposes is less determined by future temperature but rather depends on energy policy and the willingness to design a low-carbon, energy-efficient heating and cooling system, which is flexible enough to adapt to changing temperatures.

Further investigations in the EL.ADAPT project will contribute to an understanding on how the demand effects described in this part will interact with supply side effects, such as potential reduced hydropower availability in summer or changes in the availability of wind power and photovoltaic energy production. This will be important to give an assessment of the total effects of climate change on the electricity sector. In addition, energy models will be coupled with a macro-economic CGE model in order to examine spill-overs to other sectors of the economy and to be able to determine overall macro-economic effects.

### **3.3.2 Uncertainties related to future heating and cooling electricity needs**

For most Continental European countries a temperature-induced demand reduction is observed, that means that decreases in heating electricity demand more than outweigh increases in cooling electricity demand. However, these results were obtained using a strong assumption, namely that the sensitivity of heating and cooling systems stays the same as in the calibration period 2006-2010. In other words, cooling demand is not expected to change for other reasons than temperature increase, e.g. general changes in behavior and comfort levels, a higher market penetration of cooling devices, changes in the efficiency of cooling technologies. Likewise, heating electricity demand might not only be influenced by temperature change, but e.g. also by efforts to improve building insulation, the change to other less-carbon intensive heating fuels, or in the other direction, the use of additional electricity for powering thermal heat pumps. Many of these non-climatic changes are implicitly also strategies to adapt to climate change, or might be driven by mitigation policies.

While the focus of this study is not on describing the total effects of these changes in heating and cooling technologies and consumer behavior in more detail, in this section we will show (based on some assumptions) what happens if the relationship between temperature and electricity consumption changes over time. For the sake of simplicity, we carry out a sensitivity analysis for Austria based on the following change rates:

- The future development of heating electricity demand is highly uncertain. On the one hand, it might become significantly lower due to energy policies like better building insulation (as proposed by the EU directive 2010/31 on the energy performance of buildings) or a switch to other than conventional electricity heating systems. On the other hand, it might even increase in the coming decades for the reason that a

lowering heating energy demand due to better building insulation or milder winters will make heating with electricity more attractive again (because fixed costs are comparatively low to other technologies). The sharp increase in installed heat pumps, mainly used for low-energy houses, as well as the fact that the share of electricity based heating systems is higher in countries with milder winter temperatures, point in this direction. Therefore, in the following we assume growth rates for heating electricity demand of at minimum -2% p.a. (HED.low), 0% p.a. (HED.medium) and at maximum +2% p.a. (HED.high).

- Basically, it needs to be expected that cooling electricity demand in Europe will further grow, not only because of climatic pressure but many other reasons. Comprehensive studies on this topic, like Adnot et al. (2003), assume annual growth rates for Austria of around 2% p.a. until 2020, but much stronger growth rates for Germany and France, which are countries with a similar summer climate to Austria. Therefore, for the temperature sensitivity of cooling demand we assume a best case growth rate of 0 % p.a. (CED.low), which would presumably only be achievable with very stringent regulatory measures, an intermediate growth rate of +2 % p. a. (CED.medium) and a high growth rate of +4 % p.a. (CED.high).
- Results from this sensitivity analysis (see Figure 47) allow understanding some very distinctive features of future heating and cooling electricity demand in Austria. Firstly, even if cooling electricity demand would increase much faster than heating electricity demand (up to + 4 % p.a. faster) temperature-related peak demand for single days would still be higher in winter until 2050. Secondly, as the average annual temperature is still far below the transition point temperature, the overall annual change in electricity demand will be almost certainly negative. This means that climate change will very likely lead to decreasing electricity demand in Austria. Dependent on the climate scenario, the difference in the annual growth rate of the temperature sensitivity of cooling and heating electricity demand would have to be 7 % to 14 %. This unlikely case would mean that under a constant heating sensitivity, the cooling sensitivity would need to double every 5 to 10 years.

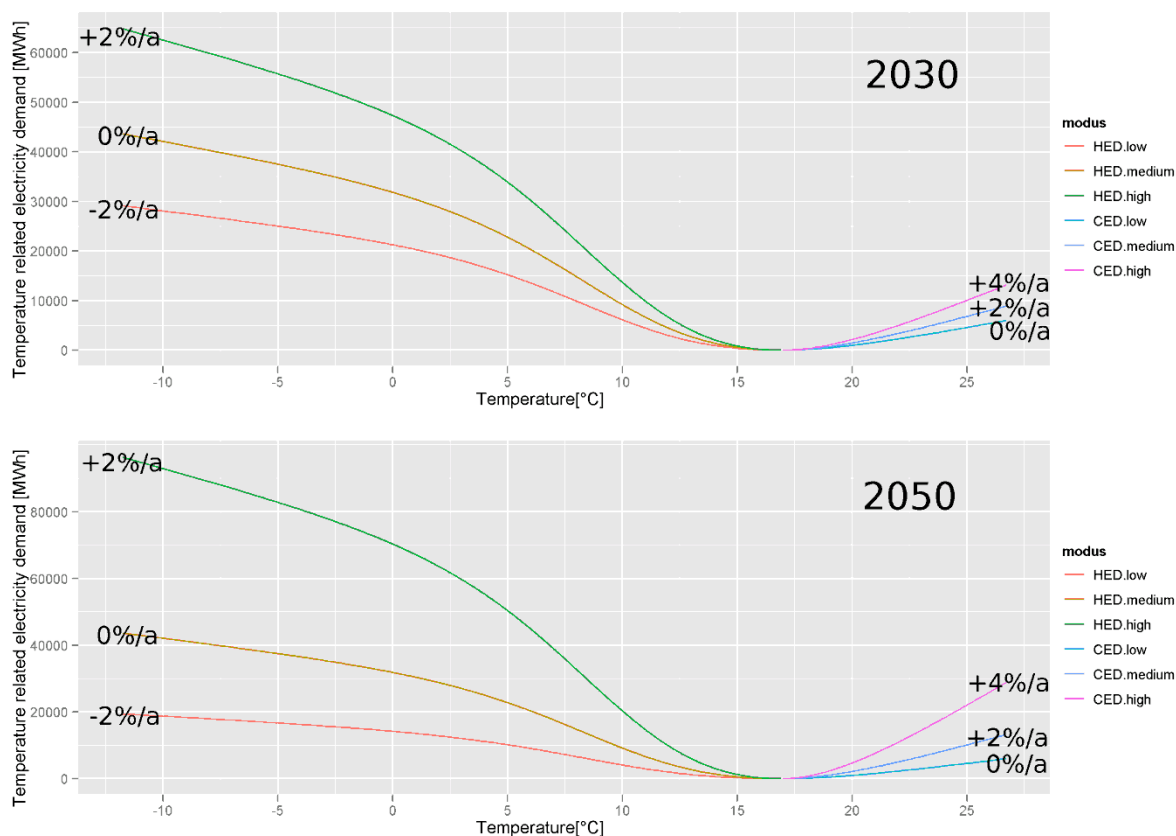


**Figure 47: Sensitivity analysis for different assumptions on changes in the temperature sensitivity of heating and cooling electricity demand in Austria**

Doing the same calculations for Continental Europe largely confirms the results obtained for Austria (see Table 9). The difference in the annual growth rate of the temperature sensitivity of cooling and heating electricity demand would have to be on average 5 % to 9 %<sup>7</sup>, again dependent on the climate scenario. This high rates are not surprising given the fact that 70 % of the electricity consumption takes place in countries with relative moderate temperatures, while only 30 % are consumed in the warmer southern countries (BG, HR, IT, ES, PT)<sup>8</sup>. In addition, for some of the latter countries, such a strong growth difference between cooling and heating would hardly be feasible due to network constraints.

<sup>7</sup> Note that the lowest value of 5 % corresponds to the scenario CNRM, where temperature change is much stronger in summer than in winter and the impact on cooling is therefore stronger than the impact on heating.

<sup>8</sup> The overall picture presented in this analysis may not change when extending the scope to the remaining countries in Europe: Effects for all the heating-oriented Scandinavian, Baltic and Non-EU-Eastern-European countries as well as Great Britain and Ireland should far outweigh the dominance of cooling in Greece, Non-EU-Balkan states as well as the European part of Turkey.

**Table 9: Difference in the annual growth rate of cooling and heating demand, where additional cooling electricity demand would equal reduced heating electricity demand**

Country	Scenario			
	C4IRCA	CNRM	HC	RACMO
PL	18,66	12,31	18,10	18,91
CZ	17,06	10,36	16,61	15,64
SK	20,10	12,02	18,07	20,05
DE	15,95	10,69	15,16	12,73
AT	14,30	7,16	12,96	12,09
NL	7,17	5,07	6,33	2,40
SI	6,93	0,64	5,84	2,96
RO	7,70	3,85	7,66	11,72
BE	22,50	17,11	21,05	16,40
HU	5,95	-1,53	4,10	4,08
FR	16,72	12,41	17,07	12,99
BG	8,24	4,26	8,41	13,95
HR	7,28	0,53	6,17	3,39
IT	-1,19	-4,95	-0,05	-4,02
ES	2,85	2,96	3,22	-0,37
PT	6,84	7,24	6,24	2,80
ALL	7,96	4,75	8,49	5,68

Summing up, it can be said that while there exist large uncertainties on the development of future heating and cooling needs, results are relatively robust in the sense that only a radical change in patterns (much less heating with electricity, much more cooling) would mean that the described positive effects for Continental Europe would turn into negative ones. Of course, one needs to be aware of the fact that our modeling activities do not account for electricity prices.

### 3.3.3 Impact on electricity demand

Total electricity demand needs to be broken down in two main components: industry demand and demand of private households. The climate change signal affects the electricity demand of private households in terms of an inner-annual demand shift due to a change in heating behavior in ATLANTIS. The total changes in electricity demand induced by climate change are considered within the CGE model.

### 3.4 Climate change impacts on the electricity sector

Climate change impacts on the electricity sector can be categorized in two fields: the impacts on the electricity generation in terms of generation technologies directly influenced by changes of climatic parameters (renewable energy sources), and the impacts resulting from those changes in electricity generation as well as electricity demand, regarding the electricity market or CO<sub>2</sub> emissions, for example.

#### 3.4.1 Impacts on electricity generation

The direct impacts of long-term average climate changes can be estimated by investigating changes of the standard capacity<sup>9</sup> of renewable energy sources. Within the model chain briefly described in chapter 2.4.2, the influence of changes in river runoff, average wind speeds and average solar radiation on hydro power, wind power, solar power and the natural inflow into reservoirs of storage power plants are analyzed. The results are given in relative changes of standard capacity compared to the BASE scenario (without consideration of climate change) and are shown for Continental Europe in Figure 48 and for Austria in Figure 49<sup>10</sup>.

---

<sup>9</sup> „Standard capacity“, „standard operation capacity“ or „standard production capacity“ is defined in this study as the long-term average annual net electrical energy output. These terms are commonly used with generation units using renewable energy sources.

<sup>10</sup> The results of all other country aggregates can be found in the annex.

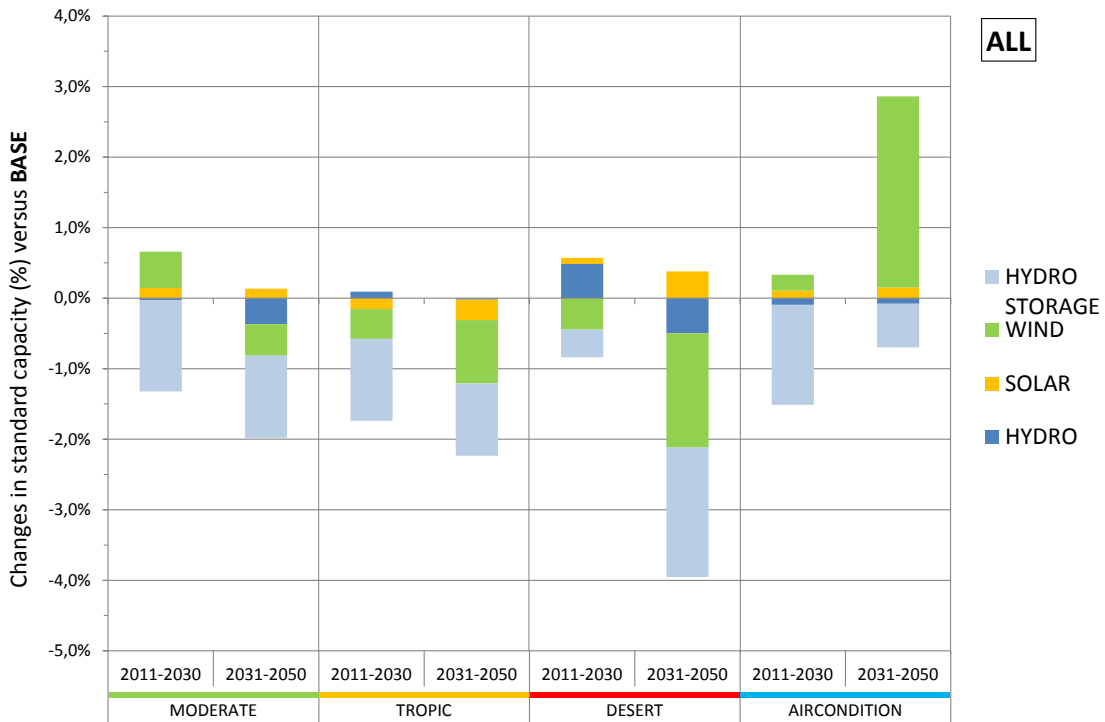


Figure 48: Changes in standard capacity in Continental Europe11



Figure 49: Changes in standard capacity in Austria

<sup>11</sup> Please note: for hydro and hydro storage, only the Greater Alpine Region (GAR) is considered

Figure 48 shows that the climate change leads to an increase of 3 % of total standard capacity in Continental Europe in the best case (AIRCONDITION), respectively to a decrease of -4 % in the worst case (DESERT scenario). The most affected technologies in this simulation are wind power, due to the high share of installed capacities, and hydro storage power plants. Regarding hydro storage, the uncertainties of the results are presumably higher than for all other technologies, mainly because of the simplified approach used to model this technology. As expected, the MODERATE scenario shows the lowest changes, though facing a negative impact similar to TROPIC. To sum it up, it can be seen that climate change impacts show negative trends in most cases. However, the variation bandwidth is not very high.

In Austria, the bandwidth of possible impacts is slightly higher compared to Continental Europe, reaching from an increase of about 2.5 % in the best case to a decrease by -5 % of Austria's standard capacity in the worst case. However, the TROPIC scenario shows positive results for Austria in contrast to the European trend. Due to its high share in electricity generation in Austria, hydro power is the most affected technology and is also responsible for the positive results in the TROPIC scenario.

Besides the changing annual production, seasonal shifts are very important for the electricity system. All electricity generation technologies that directly depend from climatic parameters feature their own seasonally and regionally different characteristic. For example, hydro power in Austria reaches its maximum production in spring, due to melting snow in the Alps, and its smallest production usually in February. In contrast, hydro power in Spain normally reaches its maximum in winter (January or February), cf. (Schüppel, 2010) and (Maier, 2011).

As an example, the seasonal shifts of hydro power are shown for Continental Europe (GAR) in Figure 50 and for Austria in Figure 51. The trends are quite the same in both cases, pointing to an increased generation in winter and a decrease in summer, probably resulting from the general trend of rising temperatures throughout all climate scenarios. For those countries in Continental Europe having their peak load in winter, this is a positive development, because the additional energy yield caused by the climate change supports and maybe stabilizes the energy system. The simulation results for Austria show a more distinct shift towards the winter months, although this has to be put into perspective, since the GAR is only considered within the results for Continental Europe.

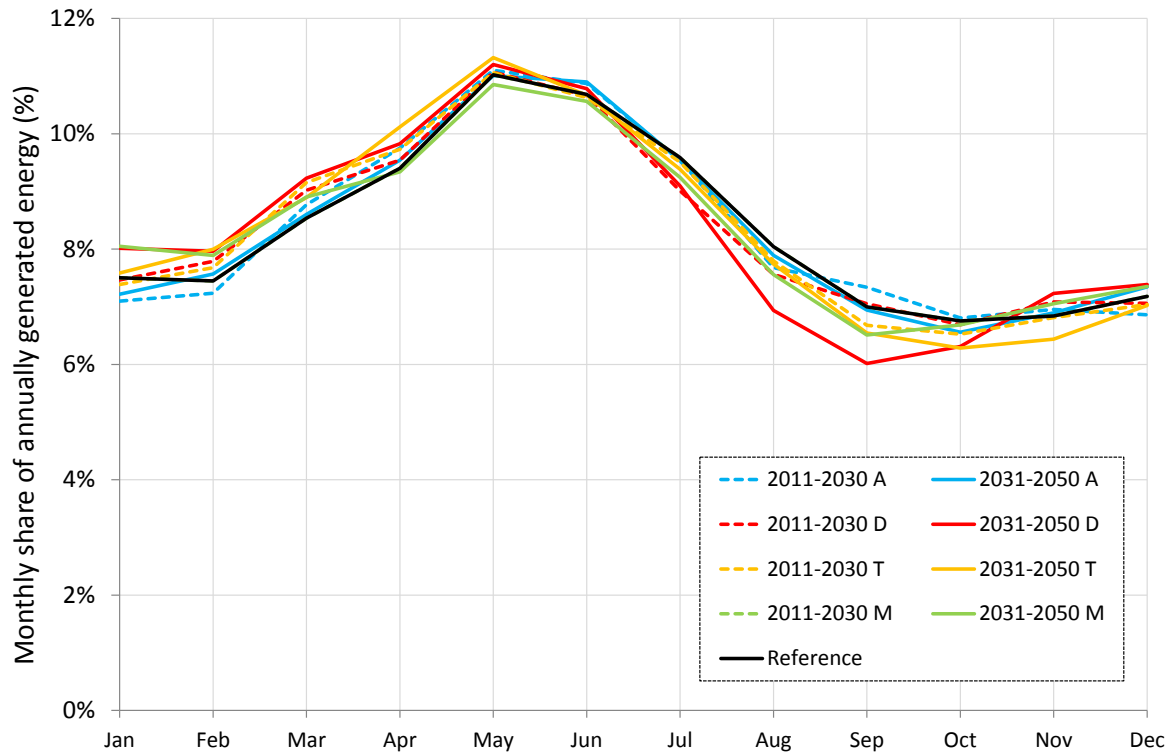


Figure 50: Seasonal characteristics of hydro power (run-of-river) in Continental Europe (GAR)

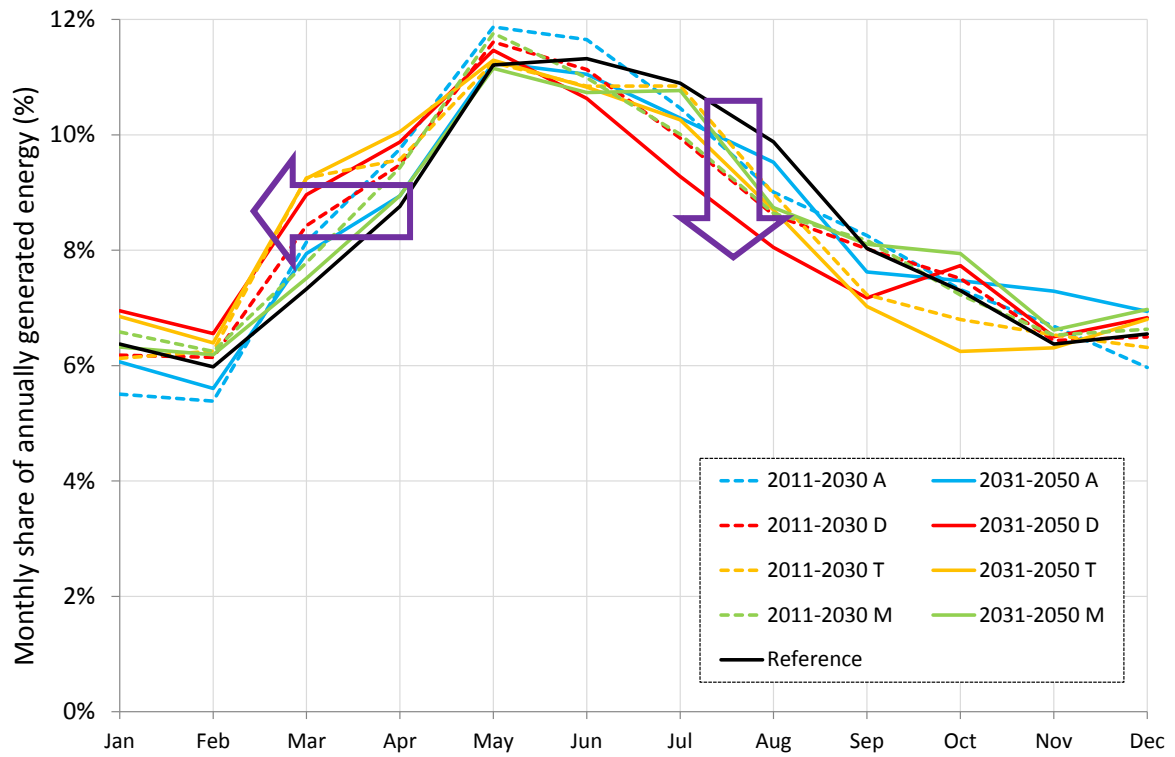


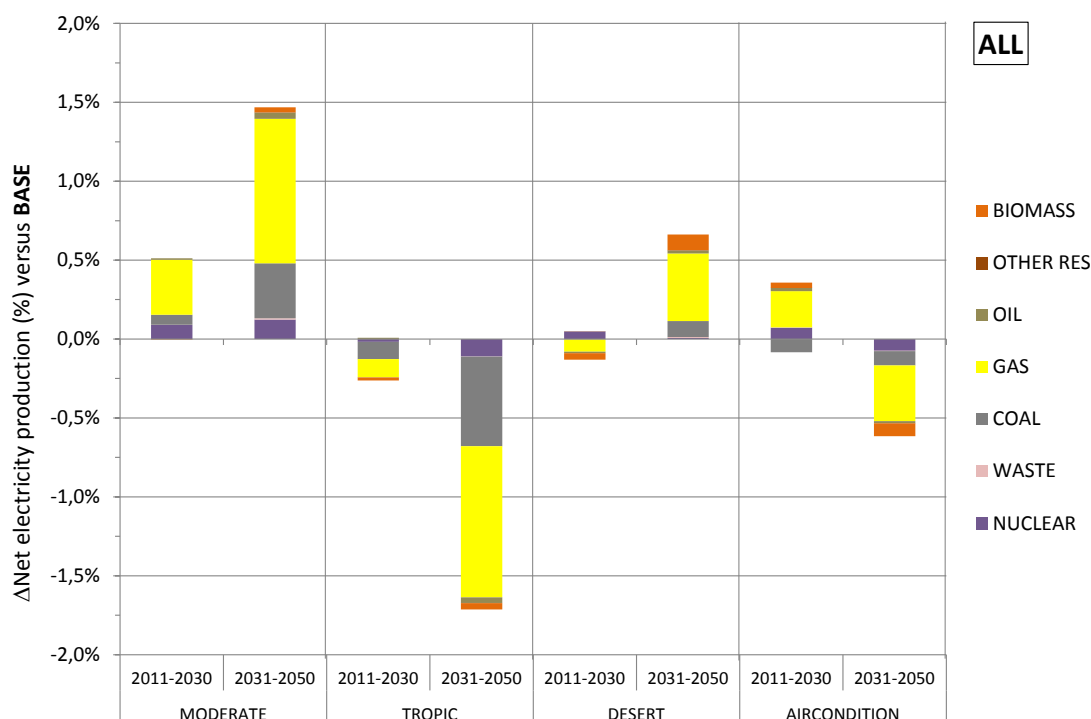
Figure 51: Seasonal characteristics of hydro power (run-of-river) in Austria

EL.ADAPT

Wind power and photovoltaics in Continental Europe face a slight increase in winter and a slight decrease in summer. In the MODERATE and the DESERT scenario, those trends are reverted in the climate period 2031-2050, almost compensating the changes of the previous period. In Austria, there is no general trend for wind power derivable from the simulation results, whereas photovoltaics show a generation shift from winter towards summer. This effect may support the electricity system to compensate increasing demand in summer months due to electricity-powered air conditioning systems.

Since generation has to be equal to demand within the electricity system, the impacts of climate change on renewables and electricity demand need to be compensated by available conventional generation capacities. Depending on fuel prices and CO<sub>2</sub> price, different technologies may be dispatched in order to perform that compensation.

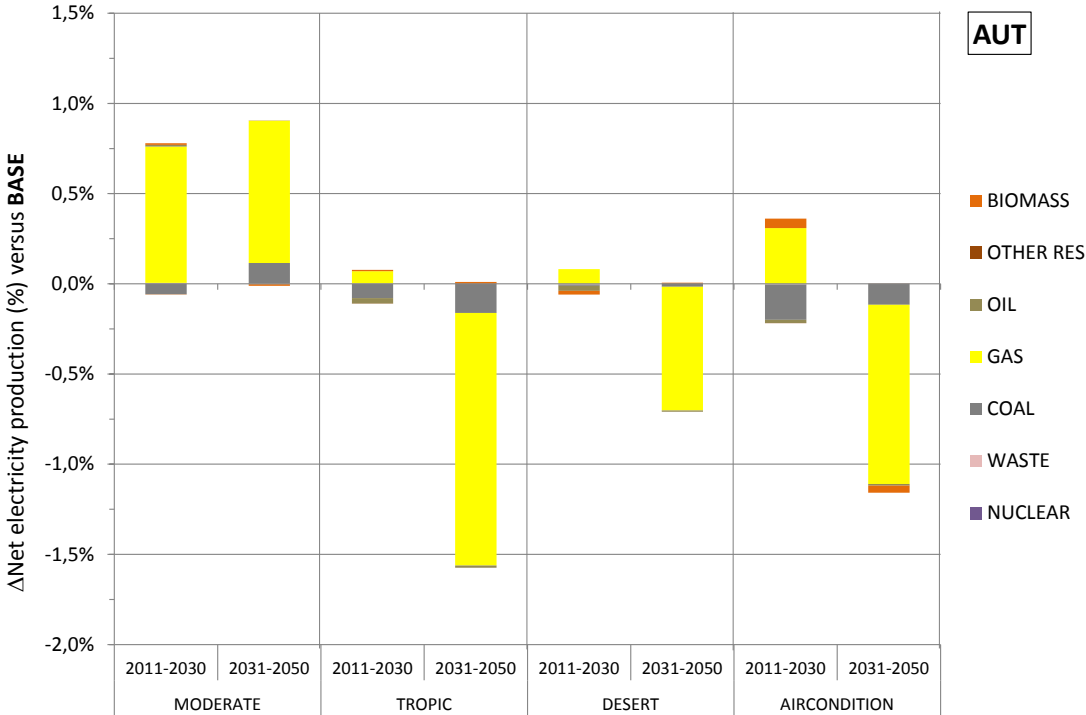
Figure 52 shows the changes in average net electricity production of conventional generation technologies in Continental Europe per climate scenario and period, compared to the total net electricity generation. It can be seen that gas fueled power plants contribute the major share to compensate changes. Due to merit order effects, this is an expected result: this technology determines the market clearing price (MCP) in many cases. Thus, it is the most sensitive technology to changes in demand or renewable energy sources.



**Figure 52: Avg. changes in net electricity production of conventional technologies in Continental Europe**

The shown changes are made up by two concurrent effects: either the impacts on the electricity demand dominate, or the impacts on renewable energy generation. In the case of

the MODERATE and the DESERT scenario, both effects work together: decreasing generation capacities occur along with the highest increase of electricity demand (see chapter 3.4.2). Likewise, in the AIRCONDITION scenario the increasing standard capacity (in the second period) occur along with a decreasing demand, leading to a decrease of conventional generation. In the remaining TROPIC scenarios, both effects compete. In doing so, the decreasing demand outweighs the decreasing generation, again leading to a decrease of generation from conventional technologies.



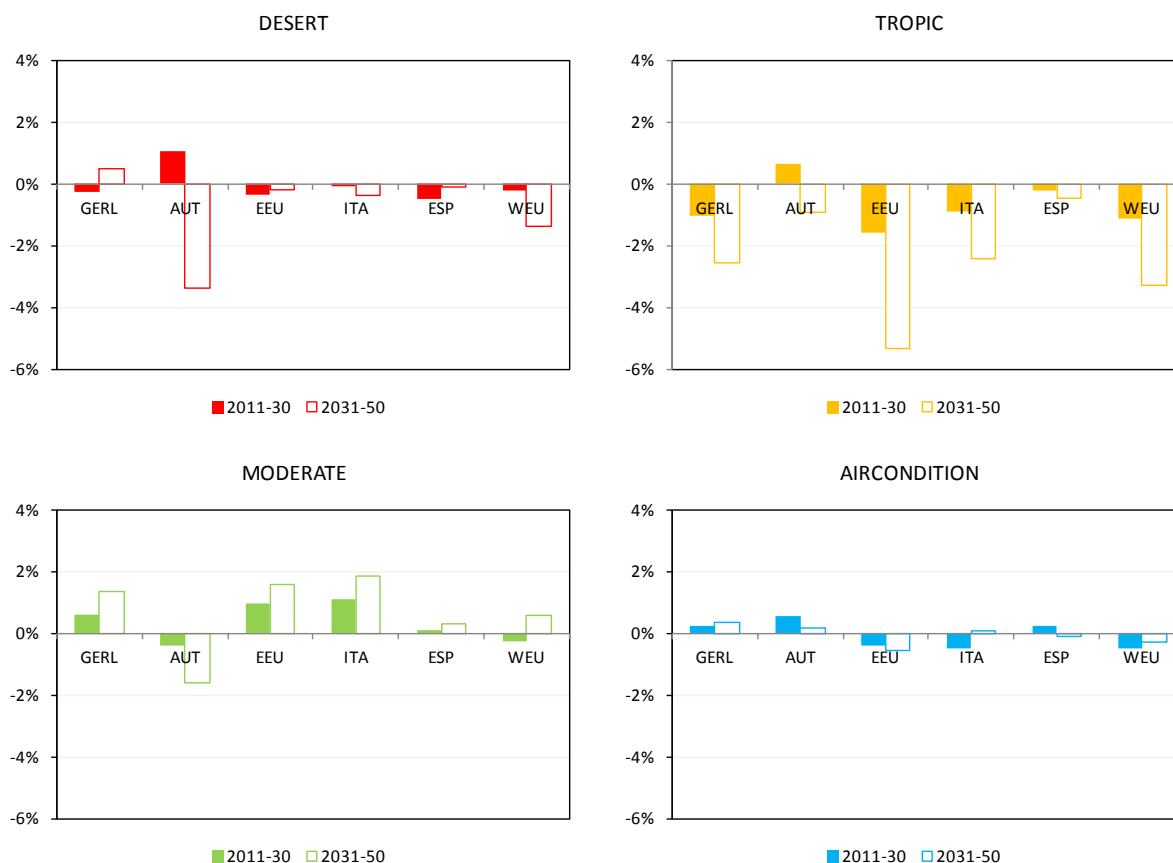
**Figure 53: Average changes in net electricity production of conventional technologies in Austria**

Figure 53 shows the changes in average net conventional production for Austria, compared to the total net electricity generation. Gas-fired power plants are contributing a vast share to compensate climate change impacts, making other technologies almost negligible. However, if one single country is investigated, the cross-border electricity trade has to be considered (see 3.4.3).

Finally, an overview of climate change impacts on the electricity generation is given in Panel 6 illustrating the respective results on (physical) power generation compared to BASE. In TROPIC, impacts are the strongest among all climate scenarios. In nearly all regions, power generation is decreasing relative to the BASE scenario (with much stronger effects in the second period under consideration). This result is mainly driven by reduced energy demand because of a higher CO<sub>2</sub> price. In contrast, in MODERATE power generation is rising in most regions due to risen (intermediate) demand. We find that in AIRCONDITION

EL.ADAPT

impacts on power generation are negligible. Also DESERT does not affect power generation strongly, except for AUT and WEU in the second period under consideration (This is because of less heating demand in winter season).

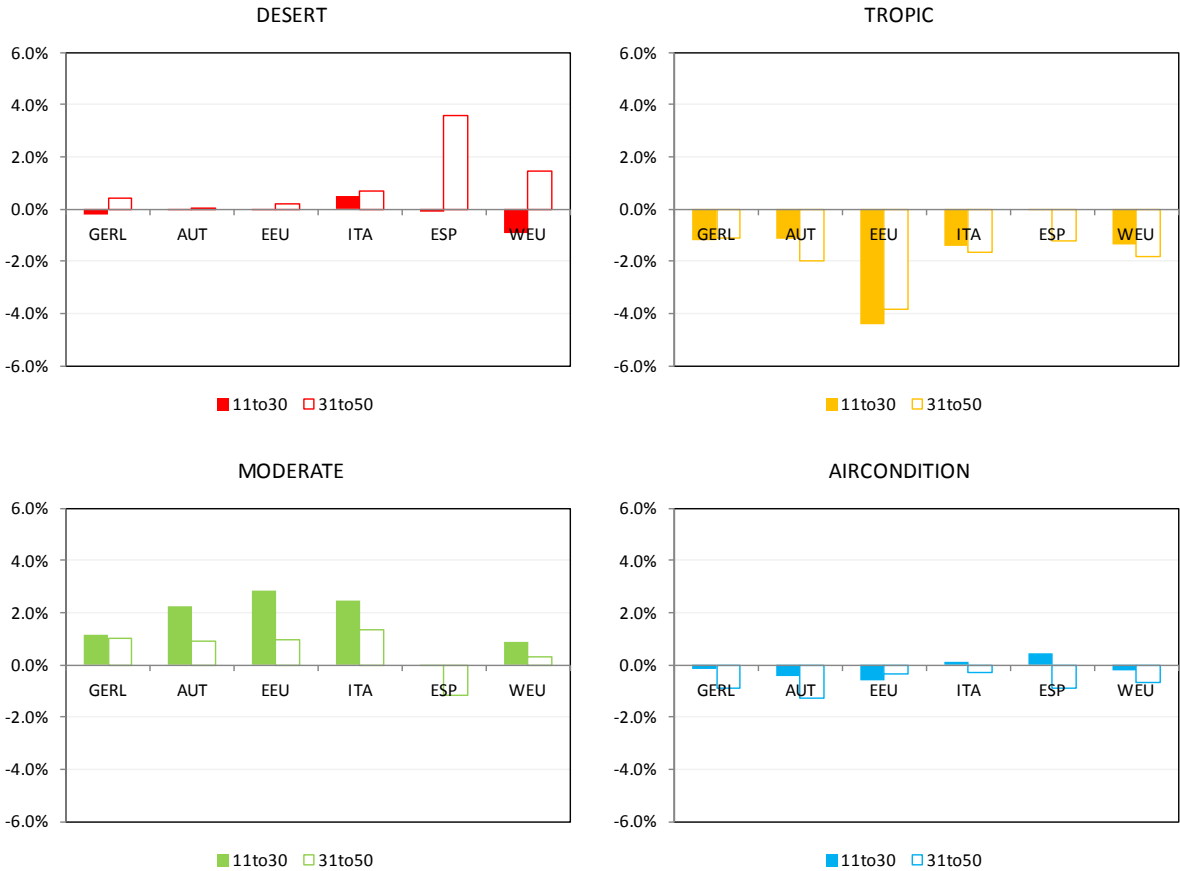


**Panel 6: Percentage change of power generation (based on TWh) for all climate change scenarios, on average for periods 2011-30 and 2031-50 relative to BASE.**

### 3.4.2 Impacts on the electricity demand

We start by analyzing impacts of climate change scenarios on intermediate electricity demand (i.e. demand by other sectors) as this is a main driver for the output level of the electricity sector. Panel 7 shows the average impact for all climate change scenarios compared to BASE (scenario with climate policy but without climate change). In general, we find that intermediate electricity demand is falling relative to BASE in TROPIC and AIRCONDITION, while it is rising in DESERT in MODERATE. As all sectors are affected by climate policy, this result on intermediate electricity demand is mainly driven by changes in CO<sub>2</sub> prices and electricity prices which differ across scenarios due to different generation mixes. For instance, in TROPIC CO<sub>2</sub> prices are higher than in the other climate scenarios and thus energy demand is falling implying reduced electricity use. The same holds for the scenario AIRCONDITION, but on a smaller level. In contrast, MODERATE is characterized

by a rise in electricity demand because of a stronger shift from fossil fuels to electricity in domestic production and because of a CO<sub>2</sub> price is below the BASE-level.



Panel 7: Average changes in intermediate electricity demand compared to BASE.

### 3.4.3 Impacts on the electricity market

In this chapter, the impacts of climate change on the electricity market are illustrated. In special, changes in wholesale market prices of Austria’s price zone, production costs and CO<sub>2</sub> emissions of the electricity sector are investigated.

Austria and Germany are interconnected by cross-border transmission lines without declared congestions (ENTSO-E, 2013). Thus, both countries share the same market area and, resulting from that, the same wholesale market clearing prices (MCP). However, it follows that impacts on German generation and demand will influence the market price in Austria and vice versa. Figure 54 shows the bandwidth of the climate period’s average maximum and minimum MCP as well as the corresponding period mean value. The diagram shows that the mean MCPs of the climate change scenarios (colored diamonds) are at the same level as the BASE scenario (black diamonds). Thus, climate change does not affect the mean value of the wholesale MCP. However, changes in the bandwidth can be observed. The

EL.ADAPT

maximum MCP -representing the peak load price - is significantly reduced in the AIRCONDITION scenario 2031-50, possibly caused by the sharp increase of hydro generation and wind power induced by climate change. The minimum value also is significantly reduced in the TROPIC scenario 2031-2050. In this case, the decrease is presumably caused by a decrease of electricity demand in Austria.

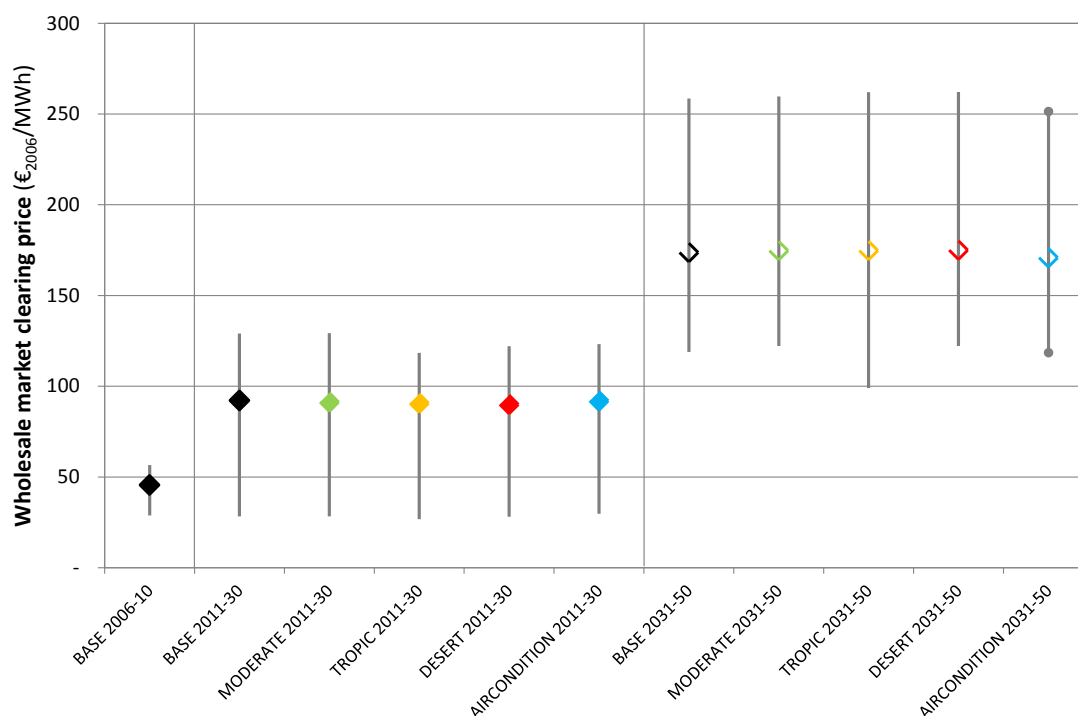


**Figure 54: Bandwidth (grey) and mean (diamonds) of wholesale market prices by climate scenario**

The simulated changes in average variable production costs of electricity in Continental Europe are shown in Figure 55, and the impacts in Austria are shown in Figure 56. In both diagrams, the same trends are depicted, although having different intensities.

Basically it can be found that generation costs will rise in case of decreasing standard capacities induced by climate change, due to conventional power plants compensating the missing energy (MODERATE and DESERT scenario). However, the TROPIC scenario faces a decrease of standard capacities in Continental Europe, showing a reduction in production costs anyway. This is presumably caused by the comparably strong decrease of electricity demand.

In the DESERT scenario, the increase of production costs in Austria is comparably low in contrast to Continental Europe. Founded by the increasing standard capacity in Germany (see annex) and the observed increase of electricity imports to Austria, losses of standard capacity in Austria may be compensated by German power plants rather than “homemade” conventional generation in this scenario.

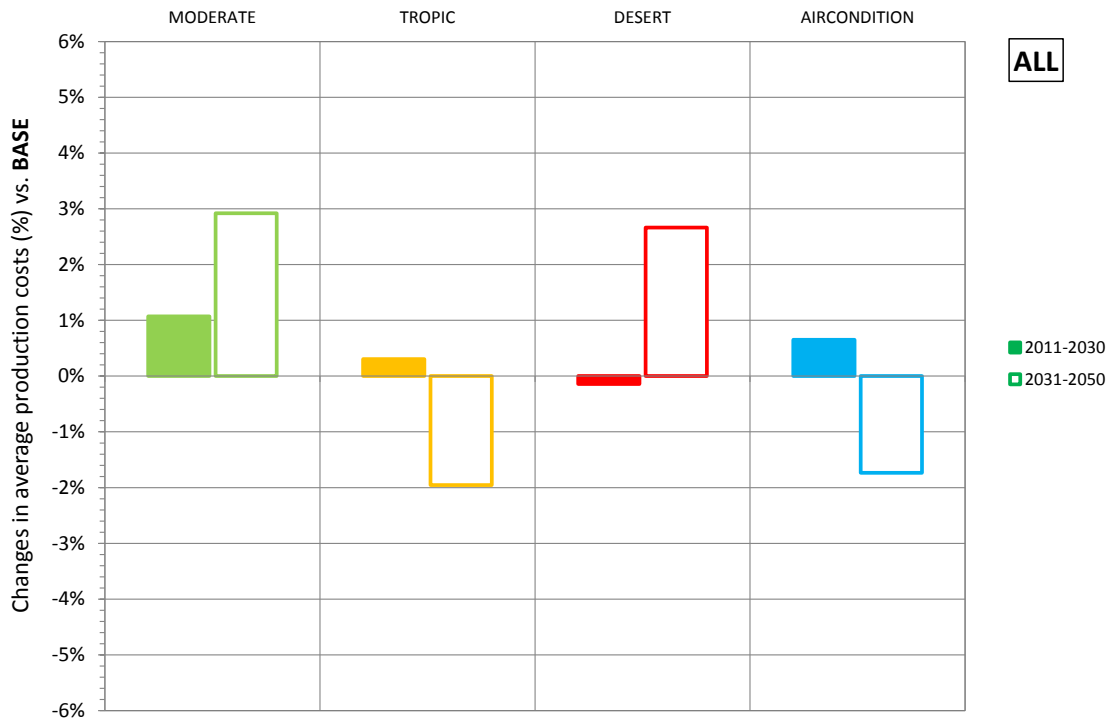


Figure 55: Changes in average variable production costs in Continental Europe

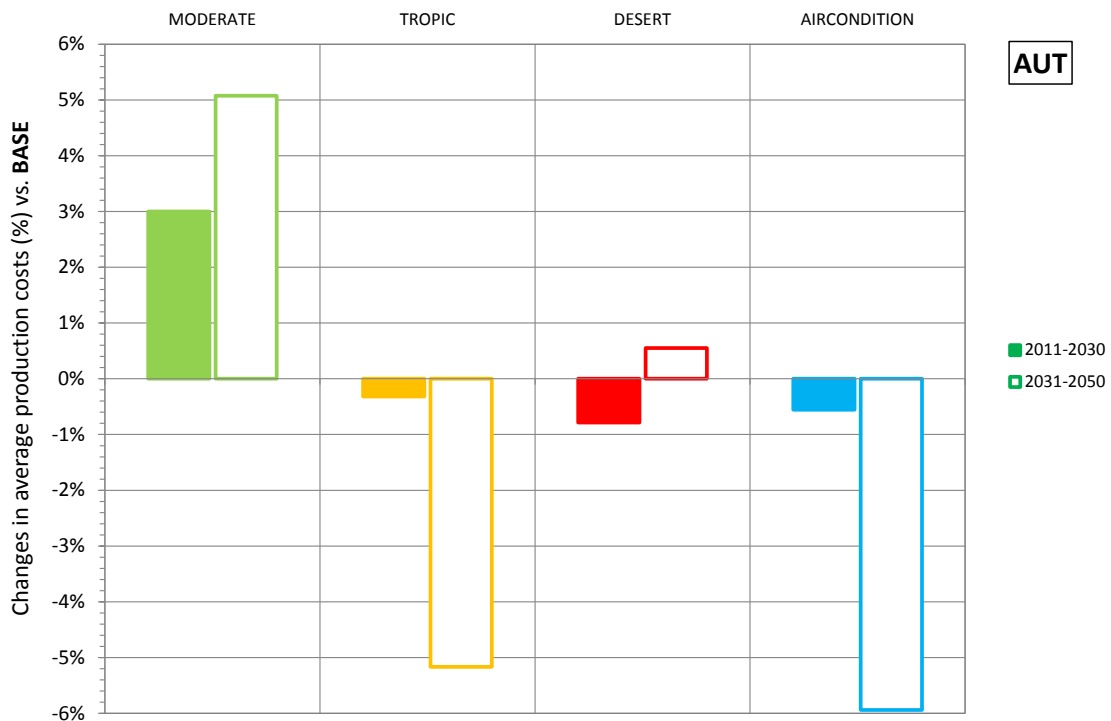
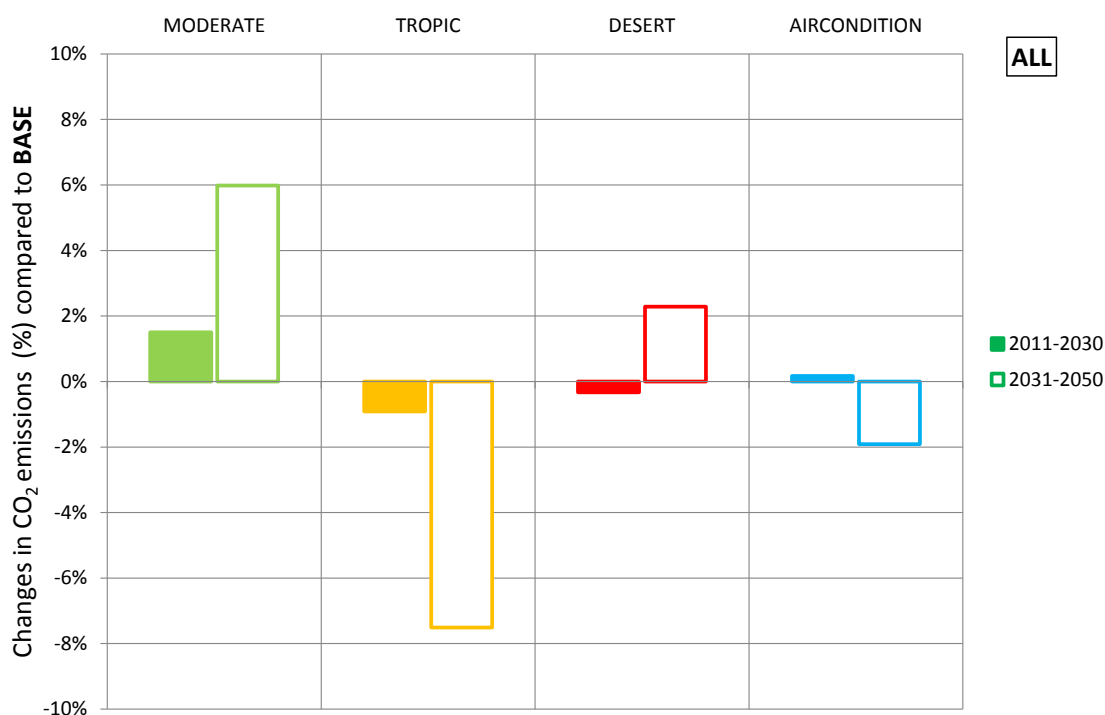


Figure 56: Changes in average variable production costs in Austria

When it comes to CO<sub>2</sub> emissions in the electricity sector, a general reduction in Continental Europe may be expected due to the decreasing demand induced by climate change.

EL.ADAPT

Uncoupled simulations using ATLANTIS confirm this assumption; cf. (Feichtinger et al., 2013). However, taking further, indirect effects under consideration by using the coupled model framework, CO<sub>2</sub> emissions may even rise due to substitution of other primary energy sources.



**Figure 57: Changes in CO<sub>2</sub> emissions of the electricity sector in Continental Europe**

Figure 57 shows the simulation results for changes in CO<sub>2</sub> emissions of the electricity sector in Continental Europe. The results are similar to the changes in conventional power generation as shown in Figure 52, as expected. The total amount of CO<sub>2</sub> emissions also depends on the generation technologies used, e.g. substituting coal power plants by gas-fueled power plants producing the same amount of energy may result in a reduction of CO<sub>2</sub> emissions by about 50 %<sup>12</sup>. This effect can be observed in the AIRCONDITION scenario 2011-2030, for example, showing a low rise of CO<sub>2</sub> emissions compared to the increasing generation.

Sectoral CO<sub>2</sub> emissions in Austria follow the same trends as in Continental Europe for all scenarios except for the DESERT scenario. As described above regarding production costs, Austria is importing electrical energy in this scenario, leading to a decreased dispatch of thermal generation units and therefore reduced CO<sub>2</sub> emissions, as shown in Figure 58. The changes in CO<sub>2</sub> emissions for all country aggregates are shown in Panel 8.

<sup>12</sup> assuming specific CO<sub>2</sub> emissions of 800 g/kWh for coal and 400 g/kWh for gas-fired power plants

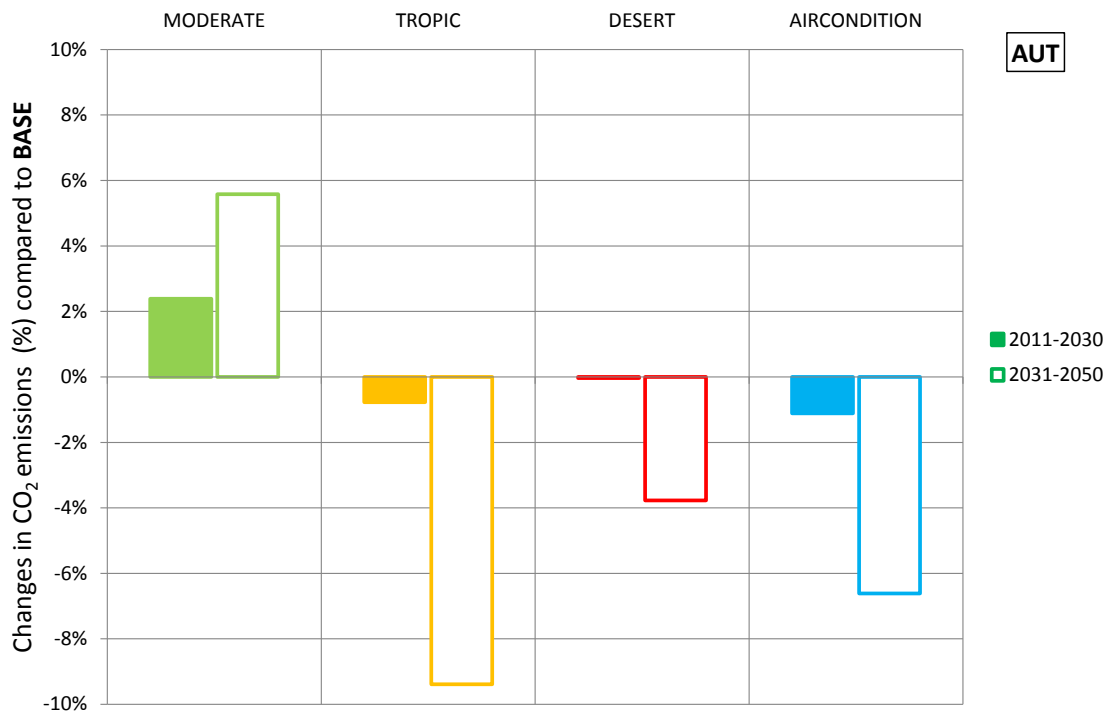
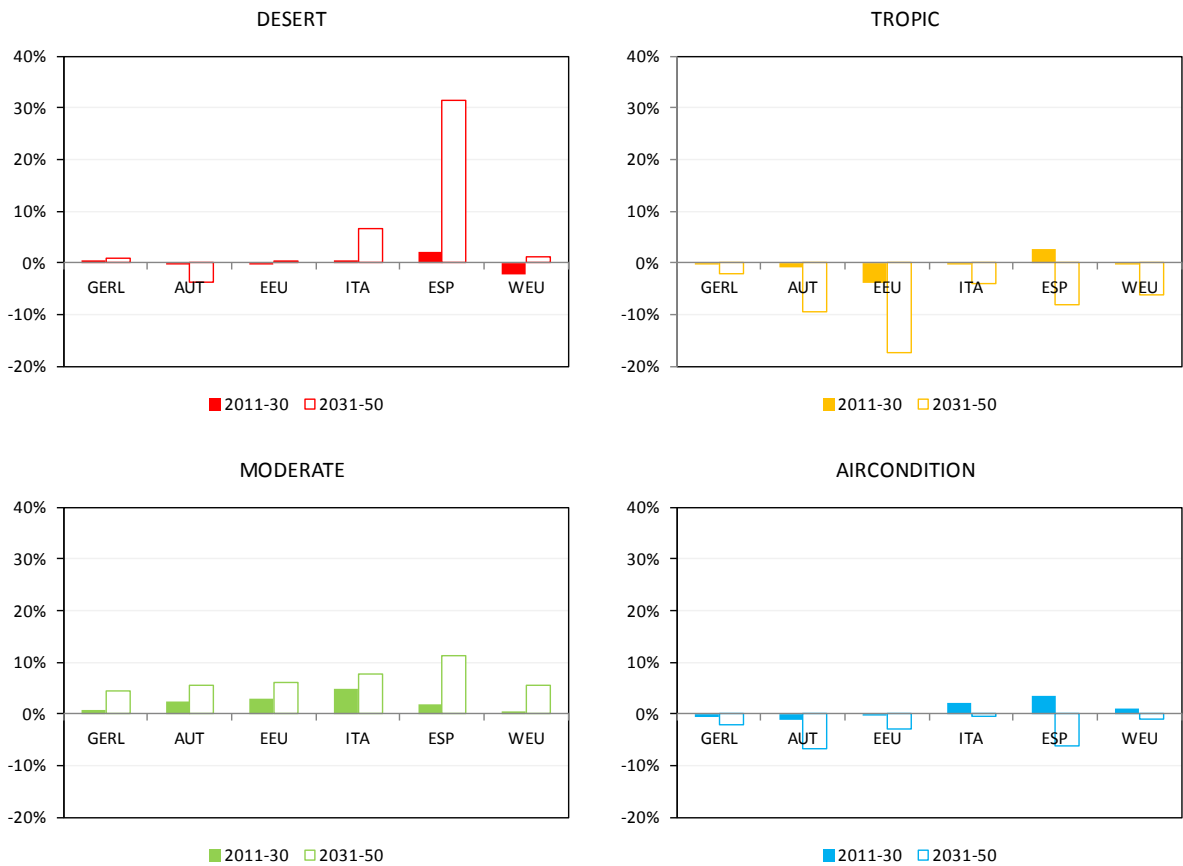


Figure 58: Changes in CO2 emissions of Austria's electricity sector



Panel 8: Impacts on CO2 emissions of the electricity sector

EL.ADAPT

Please note that the vast increase of CO<sub>2</sub> emissions in ESP (Spain and Portugal) in the DESERT scenario result from the very low level of emissions in that countries. Thus, a slight increase expressed in absolute numbers results in a quite high percentage of relative changes.

To conclude the findings shown, it can be stated that climate change does not affect the average wholesale market price significantly, though influencing the maximum peak and minimum off-peak prices depending on the selected climate scenarios. Regarding production costs, the simulation shows strong dependencies to other countries in terms of changes in standard capacities. Thus, effects on production costs can solely be investigated in a Continental European context. The results for Austria show, that production costs are rising by up to 5 % in case of thermal power plants compensating losses of standard capacity. In contrast, production costs are reduced by about 6 % in the best case (AIRCONDITION scenario), due to an increase of standard capacities of RES generation units. The simulation results for CO<sub>2</sub> emissions show a decrease of up to 10 % in three of four selected climate scenarios, due to increases of standard capacities in Austria and its neighboring countries as well as decreasing electricity demand. The MODERATE scenario only shows an increase of about 6 % of CO<sub>2</sub> emissions in the second period 2011-2030.

#### **3.4.4 Sensitivity analysis and uncertainties**

The first part of this chapter deals with the last step of the hydro power plant model chain – the power plant models. To be able to estimate the uncertainties along the whole model chain, the model quality of these individual power plant models were investigated. The second part consists of a sensitivity analysis of the standard capacity changes shown in chapter 3.4.1 in terms of renewable energy sources.

##### **3.4.4.1 Hydro model chain**

In order to continue the detailed uncertainty analysis carried out in section 3.2.3, a brief description of uncertainties within the hydro power plant model for Austria is given in this chapter. The power plant model is based on the linear relationship between generated power and runoff at a given hydraulic head.

$$P_{el} = \rho \cdot \eta_{tot} \cdot g \cdot \Delta H \cdot Q$$

where:

$P_{el}$	generated electrical power
$\rho$	density (of water)
$\eta_{tot}$	total degree of efficiency (turbine, generator, penstock...)
$g$	acceleration of gravity
$\Delta H$	average effective net hydraulic head
$Q$	turbine inflow (runoff)

Besides the physical constants, technical data like hydraulic head and maximum (nominal) turbine inflow are given by several publications and information sites. However, the degree of effectiveness is unpublished or estimated only in most cases. Thus, the degree of effectiveness was chosen as a degree of freedom to calibrate the hydro power plant model, cf. Schüppel (2010). Furthermore, the catchment sizes of power plants and assigned gauges differ, resulting in deviating runoff values. Thus, a linear catchment size correction was introduced in the model, using a catchment size correction factor as a second degree of freedom:

$$Q_{pp} = \frac{A_{c,pp}}{A_{c,g}} \cdot Q_g = f_c \cdot Q_g$$

where:

$Q_{pp}$	runoff at the power plant site
$A_{c,pp}$	catchment size of power plant (unknown/unpublished)
$A_{c,g}$	catchment size of gauge
$Q_g$	runoff at the gauge site (results from hydro model)
$f_c$	catchment size correction factor

While the degree of effectiveness influences the maximum output power of the power plant directly, the catchment size correction factor influences the standard capacity, without changing the maximum output power<sup>13</sup> due to the limitation of the nominal inflow. Thus, the model calibration was carried out using the degree of effectiveness to calibrate the maximum output power of the model, and in a second step, the catchment size correction factor was used to calibrate the standard capacity.

Due to the physical foundation of both degrees of freedom, an uncertainty estimation can be done by analyzing the range of both parameters graphically and checking whether the calibrated values make sense or not. In Figure 59, the resulting degrees of efficiency after

---

<sup>13</sup> Assuming that the runoff exceeds the nominal inflow at least once in the given time series.

EL.ADAPT

the calibration process are shown by power plant<sup>14</sup>. The area marked green in the diagram represents a range of possible values that can be found in the literature. It is shown that the degree of effectiveness fits very well in the expected range, verifying a good quality of this parameter.

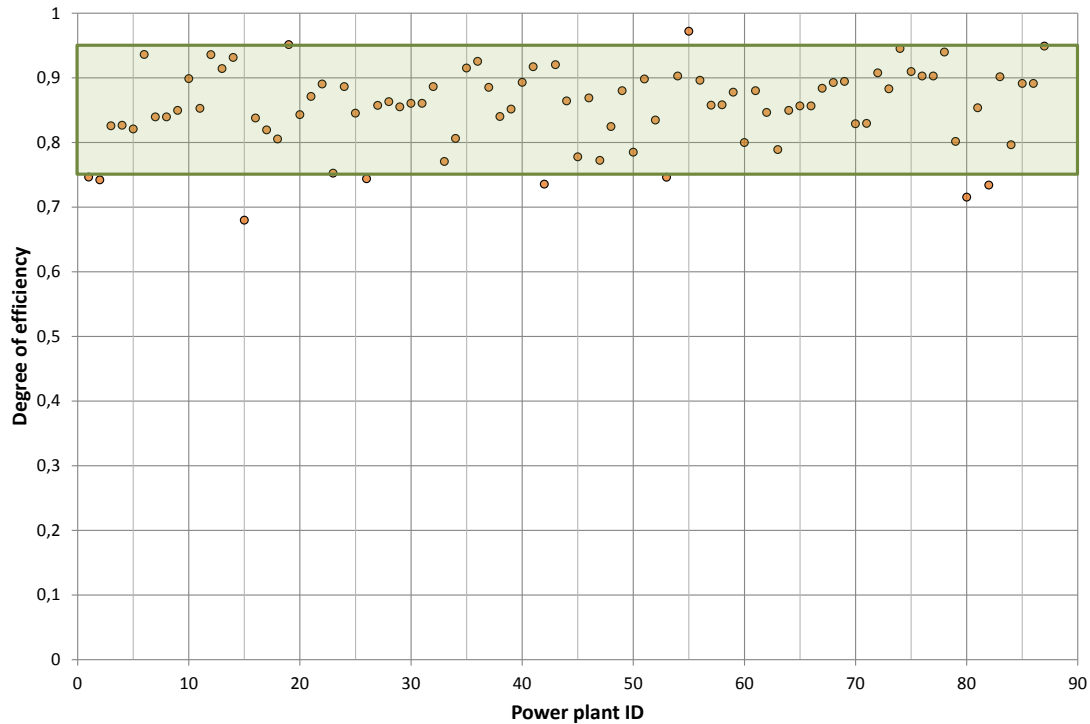


**Figure 59: Resulting degrees of efficiency after model calibration by power plant**

The resulting catchment size correction factor compared to the measured distance between gauging station and corresponding power plant on the x-axis is shown in Figure 60.

---

<sup>14</sup> To assure a high model quality, almost 90 run-of-river hydro power plants in Austria have been modeled individually.

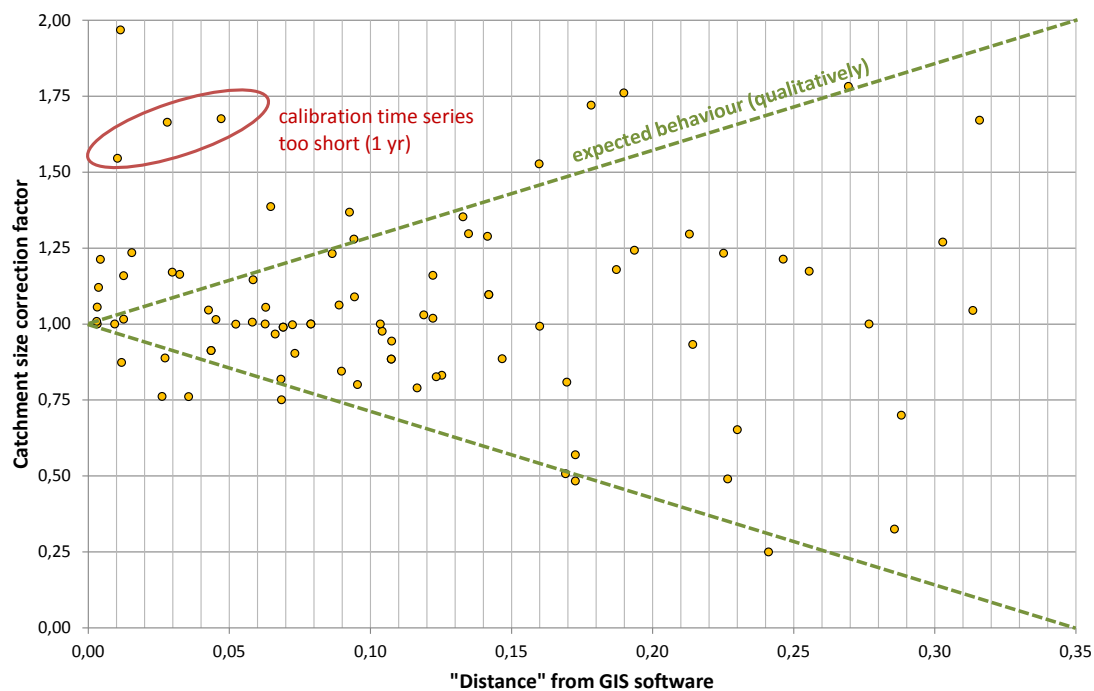


**Figure 60: Resulting catchment size correction factors after model calibration by distance**

The diagram shows quantitatively, that the absolute value of the correction factor depends on the distance between power plant and gauging station. In some cases, the results are unexpected – the outliers marked red, for example, show a very short time series of reference values. Thus, the correction factor possibly includes other calibration aspects, too.

Some values are set to 1.00, although there is a certain distance between gauging station and power plant. In this case, the calibration routine provided nonsensical results. Therefore the value was set to 1.00, assuming as an approximation, that the power plant faces the same catchment size as the gauge.

Resulting from this uncertainty estimation, it was found that the power plant models seem to face low uncertainties, except from those plants providing insufficient time series of calibration data. Especially diversion power plants with unknown residual water flows show higher uncertainties, because the share of runoff passing through the turbine must be estimated. All in all, the analysis and estimation of uncertainties suggests that the hydro power plant model chain provides stable results.

#### 3.4.4.2 Influence of RES development paths on climate change impacts

To determine uncertainties within the impacts on electricity generation in terms of RES generation units, further simulations were carried out using ATLANTIS (standalone) with a

different power plant development path, reflecting the actual development extrapolated into the future as shown in Figure 61 (further referenced as BAU scenario).

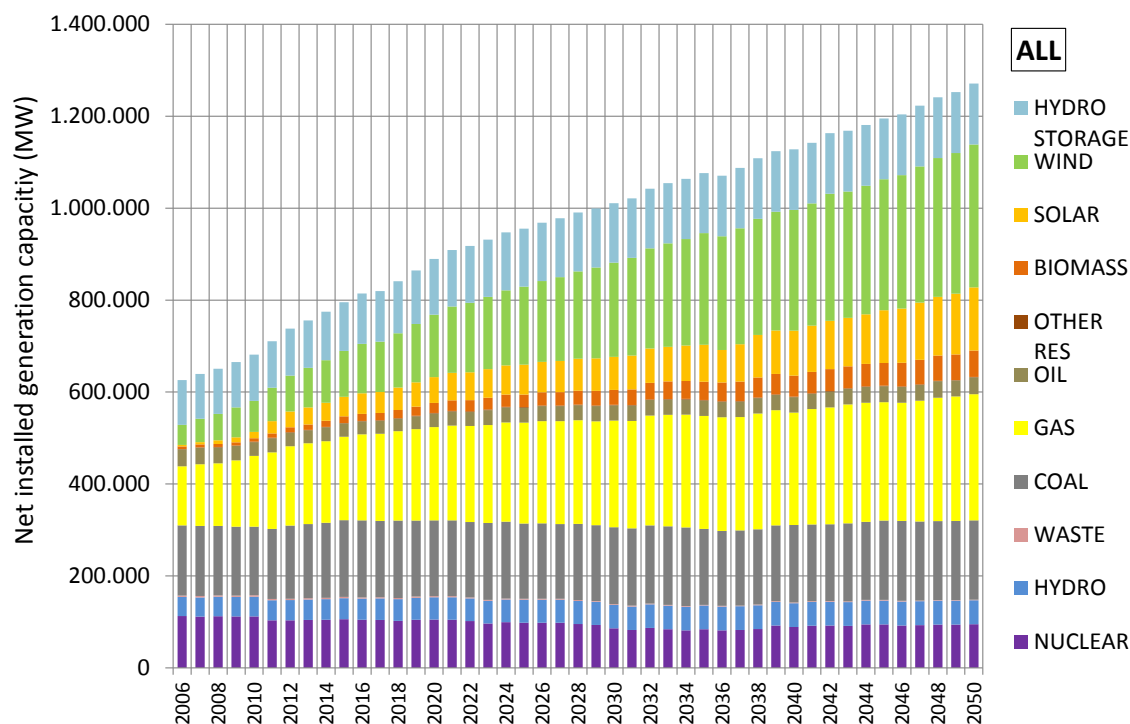


**Figure 61: Assumed business-as-usual (BAU) power plant development path for sensitivity analysis**

To be able to compare the impacts on standard capacities of RES generation between both scenarios, the absolute changes in GWh in relation to the corresponding installed standard capacity are determined and compared.

Figure 62 shows the results of the sensitivity analysis. For every climate scenario, climate change impacts on the standard capacity are compared between the BAU scenario and the scenario used in all other investigations within this study (referenced as “EU2020” scenario). On a Continental European level (left column), the results show stable values for hydro and wind power as well as photovoltaics, indicated by almost equal relative changes for all mentioned technologies. Regarding hydro storage power plants, the comparably high climate change signals as well as the rough approach by using a climatic water balance only are presumably responsible for the quite high uncertainties proven by this sensitivity analysis. For example, locating a new power plant in the NW region instead of the SW region (see Figure 10 on page 24) will cause a significant difference in terms of climate change impacts, even if the distance between both sites is short. In reality, there will be possibly far less difference than estimated within the model framework.

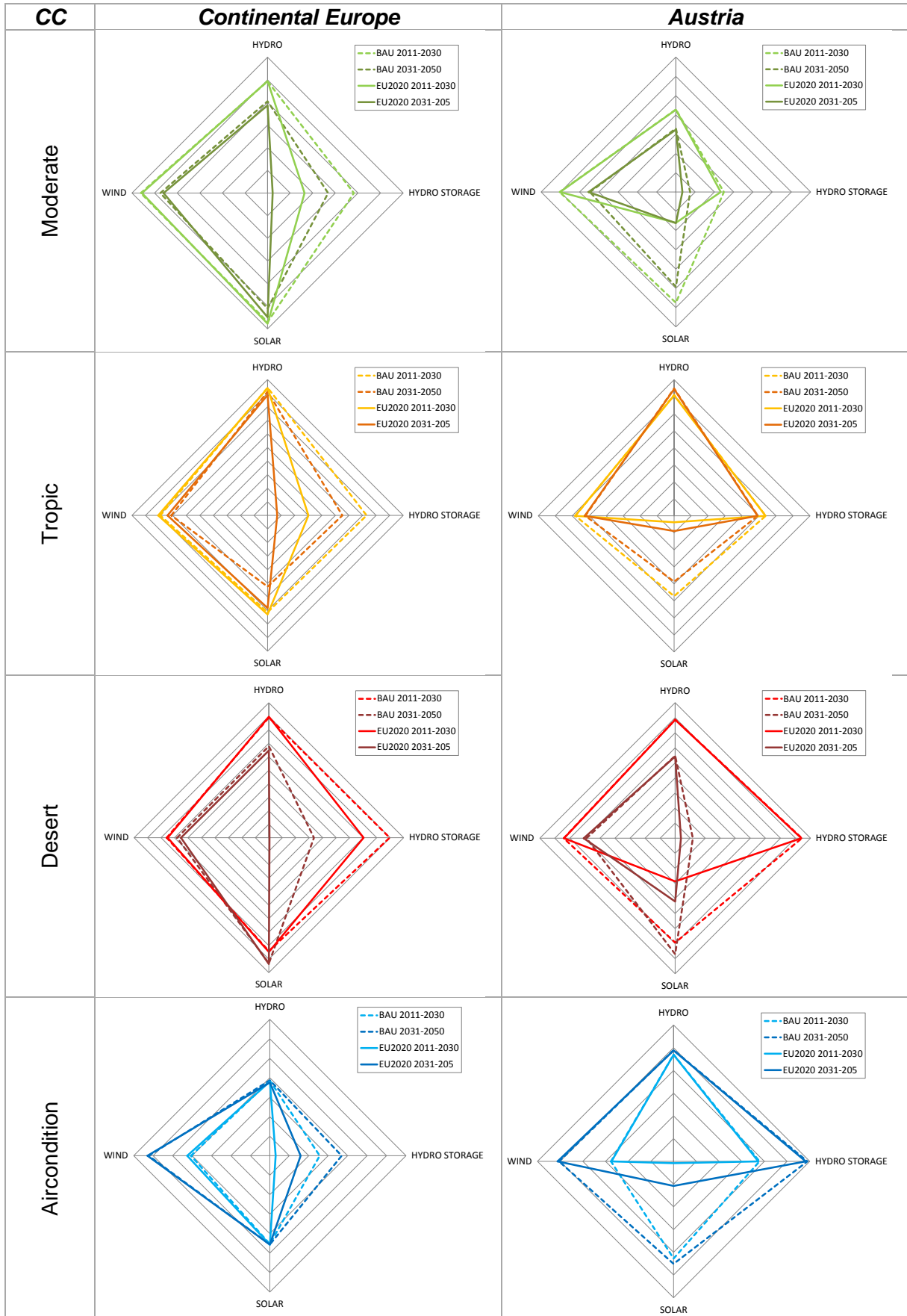


Figure 62: Results of the sensitivity analysis of standard capacity changes

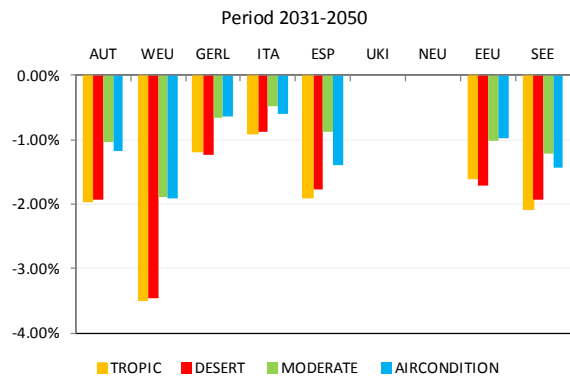
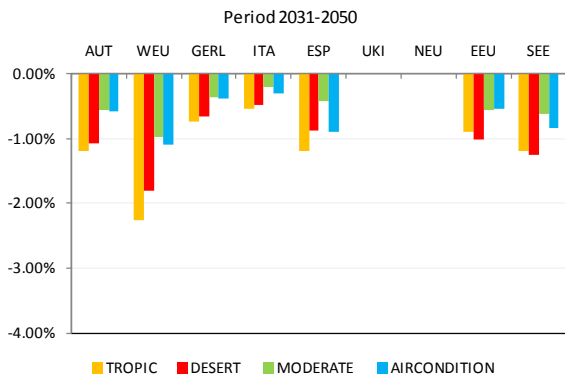
The diagrams for Austria (right column) prove stable results for wind power and hydro power, but also for hydro storage power plants. Due to the high degree of already installed power plants, there is little potential left for new capacities. Thus, the difference between the BAU scenario assumptions and the EU2020 scenario assumptions is small, resulting in a lower sensibility concerning climate change impacts. Because of similar reasons, the uncertainties regarding photovoltaics in Austria are high in contrast to the results for Continental Europe. The installed capacity of photovoltaics in Austria is currently low compared to other generation technologies. Furthermore there is a high potential of possible sites to construct photovoltaic units, compared to e.g. wind power with a high potential concentrated in the north west of Austria. Therefore the impacts of climate change on electricity generation from photovoltaics are quite sensitive to the degree of exploited potential, equivalent to the amount of installed capacities.

#### 3.4.4.3 Uncoupled simulations using ATLANTIS

To be able to estimate direct impacts of climate change on the electricity system without taking spill-over effects and economic feedback effects under consideration, uncoupled (“standalone”) scenario simulations have been carried out using ATLANTIS. Due to the fact that those simulations are not part of the intended model coupling, the results are not published in this report. However, the results already have been published in Feichtinger et al. (2013); please refer to this contribution for further details on uncoupled simulations.

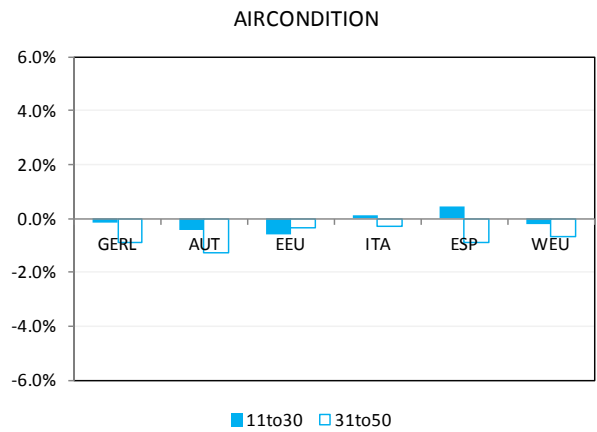
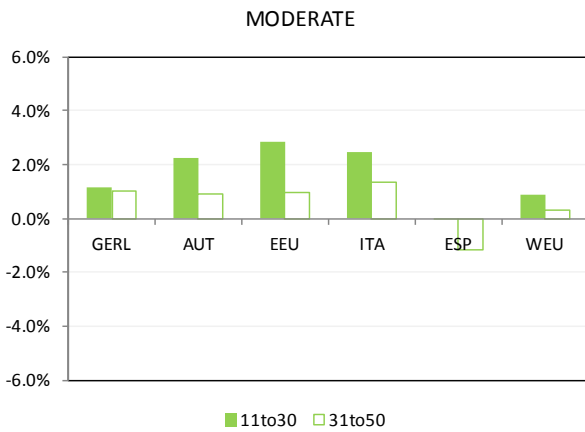
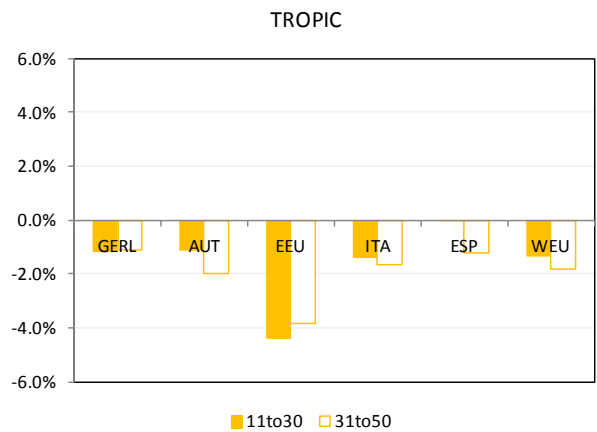
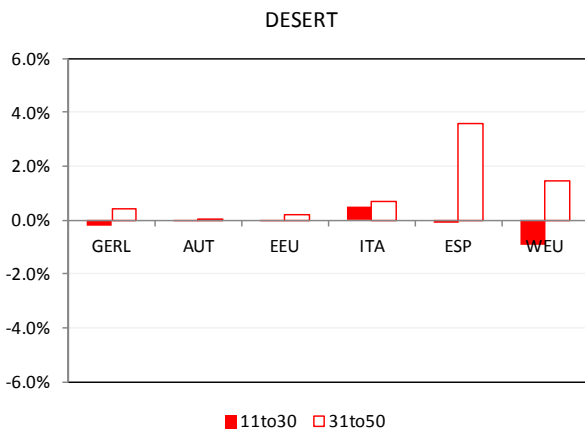
### 3.5 Macroeconomic effects

As the electricity sector is linked to other sectors both up- and downstream, we now investigate so-called indirect effects. To get an understanding how effects on electricity generation and consumption patterns affect other sectors, it is essential to understand the implementation of impact chains in the coupled modeling framework. Panel 9 illustrates the impacts on electricity demand of private households which are implemented as demand shocks in the CGE model.



**Panel 8: Climate change impact on electricity demand of private households by region.**

The impacts on electricity use per unit output in economic sectors correspond to changes in electricity demand as well (see Panel 2). Panel 9 shows the average impact for all selected climate change scenarios for expenditures on electricity by all sectors compared to BASE (scenario with climate policy but without climate change).



**Panel 9: Percentage change of expenditures on electricity by all sectors (= value of electricity demand in Euros) for all climate change scenarios, on average for periods 2011-30 and 2031-50 relative to BASE.**

In general, we find that expenditures on electricity by all sectors are falling relative to BASE in TROPIC and AIRCONDITION, while it is rising in DESERT in MODERATE. As all sectors are affected by climate policy, this result on expenditures on electricity by all sectors is mainly driven by changes in CO<sub>2</sub> prices and electricity prices which differ across scenarios due to different generation mixes. For instance, in TROPIC CO<sub>2</sub> prices are higher than in the other climate scenarios and thus energy demand is falling implying reduced electricity demand. The same holds for the scenario AIRCONDITION, but on a smaller level. In contrast, MODERATE is characterized by a rise in electricity demand because of a stronger shift from fossil fuels to electricity in domestic production and because the CO<sub>2</sub> price is below the BASE-level.

In addition to electricity demand, changed generation mixes lead to altered cost structures in the electricity sector of each linking region, information on which is supplied by ATLANTIS. Figure 63 depicts altered costs structures in MODERATE for Austria on average for in periods 2011-30 and 2031-50.

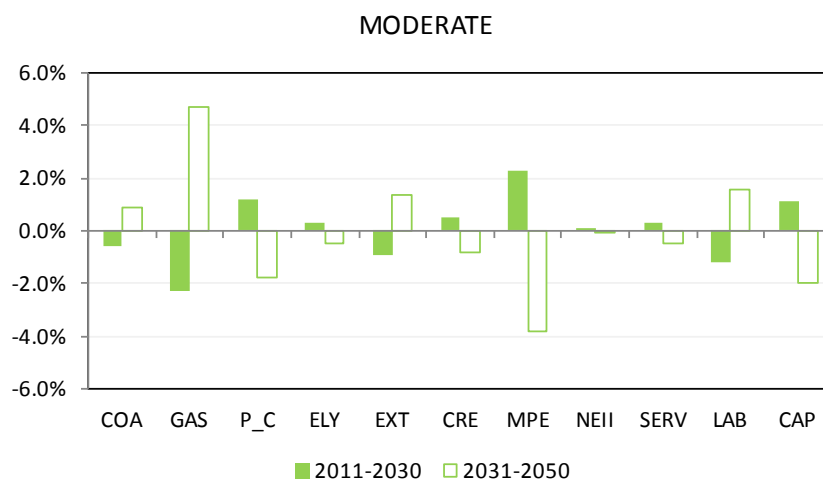
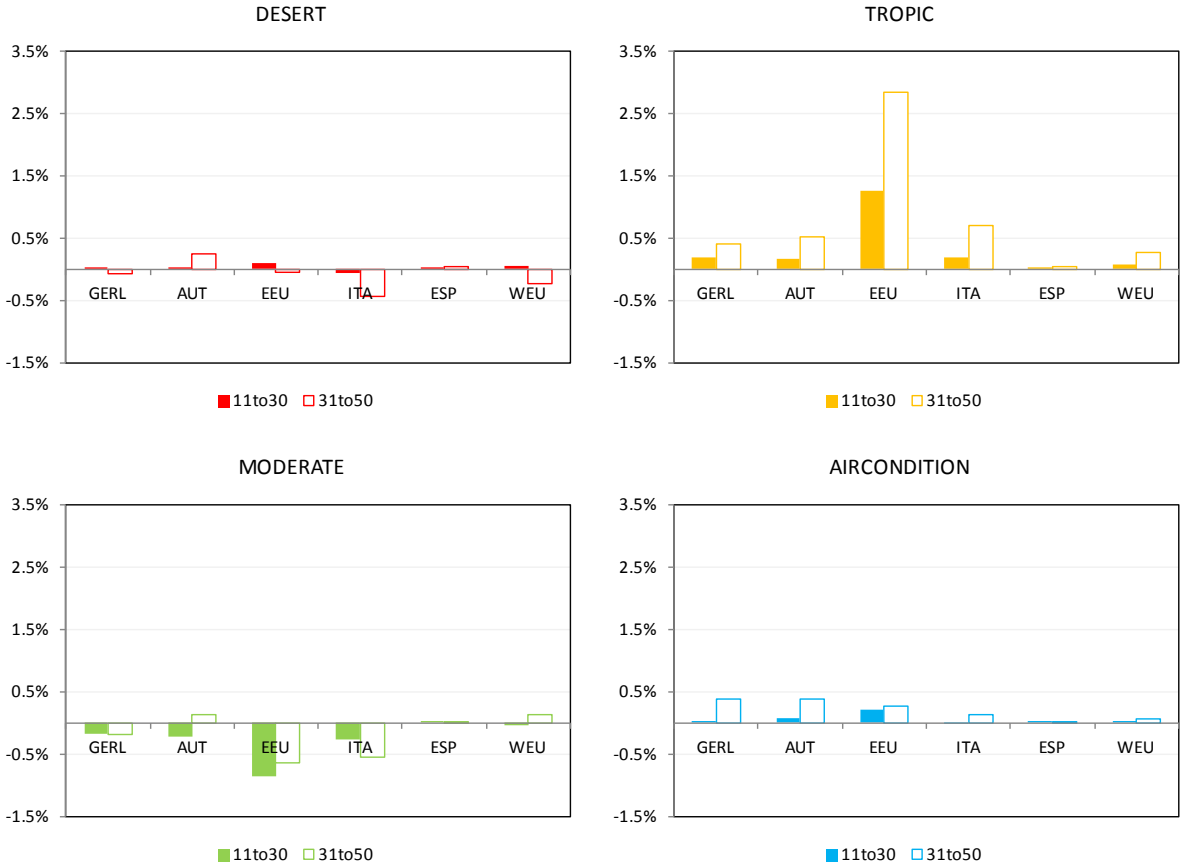


**Figure 63: Percentage change of production cost in the electricity sector in Austria for MODERATE scenario, on average for periods 2011-30 and 2031-50 relative to BASE.**

### 3.5.1 Indirect effects of climate change impacts in the electricity sector

Furthermore, we take a closer look on sectoral effects comprising the indirect effect of climate change for the electricity sector. Electricity intensive sectors (EIS) – comprising CRP, IS, NMM, OMN, PPP and P\_C – are investigated concerning change in output value compared to the BASE scenario. More precisely we observe average output value relative to the BASE scenario for EIS across regions for the two periods 2011-30 and 2031-50. In general, we find that the impact is stronger in period 2031-50 and that effects in scenarios DESERT and AIRCONDITION are negligible. Concerning the MODERATE scenario there

are almost only negative effects, yet of small magnitude. The strongest effects can be observed in the TROPIC scenario, where all effects are positive; meaning higher output value compared to the BASE scenario for all regions in all periods, with a stronger change in the latter period. These impacts of climate change on output of EIS mainly result from changes in the fossil fuel use in the electricity generation and altered electricity prices. For instance, in TROPIC where fossil fuel use in the electricity generation is considerably below the level of BASE (Panel 10), the respective electricity price is also falling and thus demand is rising (especially in EIS). Consequently output of EIS is also boosted. In contrast, in MODERATE fossil fuel use in electricity generation is substantially higher (relative to BASE) and hence production costs are rising. Thus output of EIS is falling.

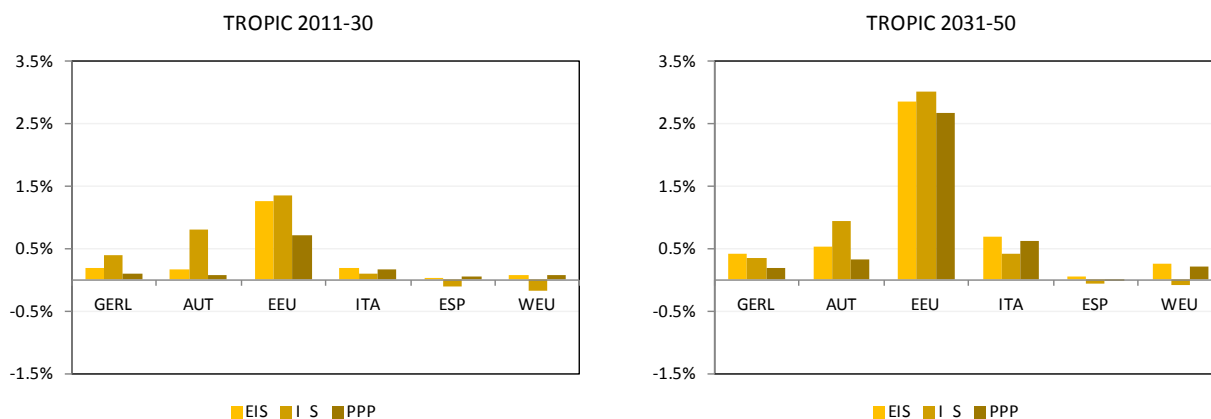


**Panel 10: Impacts on EIS output values (% relative to BASE)**

Since climate change impacts on the output of EIS are by far the strongest under TROPIC, we take a closer look. Our results show differences in sectoral responses to climate change. Panel 11 shows the impact of climate change on the electricity intensive sectors I\_S and PPP and EIS in total. Regarding the first period, sector I\_S is affected relatively strong in 100

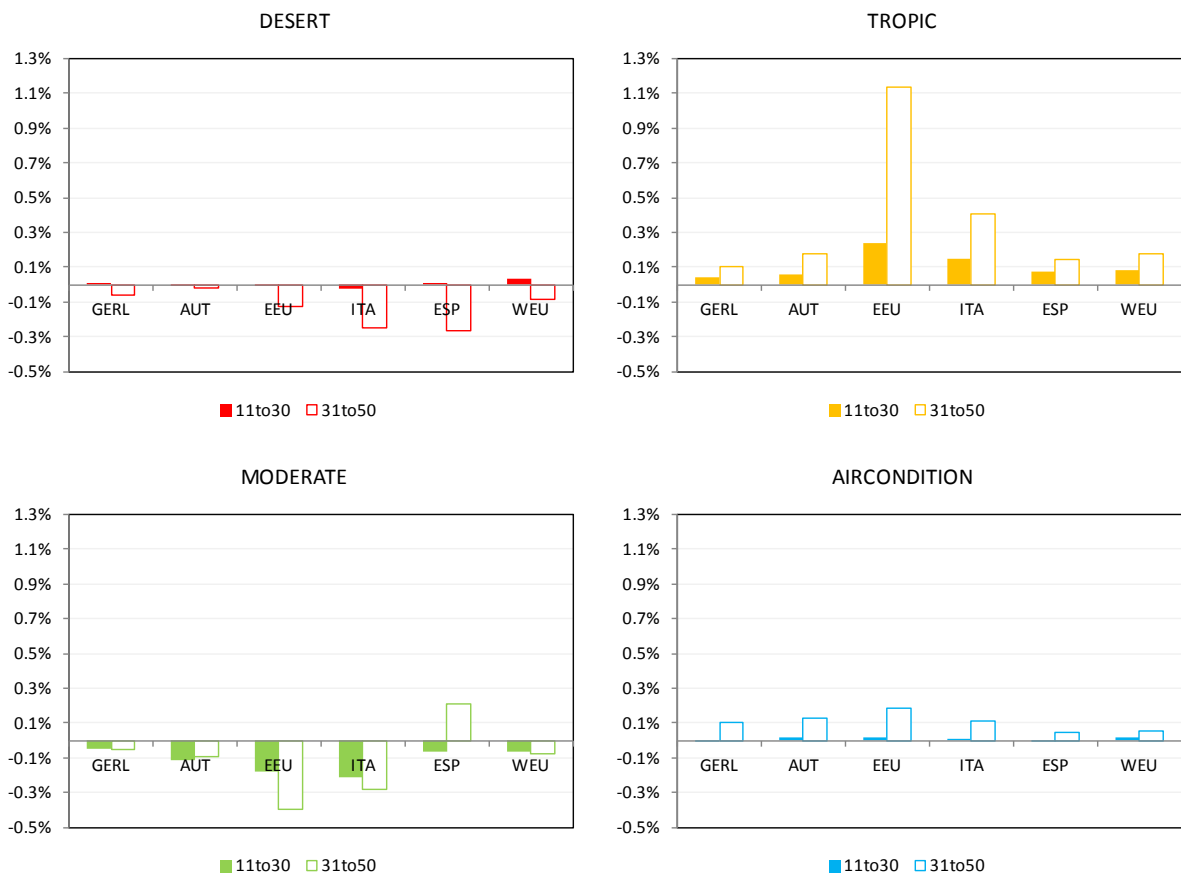
EL.ADAPT

EEU, GERL and especially in AUT (compared to the aggregate EIS). Sector PPP is affected only moderately in period 2011-30. In period 2031-50 sector I\_S is affected again strongly, but this time PPP is also stroke by climate change, especially in EEU and ITA. Although electricity consumption is by far the highest in PPP, output of I\_S is boosted most strongly.



**Panel 11: Average change of EIS, I\_S and PPP output value under TROPIC scenario relative to BASE.**

Regarding non-energy intensive sectors (NEIS) Panel 12 illustrates the effects arising through climate change, which are again stronger in the second period under investigation. Nevertheless, the effects are less stronger compared to EIS, but the direction in the respective scenarios is the same. Again we see positive effects in TROPIC and negative effects in MODERATE, which can be explained according to the same mechanisms as in the explanation for effects in EIS. To summarize, the effects of changed output value compared to BASE lies between 0.2% and -0.2% in period 2011-2030 and between 1.1% and -0.4% in period 2031-2050.



**Panel 12: Impacts on NEIS output value (% relative to BASE)**

Concerning AUT the effects are similar to the rest of Europe (see columns for AUT in Panel 10 and Panel 12). For EIS the strongest effects can be investigated again in TROPIC and MODERATE. There is a change in output value compared to BASE of -0.24% (MODERATE) to +0.16% in period 2011-2030 and +0.13% (MODERATE) to +0.52% (TROPIC) in period 2031-2050. Regarding NEIS in AUT the strongest effects are also in TROPIC and MODERATE. In the first period changes in output value compared to BASE are between -0.12% (MODERATE) and 0.06% (TROPIC) whereas for the second period it's -0.09% (MODERATE) and +0.18% (TROPIC).

**3.5.2 A comparison of direct and indirect effects of climate change impacts in the electricity sector**

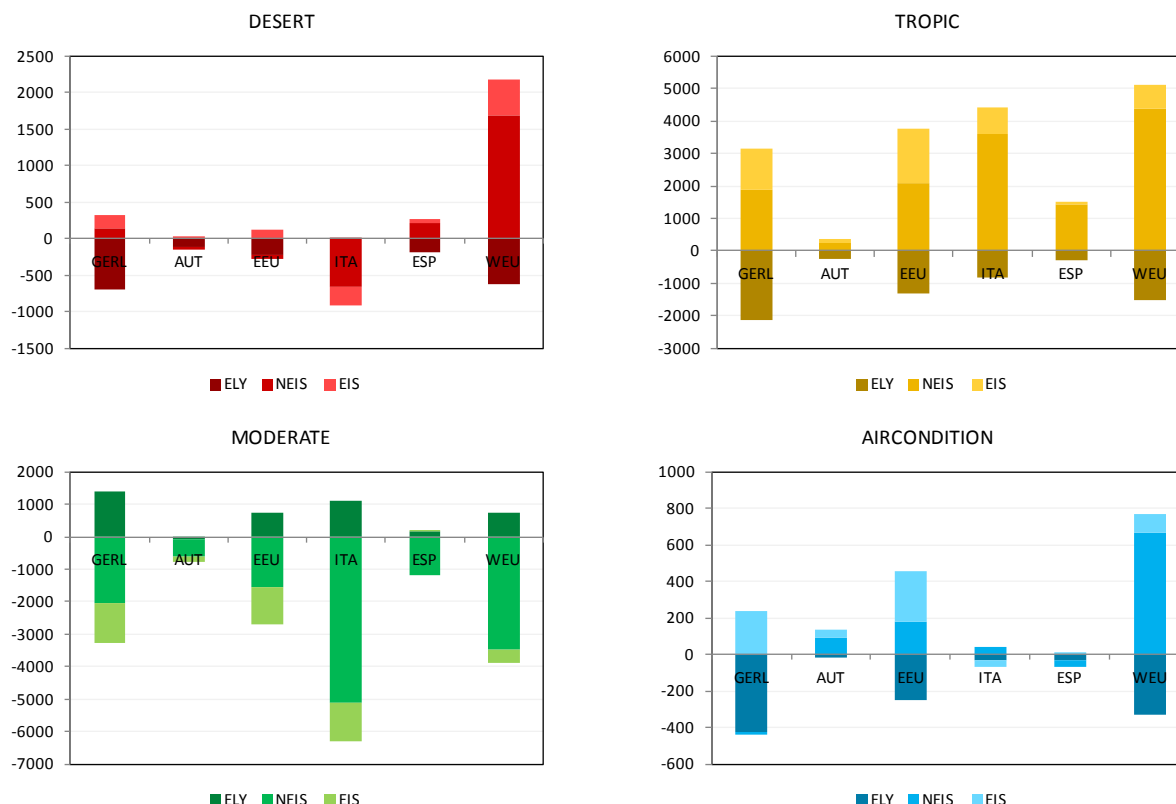
In a next step, we compare direct and indirect costs of climate change in absolute output values (see Panels 13 and 14 for periods 2011-2030 and 2031-2050). Direct costs are expressed as changes in ELY output value, whereas indirect costs are changes in NEIS and EIS output values. Again we see significant differences between regions in all scenarios. The strongest impacts can be observed in TROPIC and MODERATE.

EL.ADAPT

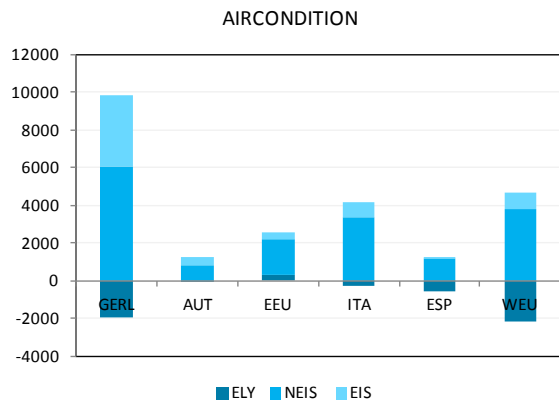
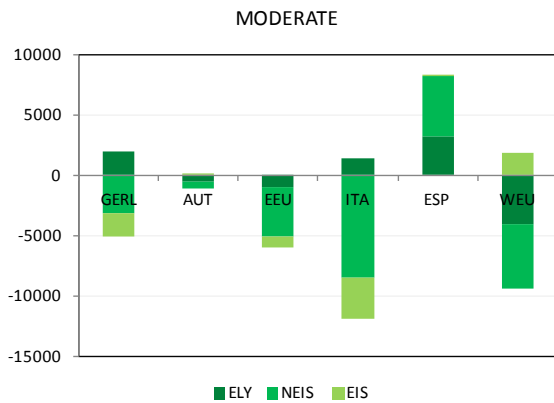
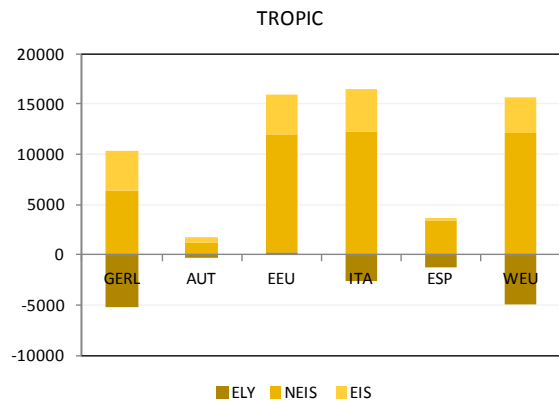
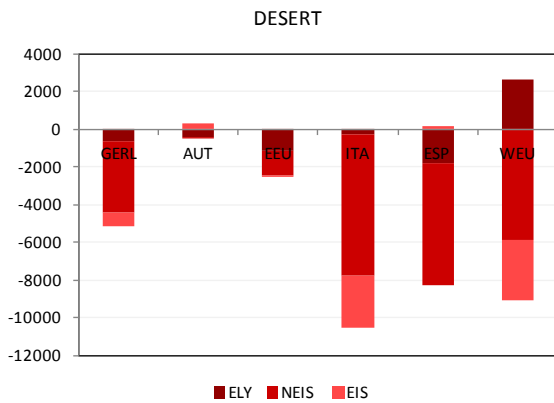
Comparing the relative magnitude of direct and indirect costs of climate change in absolute output values for period 2011-2030, we find that in TROPIC output value of ELY is falling compared to BASE (positive direct costs) in period 2011-2030, but this loss is compensated by an increase in output value in EIS and NEIS in every region (negative indirect costs) such that the total economic output increases range from +0.02% for GERL to +0.23% for EEU (see Table 10). In MODERATE, a net loss in output results as positive effects in ELY output value (gains) are compensated by much higher negative effects in EIS and NEIS (losses). The net effect thus ranges from -0.19% for EEU to -0.04% for GERL. In DESERT and AIRCONDITION, ELY experiences a loss in output value across all regions, whereas the direction of effects in EIS and NEIS varies, leading to net effects from -0.03% to +0.02%. Net effects for Austria range from -0.14% in MODERATE to + 0.03% in TROPIC.

**Table 10: Change in net effects of direct and indirect effects relative to BASE, 2011-30 (% change in total production value of EIS, NEIS, ELY)**

	GERL	AUT	EEU	ITA	ESP	WEU
<b>DESERT</b>	-0.01%	-0.02%	-0.02%	-0.03%	+0.00%	+0.02%
<b>TROPIC</b>	+0.02%	+0.03%	0.23%	0.12%	+0.05%	+0.06%
<b>MODERATE</b>	-0.04%	-0.14%	-0.19%	-0.18%	-0.05%	-0.05%
<b>AIRCONDITION</b>	-0.00%	+0.02%	+0.02%	-0.00%	-0.00%	+0.01%



**Panel 13: Output gain/loss [in Mio. EUR] of economic sectors relative to BASE for period 2011-2030.**



**Panel 14: Output gain/loss [in Mio. EUR] of economic sectors relative to BASE for period 2031-2050.**

In period 2031-2050, the direction and magnitude of effects partly change (cf. Panel 14 and Table 12). For instance in DESERT the output value of NEIS falls strongly, implying net output losses for all regions. In contrast, in AIRCONDITION we see output gains throughout all regions due to strong positive effects in NEIS. In TROPIC and MODERATE, the results of the second period resemble the results of the first period in nearly all regions.

**Table 11: Change in net effects of direct and indirect effects relative to BASE, 2031-50 (% change in total production value of EIS, NEIS, ELY)**

	GERL	AUT	EEU	ITA	ESP	WEU
DESERT	-0.07%	-0.03%	-0.20%	-0.28%	-0.27%	-0.08%
TROPIC	+0.07%	+0.18%	+1.28%	+0.37%	+0.08%	+0.13%
MODERATE	-0.04%	-0.12%	-0.48%	-0.28%	+0.28%	-0.09%
AIRCONDITION	+0.11%	+0.16%	+0.21%	+0.10%	+0.02%	+0.03%

Concerning AUT direct and indirect effects for all four scenarios and periods are shown in Figure 64. Again, the two extremes are TROPIC and MODERATE. In TROPIC ELY production value is decreasing compared to BASE because of a lower ELY price (As the share of renewables is relatively high). Due to this relatively low ELY price demand is rising

EL.ADAPT

and in combination with a low CO<sub>2</sub> price this is boosting output of EIS and NEIS, who are both winners in TROPIC. In MODERATE there is a relative low share of renewables (see Figure 48 and Figure 49 for the decreasing capacity of renewables in power generation) which has to be compensated with fossil inputs. Therefore the resulting ELY price is relatively high which is dampening ELY demand (in quantities) and leading to a reduction in EIS and NEIS output. To put these effects into perspective, the net effect of gains and losses is compared to total output value in the regarded periods. In 2011-2030, net effects (the sum of gains and losses) compared to total production value range from -0.14% in MODERATE to +0.03% in TROPIC. In period 2031-2050 the effect is between -0.12% (MODERATE) and +0.18% (TROPIC) Note, that the effects are mostly larger in NEIS, as this aggregate is much larger than EIS in absolute terms. Furthermore the effects are always larger in the second period, as the numbers are not inflation-adjusted.

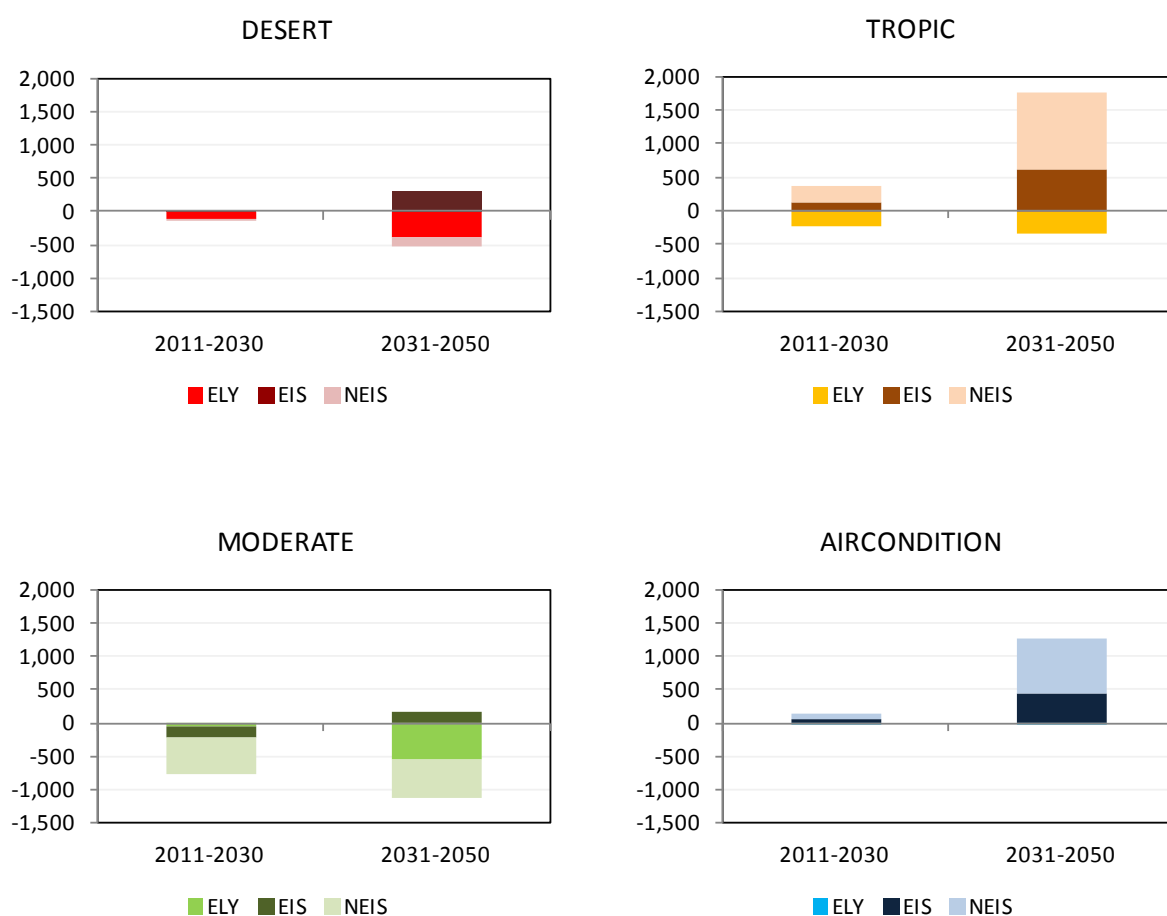
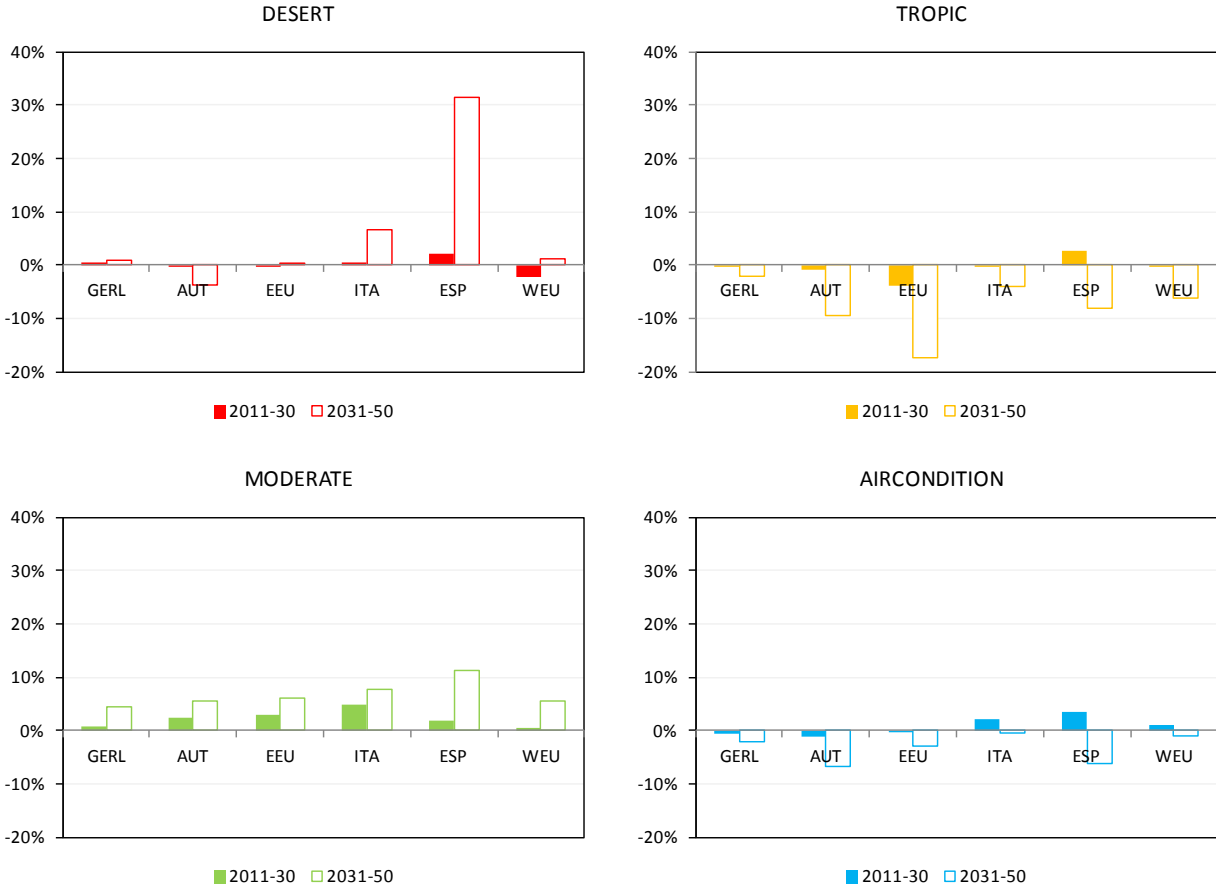


Figure 64: Output gain/loss [in Mio. EUR] of economic sectors relative to BASE for AUT.

### 3.5.3 Environmental effects

Since climate policy assumptions do not vary across impact scenarios, the overall emission reduction target is the same for all scenarios. However we find considerable differences in emission reduction between countries across impact scenarios.

Power generation in terms of generation mix and output level is responsible for the CO<sub>2</sub> emissions of the electricity sector. First of all, the particular share of renewables, which do not produce CO<sub>2</sub> emissions in operation, determines the dispatch of fossil fueled power plants and therefore affects emissions directly. Second, only fossil fueled units respond to changes in electricity consumption due to the Merit Order effect and the priority of RES generation units.



**Panel 15: Change of CO<sub>2</sub> emissions for all climate change scenarios, on average for periods 2011-30 and 2031-50 relative to BASE.**

However, the influence of both renewables and consumption is nonlinear due to the different specific CO<sub>2</sub> emissions of fuels. Because of these relationships, it is of no surprise that in general climate change impacts on CO<sub>2</sub> emissions, as illustrated in Panel 15, resemble results on power generation in direction of effect. However, the magnitude of effect differs

EL.ADAPT

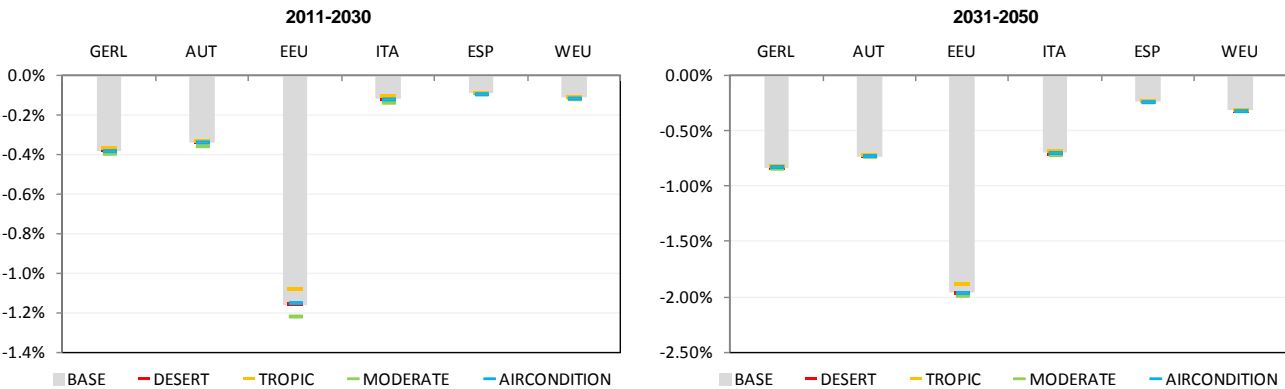
and for some regions we also observe a change in direction of effects. For instance, in DESERT, emissions in ESP rise by 33% relative to BASE which is however rather small in absolute terms because emissions in ESP are by far the smallest in all scenarios (Panel 15). Still, we find a rise in the fossil fuel use in ESP in DESERT (e.g. reduction of RES generation due to climate change is compensated by gas units). Since power generation falls in TROPIC, emissions are also lower, but the effect is more pronounced relative to the change in power generation because electricity is generated from energy sources with less emissions (e.g. wind) implying that the available capacity of fossil power plants is not employed (see Panel 16). In contrast, in MODERATE, the rise in power generation is met with a rise in use of fossil fuels. Thus, emissions are considerable above the BASE level.



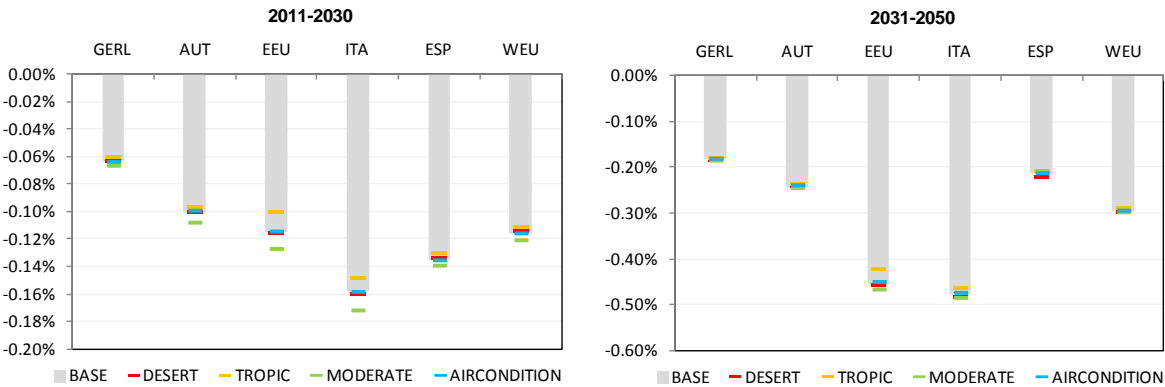
**Panel 16: Percentage change of fossil fuel consumption (based on quantities) for all climate change scenarios, on average for periods 2011-30 and 2031-50 relative to BASE.**

### 3.5.4 Interactions with climate policy

Since the electricity sector is affected by both climate change impacts and climate policy, we finally study the impacts of climate change relative to a non-climate policy BASE scenario (BASE0) to decompose the effects on output into a climate policy effect and a climate change impact effect (see Panel 17 for EIS and Panel 18 for NEIS). Regarding the climate policy effect, reductions of average annual growth rates in EIS output value (relative to BASE0) range from -0.09%-points for Spain and Portugal (ESP) to -0.38%-points for GERL in the first period and in the second period from -0.24%-points for ESP to -1.19%-points for EEU, whereas decreases in NEIS are not higher than -0.16%-points in the first period and between -0.18% and -0.48% in the latter. Yet, these “reductions” are relative to BASE0 such that output still rises, but at a lower rate. In contrast to the effects of climate policy, climate change impact effects on production value of both EIS and NEIS are substantially smaller compared to climate policy induced effects, ranging for EIS from -0.13%-points to +0.07%-points in the first period to -0.10%-points to +0.08%-points in the second. For NEIS, climate change impacts effects range from -0.03%-points to +0.02%-points in the first period to -0.04%-points to +0.04%-points in the second.



**Panel 17: Change in NEIS output growth rates p.a. (%-points relative to BASE0) induced by climate policy (gray bars) and climate change impacts, on average for periods 2011-30 and 2031-50 relative to BASE0.**



**Panel 18: Change in NEIS output growth rates p.a. (%-points relative to BASE0) induced by climate policy (gray bars) and climate change impacts, on average for periods 2011-30 and 2031-50 relative to BASE0.**

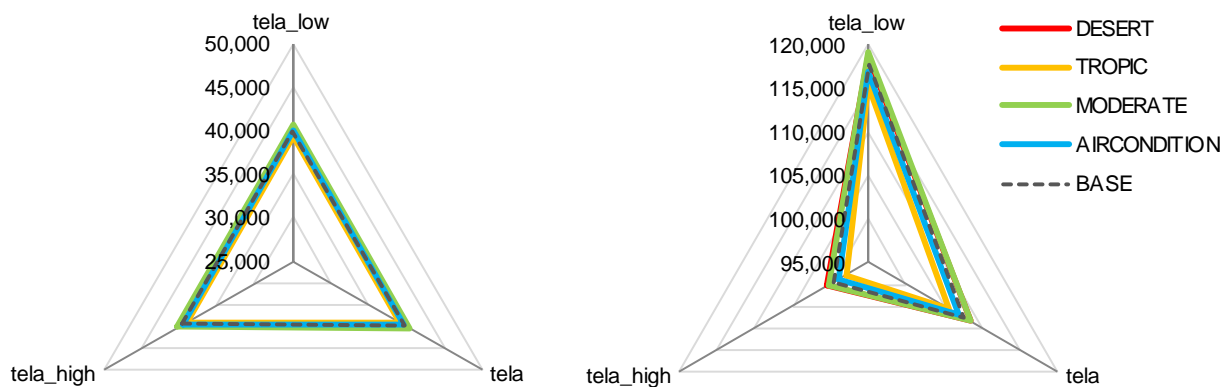
In general we can see that electricity intensive industries are hit harder by climate policy than non-electricity intensive sectors. Regarding EIS, the strongest effects emerge in region EEU reflecting the fact that fossil fuel energy intensity is relatively high in this region. Hence EEU is hit harder by climate policy while regions with low fossil fuel energy intensities remain relatively unaffected (e.g. ESP and WEU). Climate policy induced effects are getting more severe in the period 2031-2050 as reductions targets are getting more stringent leading to more economic pressure and a higher CO<sub>2</sub> price.

### 3.5.5 Sensitivity analysis and uncertainty

To conclude our analysis, we conduct a sensitivity analysis with respect to the the Armington elasticity (*te/a*) which defines the degree of substitutability between imports and domestically produced commodities. With this sensitivity analysis, we can disentangle whether the variations between the different climate scenarios are stronger or weaker as compared to parameter uncertainty in the CGE model. In order to test for sensitivity we halve as well as rise (by a factor of 1.5) the respective values of the Armington elasticity in all climate change scenarios and analyze the effects on electricity demand (industries and households).

As illustrated in Panel 19 (left), we find that in the first period (2011-2030) the effects of changed parameter setting on expenditures on electricity by all sectors are modest – for all climate change scenarios. In contrast, in the second period (2031-2050) the mean European electricity demand varies due to changes in the Armington elasticity. We find that a low Armington elasticity implies a high mean European electricity demand. More precisely, a relatively low value of the Armington elasticity hampers the degree of substitutability between imports and domestically produced commodities. Fossil fuel intermediate input, which is a key factor in production, is mainly imported in Continental Europe and hence more costly to get. Thus, in order to ensure energy supply, we observe a substitution from fossil fuel to electricity.

In general we find that in the second period the variation of *te/a* has a much stronger impact on aggregated average expenditures on electricity by all sectors than the scope of possible climate change impacts. However, putting these results into perspective, climate change may have severe consequences; depending on level of regional resolution, level of sectoral aggregation and target variable (e.g. demand vs. supply).



**Panel 19: Change in electricity demand (in value terms) for different values of tela, averaged across European regions, for periods 2011-2030 (left) and 2031-2050 (right) relative to BASE.**

### 3.6 Options for adaptation to climate change in the electricity sector

One of the crucial questions within EL.ADAPT was to find possible adaptation measures to react on the impacts of climate change found in the earlier stages of the project. Therefore, a master's thesis dedicated to this topic has been carried out at the Institute of Electricity Economics and Energy Innovation (Spindler, 2013).

The thesis investigates possible adaptation measures based on state-of-the-art technologies and measures already applied in refurbishment processes of older power plants. This section of the report gives an overview on the topics discussed in the thesis and summarizes the main findings. *All facts, findings and figures are taken from (Spindler, 2013), except for chapter 3.6.5 regarding electricity demand.*

#### 3.6.1 Overview on adaptation measures

In a first step, the major impacts of climate change on electricity generation were identified by using preliminary results of EL.ADAPT. Based on these results, a compilation of possible adaptation measures was created with the help of a comprehensive literature research.

Regarding hydro power, changes in river runoff or natural inflow are crucial. An increase of average runoff will basically have a positive effect on generation companies, leading to a higher energy yield. To be able to use the additional runoff or basin inflow to its full extent, it may be necessary to modify the turbines or to extend an existing storage reservoir. Table 12 shows the possible state-of-the-art technical adaptation measures found for hydro and storage power plants.

Table 12: Technical adaptation measures for hydro power plants (Spindler, 2013)

Climate parameter		river runoff / natural reservoir inflow		
		<i>Increasing average</i>	<i>Increasing variability</i>	<i>Decreasing average</i>
General measures	<b>Run-of-river power plants</b>	<ul style="list-style-type: none"> <li>Turbine modification</li> </ul>	<ul style="list-style-type: none"> <li>Additional storage reservoir (if possible)</li> <li>Turbine modification</li> <li>Other measures within the catchment area</li> </ul>	<ul style="list-style-type: none"> <li>Additional storage reservoir (if possible)</li> <li>Turbine modification</li> </ul>
	<b>Storage power plants</b>	<ul style="list-style-type: none"> <li>Extend reservoir capacity</li> </ul>	<ul style="list-style-type: none"> <li>Interconnect reservoirs (enables balancing)</li> </ul>	
Turbine-type specific measures	<b>Pelton</b>	<ul style="list-style-type: none"> <li>Increasing number of nozzles</li> <li>Twin turbiens</li> <li>Increasing nozzle diameter</li> </ul>		<ul style="list-style-type: none"> <li>Decreasing number of nozzles</li> </ul>
	<b>Kaplan</b>	<ul style="list-style-type: none"> <li>Additional HYDROMATRIX<sup>®</sup>-or StrafloMatrix<sup>™</sup> modules</li> <li>Extended water intake</li> <li>Modification of impeller vanes</li> </ul>	<ul style="list-style-type: none"> <li>Replacing by diagonal turbines</li> <li>Controlling attack angle of impeller vanes</li> </ul>	<ul style="list-style-type: none"> <li>Modification of impeller vanes</li> <li>Replacing by diagonal turbines</li> </ul>
	<b>Francis</b>	<ul style="list-style-type: none"> <li>Replacing by "Straflo" turbines</li> <li>Increasing cross-section of guide vane apparatus</li> </ul>	<ul style="list-style-type: none"> <li>Replacing by diagonal turbines</li> <li>Using spiral turbines with two blade wheels</li> </ul>	<ul style="list-style-type: none"> <li>Replacing by "Straflo" turbines</li> <li>Decreasing cross-section of guide vane apparatus</li> <li>Replacing by diagonal turbines</li> </ul>

The crucial climate parameter for wind power is the average wind speed. In contrast to hydro power, wind turbines may face an increase of production cutoffs due to rising wind speeds, especially taking an increased frequency of extreme weather situations into account. Thus, some of the measures found call for completely new units, e.g. switching to turbines with vertical axis. Table 13 shows the found results.

Table 13: Technical adaptation measures for wind power (Spindler, 2013)

Climate parameter	Wind speed		
	<i>Increasing average</i>	<i>Increasing variability</i>	<i>Decreasing average</i>
	<ul style="list-style-type: none"> <li>• Storm control<sup>15</sup></li> <li>• Decreasing hub level</li> <li>• Developing new areas (arising new potentials)</li> </ul>	<ul style="list-style-type: none"> <li>• Storm control</li> <li>• Enhanced rotor blades</li> <li>• Replace by units with vertical axis</li> </ul>	<ul style="list-style-type: none"> <li>• Increasing hub level</li> <li>• Replace by units with vertical axis</li> </ul>

Regarding solar power (especially photovoltaics), the crucial climate parameter is global radiation. Due to the fact that photovoltaic cells are a quite young technology being currently developed, any new measure to increase efficiency of photovoltaics can be applied as adaptation measure, too, but will be implemented anyways, as soon as they are economically efficient. To this effect, no explicit adaptation measures could be found regarding global radiation.

However, the energy yield of photovoltaic modules not only depends on global radiation. The efficiency of these modules also depends on their temperature, which is directly linked with the surrounding temperature. Therefore, measures to react on rising temperatures were investigated in this study. Table 14 depicts an overview of possible measures.

**Table 14: Technical adaptation measures for photovoltaics (Spindler, 2013)**

Climate parameter	Temperature		
	<i>Increasing average</i>	<i>Increasing extreme weather conditions</i>	<i>Decreasing average</i>
	<ul style="list-style-type: none"> <li>• Fluid cooling</li> <li>• Air cooling</li> <li>• Cooling by spray irrigation</li> <li>• Coating based on polyurethane elastomer</li> </ul>	<ul style="list-style-type: none"> <li>• Silicon lamination</li> <li>• Coating based on polyurethane elastomer</li> </ul>	

---

<sup>15</sup> “Storm control” is an invention of ENERCON GmbH, which prevents an immediate cutoff of wind turbines at their maximum wind speed, but reducing their revolution speed linearly to zero (Enercon, 2012). Thus, wind turbines lose less energy on gusts of wind, and are faster available again after such gusts.

The measures described are proven to partially/fully compensate climate change impacts on the electricity generation in a physical way, meaning that possible losses of energy yield or a rising variability may be balanced. In addition, the economic efficiency of selected measures has been estimated. The results are shown in the following chapters for every investigated generation technology.

### 3.6.2 Hydro power

By reason of its importance for the electricity system in Austria, four selected adaptation measures for hydro power have been investigated using examples based on real projects or real power plants in Austria, taking the selected climate scenarios of EL.ADAPT under consideration.

The investment in additional HYDROMATRIX<sup>®</sup> modules was simulated for the Abwinden-Asten power plant located on the Danube River. Due to their modular structure, this type of small-scale Kaplan turbine can easily be mounted in weir fields of existing power plants. At Abwinden-Asten, up to 80 units could theoretically be added. By using 80 additional modules, the impacts of climate change on this power plant are compensated in all negative climate scenarios in the first period 2011-2030, whereas in the second period the power plant will face slight losses in the energy production in the DESERT and the MODERATE scenario. However, the climate change impacts are compensated by about 75 % in those two scenarios, too.

From an economic point of view, the optimal amount of modules will be 50-60, gaining additional earnings in all climate scenarios, if a static approach is used. However, due to the long-term investment, a dynamic approach should be used. Hence, a cost-benefit analysis and a compound value method analysis - both using discounted<sup>16</sup> cash flows - were carried out. The results of the cost-benefit analysis show that a total of 10 modules are optimal, solely being economically efficient in the TROPIC scenario<sup>17</sup>. The compound value method found a bandwidth of six to twelve modules as most efficient and shows that this investment will be positive for all scenarios except from the MODERATE scenario.

At Kirchbichl power plant, an enhancement is planned until 2017, aiming at almost a doubling of installed capacity (from 25 MW to 46 MW) by building a second power house. The simulation of this project shows, that the standard capacity of this power plant will be

---

<sup>16</sup> The discount rate was set to 6 % according to (Giesecke et al., 2009, S.67) in (Spindler, 2013)

<sup>17</sup> However, the other scenario's internal rate of return is about 5 %, just a little less than the TROPIC scenario.

increased by about 35 % (without considering the climate change). The economic analysis shows, that the investment is positive in any climate scenario, due to the fact that the gain of energy production is significantly higher than the impacts of climate change. The current project shows that additional generation capacities at power plant sites, that do not utilize the total potential of the corresponding water body, may easily compensate the impacts of climate change and are economically efficient in addition.

The Pernegg power plant located at the river Mur is currently undergoing a refurbishment, looking back at almost 80 years of operation. During the refurbishment process, the turbines of the power plant are exchanged for newer turbines with slightly higher power output while using the same amount of inflow. Based on that fact, the results prove that the standard capacity increases by about 10 %, regardless of the chosen climate scenario. Thus, the simulation results show that the investment will be positive in any climate scenario by gaining a higher increase of standard capacity than the worst reduction that will be caused by climate change within the analysed climate scenarios.

Within the refurbishment process of Agonitz power plant in Upper Austria, the Kaplan turbine is renewed and, in addition, the first StrafloMatrix™ turbine will be set into commercial operation. The refurbishment results in a quadruple of the former standard capacity. Due to this, the impacts of climate change are almost negligible.

The discussed examples show that, according to simulation results, the impacts of climate change on hydro power may be well compensated, especially in Austria. In addition, the investment will show positive earnings at the end of their lifetime in almost all investigated cases.

The adaptation measures for storage power plants are difficult to investigate, due to missing information concerning investment costs in new dams or connection pumps between different catchment areas, for example, as well as the effectiveness of these measures. Therefore, no key findings could be achieved for this generation technology.

### **3.6.3 Wind power**

The newly developed “storm control” seemed to be a promising adaptation measure. Thus, this technology was investigated in detail within this study. A simulation model<sup>18</sup> for wind turbines with and without storm control was used to estimate the additional amount of generated energy induced by this new control method.

---

<sup>18</sup> Please refer to (Spindler, 2013) for a detailed description of the model.

The model shows that the most frequent activity of the storm control mechanism appears in winter. This can be explained by the fact that average wind speeds in winter are higher than in summer. Thus, gusts may exceed the maximum wind speed of wind turbines more frequently than in summer. The storm control leads to an increase of electricity generation up to 0.33 % using the example of Germany. Compared to the possible reduction of standard capacity induced by climate change, ranging between -1.3 % (TROPIC, Germany, 2011-30) and -3.1 % (TROPIC, Germany, 2031-50), it is shown that the investigated measure is not able to fully compensate the impacts of climate change.

### 3.6.4 Solar power (photovoltaics)

Regarding photovoltaics, the effects of different cooling technologies were compared, based on results found in the literature. Therefore, a virtual photovoltaic unit of 10 kWp located in the city of Graz was assumed. By using a planning software, the standard capacities of the corresponding cooling methods were determined (see Table 15).

**Table 15: Standard capacities of the reference unit by different cooling methods (Spindler, 2013)**

<i>Cooling technology</i>	<i>Average efficiency</i>	<i>Standard capacity</i>
Water fluid cooled	0.1362	14,052 kWh/a
Air cooled	0.1343	13,860 kWh/a
Without cooling	0.1302	13,432 kWh/a

The results show, that active cooling of a photovoltaic module may increase the standard capacity by 3.2 % to 4.6 %. Compared to the climate change impacts, which are unfortunately negative throughout all climate scenarios, an active cooling of photovoltaic modules is able to compensate at least 30-50 % of standard capacity reductions caused by climate change impacts on solar radiation, also depending on the changes of mean temperature. Taking a look at the economic efficiency, the analysis shows that – based on investment costs found in the literature – an investment in cooling technologies is not reasonable, unless the additionally generated low-temperature heat can be used. In this case, an additional, yet unconsidered cost reduction in terms of heating demand may turn the economically inefficient investment into an efficient one.

### 3.6.5 Electricity demand

When it comes to electricity demand, a differentiation between impacts and adaptation measures is quite difficult. The electricity demand depends - more or less – only on the

temperature, as shown in Toglhofer et al. (2011). Thus, climate change directly impacts heating and cooling demand of households. All of the climate models show an increase of temperature, leading to a decrease of heating demand in winter and an increase of cooling demand in summer. Based on many discussions within the project team, the changes in heating demand were considered as impact effect, founded by the fact that there is no need for customers to react on a warmer climate; heating systems will automatically reduce the energy needed for heating. An increasing electricity demand caused by air conditioning systems is considered as adaptation measure, due to the need of additional cooling capacities, which have to be installed to meet an increasing cooling demand.

To sum that up, an increasing electricity demand in summer is expected due to adaptation measures to react on rising temperatures, mainly caused by air conditioning systems in domestic homes and/or office buildings. Using standard electricity-driven air conditioning systems solely may be a kind of mal-adaptation. The use of so-called “solar cooling” systems might be a better way to react on rising temperatures. Starting with a simple combination of air conditioning systems and photovoltaics ranging to absorption/adsorption cooling systems, any use of solar power for cooling processes will be more reasonable, as long as they are well-planned, cf. (Preisler et al., 2012).

## 4 Outlook and recommendations for research

For the assessment of changes of natural inflow to storage power plants, the available data and methods used herein (coarse data resolution and monthly hydrological model that needs calibration to measured runoff) are not appropriate. To be able to consider possible changes in runoff due to climate changes, a climatic water balance was computed (precipitation – PET) for four sub-regions of the Alps on an annual basis. The change in runoff in these regions from the periods 2011-2030 and 2031-2050 to the reference period 1961-1990 was then used to adjust the average annually produced energy amount related to the natural inflow to the individual storage power plants. However, this can be seen only as a rough estimate and asks for further research: On the one hand, observation data of real inflow into the storage plants is preferable to be able to calibrate a rainfall-runoff model. On the other hand a finer resolution of the climate input data (e.g. 1 km) would be desirable to represent elevated regions more appropriately. Moreover, especially for high alpine regions, the influence of glaciers may be important. Changes of glacier bodies related to climate change need to be addressed in detail, and the current (as well as historical) situation/inventory needs to be accounted for.

Moreover, the simple model (structure) does not explicitly take into account artificial structures like reservoirs or dams. Water losses as a result of human abstractions can make up a significant amount of the water supply. Especially in Mediterranean basins, abstractions and losses alter runoff quantity and runoff regime. The model implicitly allows accounting for water losses (using the exchange term  $X_5$ ), however this only works if there is no considerable seasonal variation as the parameter is constant over time. Also variations in soil properties and vegetation cover obviously influences the transformation of precipitation to runoff, but as future changes are rather uncertain, incorporating these parameters at the current stage would only increase uncertainties and necessitate that more parameters are fitted based on the information content of a runoff time series. Although incorporating additional processes into the hydrological model is appealing, it bears the risk that the model is overparameterized (Loague and Freeze, 1985; Beven, 1989; Perrin et al., 2003). Only if additional data (e.g. groundwater levels) is available, more parameters are justifiable. Further research on these issues is desirable.

While the focus of this project was on modeling the aggregate impacts of temperature change on electricity demand for heating and cooling, more research should be undertaken

in order to understand the impacts of extreme hot spells or cold spells on electricity load. In fact, this could be done not only by considering hot or cold periods of climate scenario runs, but also by using stochastic modeling techniques which might also capture the time dynamics of daily temperatures. The latter modeling approach would help to assess the effects of unusually hot or cold periods (e.g. 1 in 20 year events) on loads, which are important for evaluating network reliability.

As shown in the results section, the climate change impacts on the electricity market depend from impacts on electricity demand and electricity generation in the neighboring countries. Thus, it is recommended to consider the total installed hydro power in Continental Europe rather than the Alpine region, though this region contains the major share of hydro generation capacities. At least, the generation units in the French Massif Central or the Italian Apennine Mountains should be included in further projects.

Regarding the modeling of wind power and photovoltaics, the supply with appropriate climate data is difficult for mountainous regions like Austria. To use high-quality power plant models, hourly climate data with a high regional resolution is needed, which is currently not derivable by state-of-the-art regional climate models. As soon as appropriate data will be available for Austria, an enhanced modeling of wind power and photovoltaics is recommended.

When it comes to adaptation measures regarding storage power plants, more information is needed: hydrological parameters as already mentioned, but also investment costs to estimate the economic effectiveness of measures, as well as a certain experience on the effectiveness of miscellaneous measures.

To enhance the modeling framework, a “tighter” coupling of sectoral models like ATLANTIS and CGE models may produce better results. However, considering market prices or import/export balances for example, which are calculated endogenously in both models as additional variables used to couple both models, will need a lot of effort and time.

## 5 References

- Adnot, J., Orphelin, M., Carretero, C., Marchio, D., Waide, P., Carre, M., Lopes, C., Cedral-Galan, A., Santamouris, M., Klitsikas, N., Mebane, B., Pressuto, M., Rusconi, E., Ritter, H., Becirspahic, S., Giraud, D., Bossoken, E., Meli, L., Cassadrini, S., Auffret, P., 1999. Energy Efficiency of Room Air Conditioners (EERAC). Study for the D.G. for Energy (DGXVII) of the Commission of the EU. Final Report, Paris.
- Babiker, M.H., Rutherford, T.F., 2005. The economic effects of border measures in subglobal climate agreements. *Energy Journal* 26(4), 99-125.
- Bednar-Friedl, B., Kulmer, V., Schinko, T., 2012. The effectiveness of anti-leakage policies in the European Union: Results for Austria. *Empirica* 39 (2), 233-260.
- Bessec, M., Fouquau, J., 2008. The non-linear link between electricity consumption and temperature in Europe: A threshold panel approach. *Energy Economics* 30(5), 2705-2721.
- Beven, K., 1989. Changing ideas in hydrology – The case of physically based models. *Journal of Hydrology* 105, 157-172.
- Beven, K.J., 1993. Prophecy, reality and uncertainty in distributed hydrological modeling. *Advances in Water Resources* 16, 41-51.
- Boberg, F., Berg, P., Thejll, P., Gutowski, W.J., Christensen, J.H., 2010. Improved confidence in climate change projections of precipitation further evaluated using daily statistics from ENSEMBLES models. *Climate Dynamics* 35(7-8), 1509-1520.
- Böhringer, C., 2000. Cooling down hot air: A global CGE analysis of post-Kyoto carbon abatement strategies. *Energy Policy* 28(11), 779-789.
- Déqué, M., 2007. Frequency of temperature and precipitation extremes over France in an anthropogenic scenario: Model results and statistical correction according to observed values. *Global Planetary Change* 57, 16-26.
- DoE (Department of Energy), 2010. Assumptions to the Annual Energy Outlook 2010 (with Projections to 2035): Electricity Market Module
- Edijatno, Nascimento, N.O., Yang, X., Makhlof, Z., Michel, C., 1999. GR3J: a daily watershed model with three free parameters. *Hydrological Sciences Journal* 44(2), 263-277.
- Enercon GmbH, 2012. ENERCON Produktübersicht. Aurich, Germany.
- ENTSO-E, 2012. Data downloaded from the ENTSO-E Data Portal on 2013-01-24. <https://www.entsoe.eu/data/data-portal/>
- ENTSO-E, 2013. entso-e portal. ENTSO-E homepage, accessed 04/2013. URL: <http://portal.entsoe.net/austria.aspx>

- Eskeland, G.S., Mideksa, T.K., 2010. Electricity demand in a changing climate. *Mitigation and Adaptation Strategies for Global Change* 15(8), 877-897.
- European Commission, 2008. 20 20 by 2020 Europe's climate change opportunity. Communication from the European Commission to the European Parliament, the council, the European economic and social committee and the committee of the regions. Brussels.
- European Commission, 2011. A Roadmap for moving to a competitive low carbon economy in 2050. Communication from the European Commission to the European Parliament, the council, the European economic and social committee and the committee of the regions. Brussels.
- European Environmental Agency (EEA), 2010. Corine Land Cover 2006 raster data (Version 13, 02/2010), <http://www.eea.europa.eu/data-and-maps/data/corine-land-cover-2006-raster>
- Eurostat, 2011. NUTS-3 population data, NUTS-0 GDP, Industrial Production Index (sectors B and C), <http://epp.eurostat.ec.europa.eu/portal/page/portal/eurostat/home/>
- EUROSTAT, 2012. Energy statistics - quantities, annual data. Exports (by country of destination) - electricity - annual data (nrg\_135a), Accessed July 2012. <http://epp.eurostat.ec.europa.eu/portal/page/portal/energy/data/database>
- Feichtinger, G., Schüppel, A., Stigler, H., Themeßl, M., Wagner, T., Birk, S., Gobiet, A., Kulmer, V., 2013. Auswirkungen des Klimawandels auf den Elektrizitätssektor – ein integrierter Modellansatz für Österreich. 8. Internationale Energiewirtschaftstagung, Wien.
- Giesecke, J., Mosonyi, E., 2009. *Wasserkraftanlagen - Planung, Bau und Betrieb*. Berlin Heidelberg. Springer, 2009. ISBN 978-3-540-88988-5.
- Graham, L. P., Hagemann, S., Jaun, S., Beniston, M., 2007. On interpreting hydrological change from regional climate models. *Climatic Change* 81, 97-122.
- Graus, W., Blomen, E., Worrell, E., 2011. Global energy efficiency improvement in the long term: A demand- and supply-side perspective. *Energy Efficiency* 4(3), 435-463.
- Guo, Y., Senior, M.J., 2006. Climate model simulation of point rainfall frequency characteristics. *Journal of Hydrologic Engineering* 11(6), 547-554.
- Gupta, H.V., Beven, K.J., Wagener, T., 2005. Model Calibration and Uncertainty Estimation. Part 11 Section 131 in Volume 3, *Encyclopaedia of Hydrological Sciences*, Wiley, Chichester, 2015-2032.
- Gupta, H.V., Sorooshian, S., Yapo, P.O., 1999. Status of automatic calibration for hydrologic models: Comparison with multilevel expert calibration. *Journal of Hydrologic Engineering* 4(2), 135-143.
- Gutschi, C., Bachhiesl, U., Huber, C., Nischler, G., Jagl, A., Süßenbacher, W., Stigler, H., 2009a. ATLANTIS – Simulationsmodell der europäischen Elektrizitätswirtschaft bis 2030. *Elektrotechnik & Informationstechnik* 126(12), 438–448.

## EL.ADAPT

- Gutsch, C., Bachhiesl, U., Huber, C., Stigler, H., 2009b. Business-as-usual scenario for the development of the electricity economies in South Eastern Europe. 18th International Expert Meeting Komunalna Energetika (Power Engineering) University of Maribor.
- Gutsch, C., Jagl, A., Nischler, G., Huber, C., Bachhiesl, U., Stigler, H., 2010. Scenarios for the development of the electricity economy in Continental Europe. 21st World Energy Congress, Montreal.
- Haylock, M.R., Hofstra, N., Klein Tank, A.M.G., Klok, E.J., Jones, P.D., New, M., 2008. A European daily high-resolution gridded data set of surface temperature and precipitation for 1950-2006. *Journal of Geophysical Research D: Atmospheres* 113(20), D20119.
- IEA, 2010. World Energy Outlook 2010. France: OECD/IEA.
- Klein, B., Krahe, P., Lingemann, I., Nilson; E., Kling, H., Fuchs, M., 2011. Assessing climate change impacts on water balance in the upper danube basin based on 23 member RCM Ensemble. Proceedings of the XXVth Conference of the Danube Countries, 16-17 Juni 2011, Budapest
- Klemes, V., 1986. Operational testing of hydrological simulation models. *Hydrological Sciences* 31, 13-24.
- Kling, H., Fuchs, M., Paulin, M., 2011. Ensemble Modellierung der Abflusscharakteristik der oberen Donau unter Klimaszenarien. Tag der Hydrologie, March 2011, Vienna.
- Klok, E.J., Klein Tank, A.M.G., 2009. Updated and extended European dataset of daily climate observations. *International Journal of Climatology* 29(8), 1182-1191.
- Kranzl, L., Haas, R., Kalt, G., Müller, A., Nakicenovic, N., Redl, C., Formayer, H., Haas, P., Lexer, M-J., Seidl, R., Schörghuber, S., Nachtnebel, H.P., Stanzel, P., 2010. Ableitung von prioritären Maßnahmen zur Adaption des Energiesystems an den Klimawandel - "KlimAdapt"-Endbericht. Klima- und Energiefonds des Bundes, 225 p.
- Krause, P., Boyle, D.P., Bäse, F., 2005. Comparison of different efficiency criteria for hydrological model assessment. *Advances in Geosciences* 5, 89-97.
- Lenderink, G., van Ulden, A., van den Hurk, B., Keller, F., 2007. A study on combining global and regional climate model results for generating climate scenarios of temperature and precipitation for the Netherlands. *Climate Dynamics* 29(2-3), 157-176.
- Leuprecht A, Gobiet A. 2010. Classification of precipitation regions in the alpine areas using cluster analysis. Wegener Center Verlag Graz, ISBN 978-3-9502615-9-2.
- Loague, K., Freeze, R.A., 1985. A comparison of rainfall-runoff modeling techniques on small upland catchments. *Water Resources Research* 21, 229-248.
- Maier, K., 2011. Analyse des iberischen Elektrizitätssystems unter besonderer Berücksichtigung der erneuerbaren Energien. Master's thesis. University of Graz in cooperation with the Institute of Electricity Economics and Energy Innovation (Graz University of Technology).

- Makhlouf, Z., Michel, C. (1994), A two-parameter monthly water balance model for French watersheds. *Journal of Hydrology* 162(3-4), 299-318.
- Maraun, D., Wetterhall, F., Ireson, A.M., Chandler, R.E., Kendon, E.J., Widmann, M., Brienen, S., Rust, H.W., Sauter, T., Themel, M., Venema, V.K.C., Chun, K.P., Goodess, C.M., Jones, R.G., Onof, C., Vrac, M., Thiele-Eich, I., 2010. Precipitation downscaling under climate change: Recent developments to bridge the gap between dynamical models and the end user. *Reviews of Geophysics* 48(3), RG3003.
- Mearns, L., 2003. Issues in the impacts of climate variability and change on agriculture - Applications to the southeastern United States. *Climatic Change* 60(1-2), 1-6.
- Moral-Carcedo, J., Vicéns-Otero, J., 2005. Modeling the non-linear response of Spanish electricity demand to temperature variations. *Energy Economics* 27(3), 477-494.
- Moriasi, D.N., Arnold, J.G., Van Liew, M.W., Bingner, R.L., Harmel, R.D., Veith, T.L., 2007. Model evaluation guidelines for systematic quantification of accuracy in watershed simulations. *American Society of Agricultural and Biological Engineers* 50(3), 885-900.
- Mouelhi, S., Michel, C., Perrin, C., Andréassian V., 2006. Stepwise development of a two-parameter monthly water balance model. *Journal of Hydrology* 318(1-4), 200-14.
- Nakicenovic, N., Alcamo, J., Davis, G., de Vries, B., Fenhann, J., Gaffin, S., Gregory, K., Grubler, A., Jung, T.Y., Kram, T., La Rovere, E.L., Michaelis, L., Mori, S., Morita, T., Pepper, W., Pitcher, H., Price, L., Raihi, K., Roehrl, A., Rogner, H.-H., Sankovski, A., Schlesinger, M., Shukla, P., Smith, S., Swart, R., van Rooijen, S., Victor, N., Dadi, Z., 2000. *Emission scenarios. A Special Report of Working Group III of the Intergovernmental Panel on Climate Change*. Cambridge University Press, Cambridge, UK.
- Nash, J.E., Sutcliffe, J.V., 1970. River flow forecasting through conceptual models, Part I – A discussion of principles. *Journal of Hydrology* 10, 282-290.
- OECD, 2012. OECD Environmental Outlook to 2050: The Consequences of Inaction', OECD Publishing. <http://dx.doi.org/10.1787/9789264122246-en>
- Oudin L., Hervieu F., Michel C., Perrin C., Andréassian V., Anctil F., Loumagne C., 2005. Which potential evapotranspiration input for a lumped rainfall-runoff model? Part 2 – Towards a simple and efficient potential evapotranspiration model for rainfall-runoff modeling. *Journal of Hydrology* 303, 290-306.
- Oudin, L., Andréassian, V., Mathevet, T., Perrin, C., Michel, C., 2006. Dynamic averaging of rainfall-runoff model simulations from complementary model parameterizations. *Water Resources Research* 42, W07410, doi:10.1029/2005WR004636.
- Paltsev, S.V., 2001. The Kyoto Protocol: Regional and sectoral contributions to the carbon leakage. *Energy Journal* 22(4), 53-79.

EL.ADAPT

- Pattis F., 2012. Modellierung der Stromerzeugung aus Photovoltaik in Deutschland. Master's thesis. Institute of Electricity Economics and Energy Innovation, Graz University of Technology.
- Perrin, C., Michel, C., Andréassian, V., 2001. Does a large number of parameters enhance model performance? Comparative assessment of common catchment model structures on 429 catchments. *Journal of Hydrology* 242, 275–301.
- Perrin, C., Michel, C., Andréassian, V., 2003. Improvement of a parsimonious model for streamflow simulation. *Journal of Hydrology* 279, 275-289.
- Piani, C., Haerter, J.O., Coppola, E., 2010. Statistical bias correction for daily precipitation in regional climate models over Europe *Theoretical and Applied Climatology* 99(1-2), 187-192.
- Pilli-Sihvola, K., Aatola, P., Ollikainen, M. and Tuomenvirta, H., 2010. Climate change and electricity consumption- Witnessing increasing or decreasing use and costs? *Energy Policy* 38(5), 2409-2419.
- Pöhler, H., Wendel, S., Schultze, B., Karl, S., J. Scherzer, 2010. Water Balance Modeling for the Inn River Basin (AdaptAlp technical report LfU-UDATA).
- Preisler, A., Thür, A., Neyer, D., Focke, H., 2012. SolarCooling Monitor. In Bundesministerium für Verkehr, Innovation und Technologie (ed.). Berichte aus Energie- und Umweltforschung 28/2012. [http://download.nachhaltigwirtschaften.at/hdz\\_pdf/berichte/endbericht\\_1228\\_solarcoolingmonitor.pdf](http://download.nachhaltigwirtschaften.at/hdz_pdf/berichte/endbericht_1228_solarcoolingmonitor.pdf)
- R Development Core Team, 2011. R: A Language and Environment for Statistical Computing. R Foundation for Statistical Computing, Vienna, Austria.
- Rivington, M., Miller, D., Matthews, K.B., Russell, G., Bellocchi, G., Buchan, K., 2008. Evaluating regional climate model estimates against site-specific observed data in the UK. *Climatic Change*, 88(2), 157-185.
- Robinson, S., Cattaneo, A., El-Said, M., 2001. Updating and estimating a social accounting matrix using cross entropy methods, *Economic Systems Research* 13(1), 47-64.
- Schüppel, A., 2010. Modellierungsansätze zur Beschreibung dargebotsabhängiger Stromerzeugung. Master's thesis. Institute of Electricity Economics and Energy Innovation, Graz University of Technology.
- Spindler, K., 2013. Anpassungsmaßnahmen der Elektrizitätswirtschaft an den Klimawandel. Master's thesis. Institute of Electricity Economics and Energy Innovation, Graz University of Technology.
- Stanzel, P., Nachtnebel, H.P., 2010. Mögliche Auswirkungen des Klimawandels auf den Wasserhaushalt und die Wasserkraftnutzung in Österreich. *Österreichische Wasser- und Abfallwirtschaft*, 62/9-10, 180-187; ISSN 0945-358X.

- Stigler, H., Gutschi, C., Nischler, G., Schüppel, A., Nacht, T., Feichtinger, G., Hütter, D., Bachhiesl, U., 2012. Aktuelle Weiterentwicklung des Simulationsmodells ATLANTIS. Tagungsband 12. Symposium Energieinnovation, ISBN 978-3-85125-200-2, Verlag der Technischen Universität Graz.
- Themeßl, M. J., Gobiet, A., Heinrich, G., 2012. Empirical-statistical downscaling and error correction of regional climate models and its impact on the climate change signal. *Climatic Change*, 112(2), 449-468.
- Themeßl, M. J., Gobiet, A., Leuprecht, A., 2011. Empirical-statistical downscaling and error correction of daily precipitation from regional climate models. *International Journal of Climatology*, 31(10), 1530-1544.
- UNFCCC, 2011. Greenhouse gas inventory data United framework convention on climate change. Accessed 09 Aug 2012, [http://unfccc.int/ghg\\_data/items/3800.php](http://unfccc.int/ghg_data/items/3800.php)
- Van Den Besselaar, E.J.M., Haylock, M.R., Van Der Schrier, G., Klein Tank, A.M.G., 2011. A European daily high-resolution observational gridded data set of sea level pressure. *Journal of Geophysical Research D: Atmospheres*, 116, D11110.
- van der Linden, P., Mitchell, J.F.B., 2009. ENSEMBLES: Climate Change and its Impacts: Summary of research and results from the ENSEMBLES project. Met Office Hadley Centre, Exeter. 160 pp.
- Wilcke, R., Mendlik, T., Gobiet, A., 2013. Performance and Consistency of Multi-Variable Downscaling and Error-Correction of Regional Climate Models, submitted to *Climatic Change*.
- Wilks, D.S., 2006. *Statistical Methods in the Atmospheric Sciences*. International Geophysics Series Volume 100, 2nd edition, Elsevier.
- Xu, C.-Y., Seibert, J., Halldin, S., 1996. Regional water balance modeling in the NOPEX area: development and application of monthly water balance models. *Journal of Hydrology* 180, 211-236.
- ZAMG/ TU-Wien Studie, 2011. Anpassungsstrategien an den Klimawandel für Österreichs Wasserwirtschaft. Endbericht. Lebensministerium.

**Acknowledgements:****Hydro:**

We thank all providers of historical runoff data: “The Global Runoff Data Centre, 56068 Koblenz, Germany”; „Via Donau – Österreichische Wasserstraßen Gesellschaft mbH“; Hydrographischer Dienst Steiermark; Amt der Kärntner Landesregierung; A08 Hydrographie; Amt der Oberösterreichischen Landesregierung, Direktion Umwelt und Wasserwirtschaft Abteilung Oberflächengewässerwirtschaft; Hydrographischer Dienst Salzburg, Fachabteilung Wasserwirtschaft; Amt der Tiroler Landesregierung, Sachgebiet Hydrographie und Hydrologie; Referat für Oberflächenhydrologie, Abt. BD3 - Hydrologie und Geoinformation, Amt der Niederösterreichischen Landesregierung; Amt der Vorarlberger Landesregierung, Abteilung Wasserwirtschaft; eHYD (<http://gis.lebensministerium.at/ehyd>); Banque Hydro <http://hydro.eaufrance.fr/> [equipe d'assistance]; the Slovenian Environment Agency: [http://www.arso.si/vode/podatki/arhiv/hidroloski\\_arhiv.html](http://www.arso.si/vode/podatki/arhiv/hidroloski_arhiv.html).

We also thank Ms. Kerstin Spindler and Mr. Florian Pattis for their excellent work within their master's theses, which were carried out on behalf of EL.ADAPT, and their valuable support.

# 6 Annex

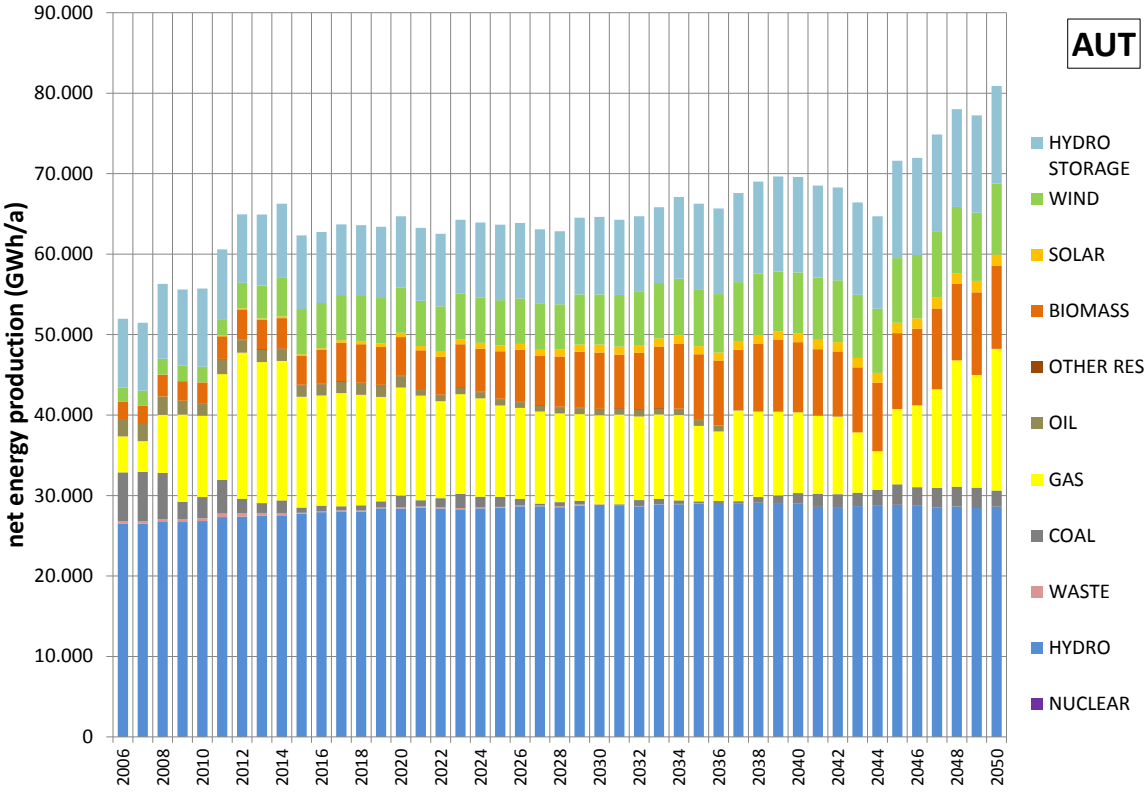


Figure 65: Net energy production in Austria (baseline scenario)

EL.ADAPT



Figure 66: Impacts of climate change on renewable generation in Germany and Luxembourg (hydro power: GAR only)

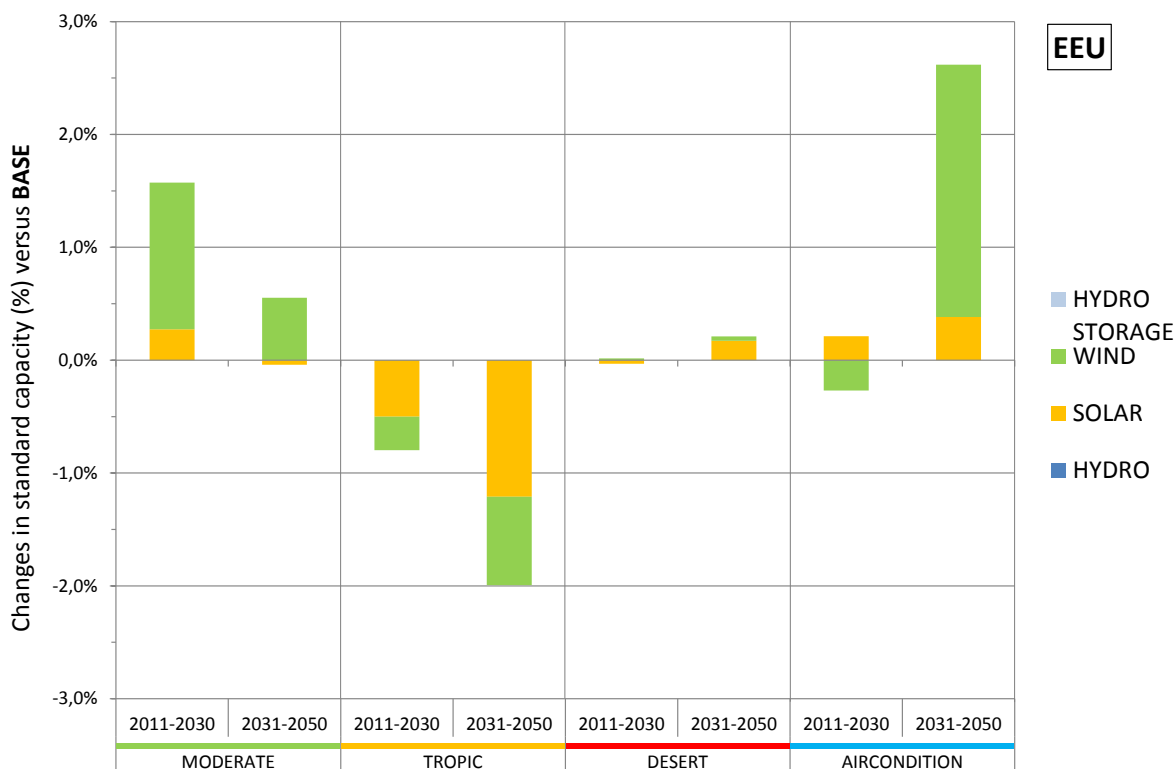


Figure 67: Impacts of climate change on renewable generation in Eastern Europe (hydro generation not investigated)

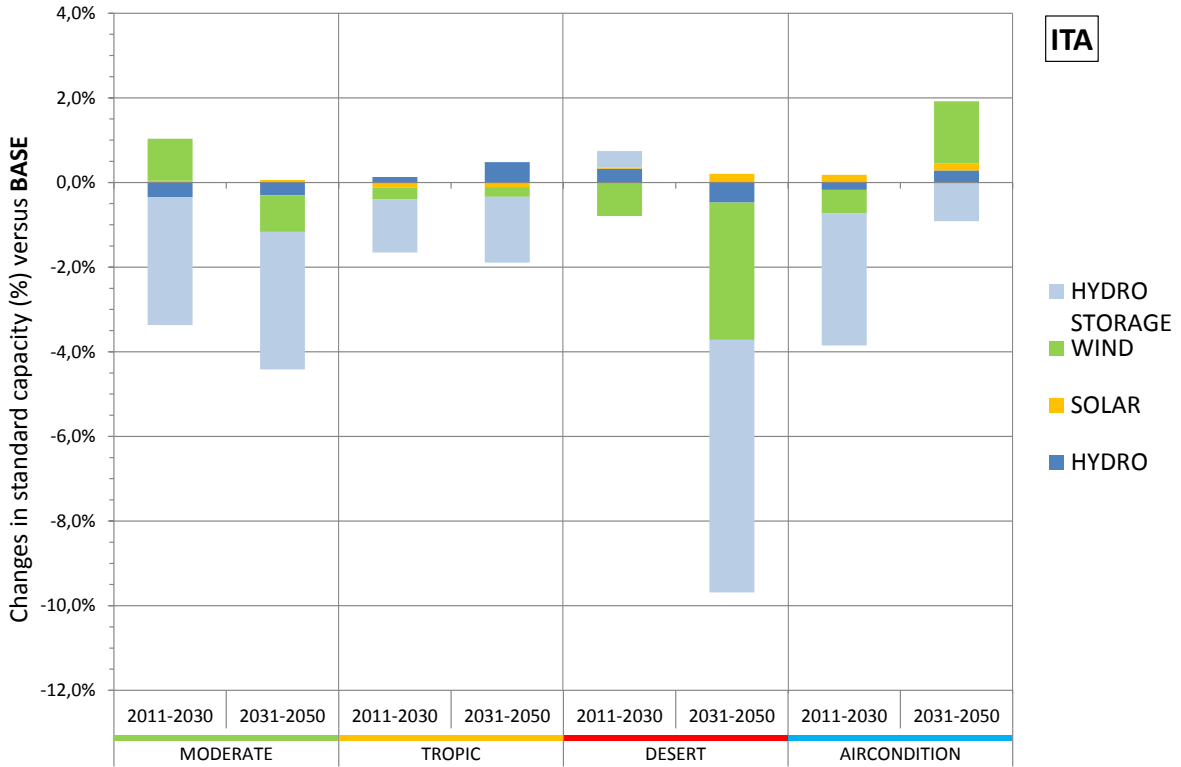


Figure 68: Impacts of climate change on renewable generation in Italy (hydro power: GAR only)



Figure 69: Impacts of climate change on renewable generation in Western Europe (hydro power: GAR only)

EL.ADAPT

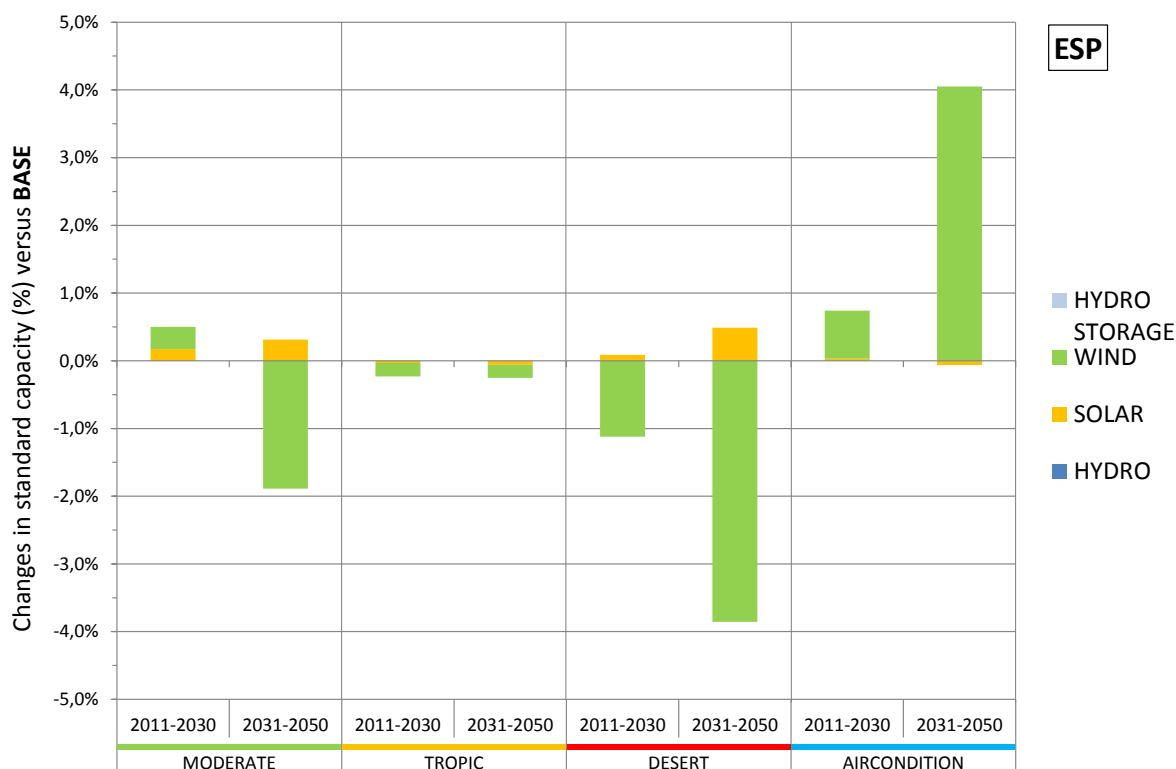


Figure 70: Impacts of climate change on renewable generation in Spain (hydro generation not investigated)

Table 16: Aggregated Region and comprising GTAP regions

Aggregated Region	Model code	Comprising GTAP regions
1 Oceania	OCEA	Australia, New Zealand, Rest of Oceania
2 Emerging economies: China, Hong Kong, India, Pakistan	ECO	China, Hong Kong, India, Pakistan
3 Tiger states	EASI	Japan, Korea, Taiwan
4 Rest of South & South East Asia ~ less developed Asian countries	RASI	Cambodia, Indonesia, Lao People's Democratic Republic, Myanmar, Malaysia, Philippines, Singapore, Thailand, Vietnam, Rest of Southeast Asia, Bangladesh, Sri Lanka, Rest of South Asia, Rest of East Asia (Korea, Mongolia, Macau)
5 North America	NAM	USA, Canada, Mexico, Rest of North America
6 Latin America	LAM	Argentina, Bolivia, Brazil, Chile, Colombia, Ecuador, Paraguay, Peru, Uruguay, Venezuela, Rest of South America, Costa Rica, Guatemala, Nicaragua, Panama, Rest of Central America, Caribbean
7 Austria	AUT	Austria
8 France + BE + CH + NL (Western Europe)	WEU	France, Switzerland, Belgium, Netherlands
9 Germany + Luxemburg	GERL	Germany, Luxemburg
10 Italy	ITA	Italy
11 Spain + Portugal	ESP	Portugal, Spain
12 UK + Ireland	UKI	UK, Ireland

13	North EU 27 + Norway + Rest of EFTA	NEU	Denmark, Estonia, Finland, Latvia, Lithuania, Norway, Sweden, Rest of EFTA (Liechtenstein, Iceland)
14	Eastern EU27	EEU	Czech Republic, Hungary, Poland, Slovakia
15	Southeastern and Rest of Europe	SEE	Albania, Croatia, Rest of Europe (Bosnia and Herzegovina, Macedonia, Serbia and Montenegro, Faroe Islands, Gibraltar, Monaco, San Marino), Turkey, Slovenia, Bulgaria, Romania, Cyprus, Greece, Malta
16	Russian Federation and CIS	CIS	Russian Federation, Armenia, Azerbaijan, Belarus, Georgia, Kazakhstan, Kyrgyzstan, Rest of former Soviet Union, Ukraine, Moldova
17	Oil / gas exporting countries (Middle East and Africa)	MENA	Iran, Rest of West Asia (Iraq, Kuwait, Qatar, Saudi Arabia, Emirates,...), Egypt, Morocco, Tunisia, Rest of North Africa (Algeria, Lybia), Nigeria, Rest of South Central Africa
18	Africa	AFR	Senegal, Rest of West Africa, Rest of Central Africa, , Ethiopia, Madagascar, Malawi, Mauritius, Mozambique, Tanzania, Uganda, Zambia, Zimbabwe, Rest of Eastern Africa, Botswana, South Africa, Rest of South African Customs Union

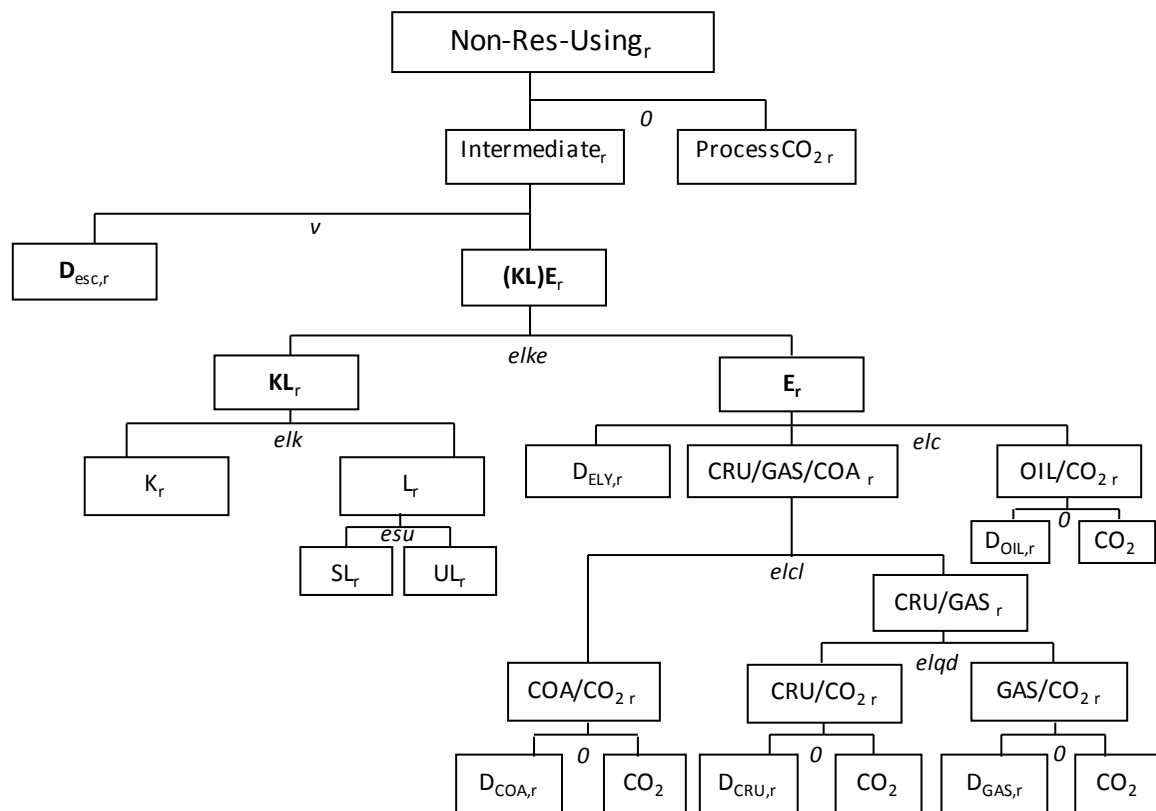


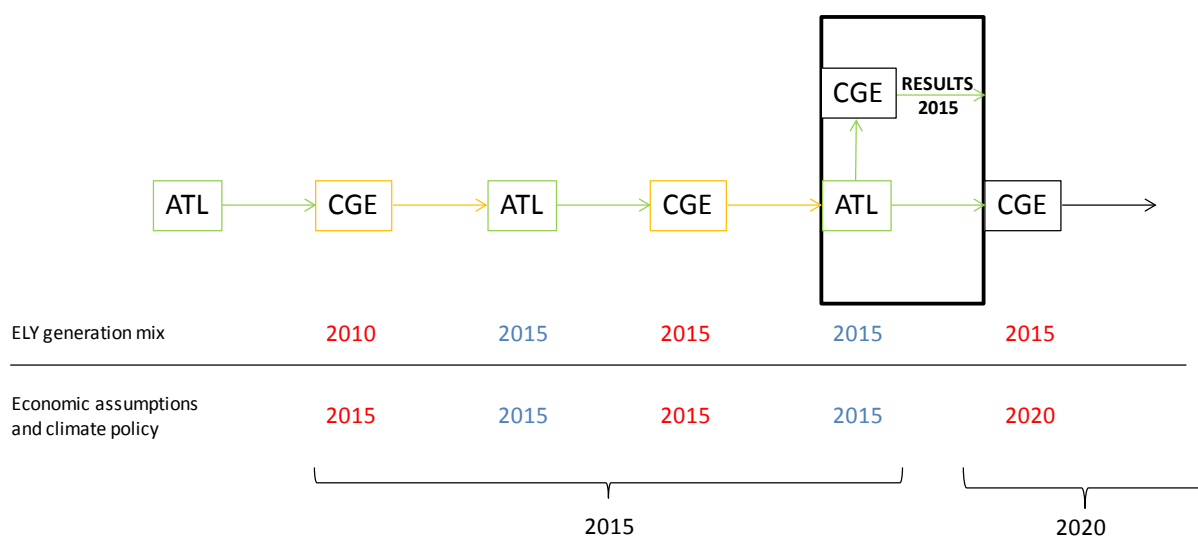
Figure 71: Nesting structure of non resource using production activities

### Details on Model Coupling between ATLANTIS and the CGE model

Oscillations in the coupled models mainly occurred due to the different nature and class of both models. The CGE model is an optimization model typically used for simulation and policy analysis, whereas ATLANTIS is a so-called ‘projection model’ which is driven by historical time paths and exogenous assumptions about future developments (‘scenarios’). By assuming a high stringency of policy measures (i.e. climate policy, renewable targets), as implemented in the CGE model, CO<sub>2</sub> price and fossil fuel input in electricity generation started to oscillate between different points in time. For example when CO<sub>2</sub> prices increased in 2015 due to the implementation of European climate policy targets in the CGE model, the response in ATLANTIS was that fossil fuel input were strongly reduced, which led to the opposed effect in 2020: A low fossil fuel input in electricity generation, therefore no scarcity of fossil fuels and a lower CO<sub>2</sub> price compared to 2015. Hence, results of both models did not coincide. Therefore, in order to ensure consistency not only between both models but also between points in time (one growth trajectory), we applied an iteration process.

More precisely, for each point in time we apply an iteration process to achieve consistency between ATLANTIS and the CGE model. Thereby, outputs of both models are exchanged in two iteration loops in each modeling step (for sequence, see Figure 1). Regarding model outputs, the CGE model delivers overall electricity demand, fossil fuel prices and the CO<sub>2</sub> price, while ATLANTIS delivers the electricity generation mix and electricity sectors’ investment demand.

**Figure A.1: Model coupling sequence and iteration steps between ATLANTIS and the CGE model**



---

*Abstract:*

This report summarizes the methodology as well as the key results of the research project EL.ADAPT. This project investigates the climate change impacts on the electricity industry and the influence of adaptation strategies on the Austrian economy up to 2050. Due to the international linkage of the electricity sector, the analysis considers the continental European context. Based on high resolution climate change and hydrology models, and an econometric electricity demand model, a techno-economic electricity sector model (ATLANTIS) is coupled with a multi-country multi-sector CGE model. The uncertainties across models are addressed by a reliability analysis. Results are presented for electricity generation (changed availability of electricity from renewable energy sources), electricity demand (due to changed heating and cooling), output of the electricity sector as well as other sectors of the economy.

*Zum Inhalt:*

Dieser wissenschaftliche Bericht fasst die Methodik sowie die Hauptergebnisse des Forschungsprojekts EL.ADAPT zusammen. In diesem Projekt wurden daher die Auswirkungen des Klimawandels auf die Elektrizitätswirtschaft sowie die Konsequenzen von Klimawandelanpassungsstrategien im Elektrizitätssektor auf die österreichische Wirtschaft bis 2050 untersucht. Ausgehend von hoch aufgelösten klimatologischen und hydrologischen Szenarien und einem ökonometrischen Elektrizitätsnachfragemodell wurden ein techno-ökonomisches Elektrizitätssektormodell mit einem Mehr-Länder-mehr-Sektoren Computable General Equilibrium-Modell gekoppelt. Mittels einer Reliabilitätsanalyse wurden die Unsicherheiten über die Modellkette beleuchtet. Es werden Ergebnisse für die Elektrizitätserzeugung (v.a. durch veränderte Verfügbarkeit alternativer Energieträger), Elektrizitätsverbrauch (aufgrund verändertem Heiz- und Kühlbedarfs), sowie Output des Elektrizitätssektors und anderer volkswirtschaftlicher Sektoren untersucht.